GeoRS

Geopedology and Landscape Development
Research Series

VOLUME 04

Detection and behavior of iron-cyanide complexes in soils of a former Manufactured Gas Plant site

Magdalena Maria Sut

b-tu

Brandenburg
University of Technology
Cottbus - Senftenberg

ISSN 2196 - 4122

ISSN 2196 - 4122

GeoRS 04

Detection and behavior of iron-cyanide complexes in soils of a former Manufactured Gas Plant site

Magdalena Maria Sut

GeoRS

Geopedology and Landscape Development
Research Series

VOLUME 04

Detection and behavior of iron-cyanide complexes in soils of a former Manufactured Gas Plant site

Magdalena Maria Sut

Brandenburg
University of Technology
Cottbus - Senftenberg

This series is edited by
Prof. Dr. Thomas Raab

Brandenburg University of Technology Cottbus - Senftenberg
Konrad-Wachsmann-Allee 6
03046 Cottbus
Germany

ISSN 2196 - 4122
www.tu-cottbus.de/geopedologie

Geopedology and Landscape Development
Research Series
GeoRS
VOLUME 04

Detection and behavior of iron-cyanide complexes in soils of a former Manufactured Gas Plant site

Dissertation approved by the Faculty of Environmental Sciences and Process Engineering of the Brandenburg University of Technology Cottbus-Senftenberg to gain the academic degree of doctor engineer (Dr. Ing.)

submitted by: M.Sc. Magdalena Maria Sut, born on 22.09.1984 from Gdynia

Reviewer: Prof. Dr. phil. Thomas Raab
Reviewer: PD Dr. rer. nat. habil. Thomas Fischer
Reviewer: Prof. Dr. M. Anne Naeth

Summary

In Germany, soil and groundwater at more than a thousand sites are contaminated with iron-cyanide complexes. These contaminations originate from the gas purification process that was conducted in Manufactured Gas Plants (MGP). There is a risk of human threat depending on the stability dissolved iron-cyanide complexes due to the potential release of toxic free cyanide, $CN_{(aq)}$ and $HCN_{(g),\,(aq)}$. The aim of this thesis was to evaluate a new method for the cyanide detection and to investigate the stability and retardation of the iron-cyanide complexes in soils by batch and column experiments in order to improve the knowledge concerning the fate of cyanide compounds in soil and groundwater. This study seeks for enhancing the efficiency of phytoremediation as a proper approach to decontaminate iron-cyanides complexes and thus tries to make a contribution to environmental protection.

Feasibility of Field Portable Near Infrared (FP NIR) Spectrometry to determine cyanide concentrations in soils of a former Manufactured Gas Plant site in Cottbus was evaluated in order to develop a rapid and non-destructive in-situ method. As known from other studies, diffuse near infrared reflectance spectroscopy has proven to be an appropriate analytical tool in soil investigation, thus various sample preparation methods were examined, including homogenizing, sieving, drying and grinding to determine the effectiveness of this method in cyanide determination. The study revealed that FP NIR could be a reliable device for detecting cyanide concentrations >2400 mg kg^{-1} in the field and >1750 mg kg^{-1} after sample preparation in the laboratory, however the limits of detection are too high to replace the traditional laboratory methods.

The applicability of neutral solution extraction to determine the water soluble cyanide fraction and the stability of Prussian Blue in surface and near-surface soils of a MGP site in Cottbus, under saturated and unsaturated water conditions, was studied in a column leaching and batch extraction experiments. Due to the lack of a standard leaching method to determine the water soluble (plant available) cyanide fraction, the efficiency of phytoremediation strategies can be decreased. Both experiments revealed high and continuous solubility of Prussian Blue, in acidic and slightly alkaline MGP soils. Dissolution of ferric ferrocyanide under circum-neutral pH and oxic water conditions was proposed to be a function of time, where the released amount is dependent on the soil pH and total cyanide content.

Modeling the long-term release of iron-cyanide complexes from the MGP soils revealed that the process is governed by two phases: one readily dissolved and one strongly fixed. The fast released phase was attributed to the transport process of readily dissolved iron-cyanide complexes (hexacyanoferrats) that is taking place in the liquid phase combined with the desorption of CN bound to heterogeneous surfaces that are in direct contact with aqueous

phase (outer-sphere complexation). The strongly fixed phase was proposed to be controlled by desorption, dissolution or diffusion processes, like the dissolution of precipitated ferric ferrocyanide or of inner-sphere complexed ferricyanides. Study revealed that the multiple first order equation, which assumed simultaneous occurrence of both phases, was the most appropriate in reflecting the probable cyanide release mechanisms from the MGP soils. The cyanide release rates increased with increasing pH, decreased with low initial CN concentration and were retarded by the increase in OM content.

The retardation of iron-cyanide in soil samples taken at MGP in Cottbus from two ≈ 7 m long boreholes was investigated in batch and column experiments. In this study, retention properties of the sandy loam MGP soil and the potential vertical movement of the solid iron-cyanide complexes, co-existing with the dissolution, sorption and precipitation reactions were investigated. Experiments revealed that the excess of the available iron, which induced the formation of the Prussian Blue colloids despite the circum-neutral pH, was a very important factor in decreasing the cyanide concentration. Additionally, despite the chemical factors influencing the potential reaction with manganese oxides, the physical factors like pore size distribution, variation in the grain size etc. can reduce the cyanide concentration due to mechanical retention (filtration) of the vertical colloidal ferric ferrocyanide movement. This study proposes colloidal vertical transport of the solid iron-cyanide complexes as a potential alternative process influencing the cyanide mobility in the circum-neutral pH and under the excess of available iron conditions.

Supplementary discussion concerning the studies presented above contains considerations on the limitations of the FP NIR spectrometry including the effect of water, OM content, color, particle size, temperature, collection point etc. of the sample. Furthermore, supplementary measurements involving batch experiments; pore volume via field capacity, porosity and particle density determination; and chemical equilibrium modeling for the stability of Prussian Blue study are discussed. Additionally, kinetic and isotherm equations were used to model long-term cyanide release, constrained by one phase, from the acidic soil.

The results presented in this thesis revealed limitations of the FP NIR in measuring the cyanide concentrations in soil. Advancing the sample pretreatment procedures can improve the feasibility of the spectrometer in detecting CN signal. Long-term extraction with the distilled water provides reliable assessment of the potential environmental hazard due to continuous dissolution of the solid iron-cyanide complexes demonstrated in this thesis. Inconsistency of the Prussian Blue stability reported in the literature to the one obtained in this study imply usage of the CN contaminated MGP soils, instead of synthetic solutions, to advance the knowledge concerning the solid iron-cyanide dissolution behavior. Furthermore, in the non-acidic soils the cyanide solubility might be influenced by the equilibrium with manganese iron-cyanide mineral.

Contents

List of abbreviations and symbols

a	Constant related to the initial velocity of the reaction
BBodSchG	Bundes-Bodenschutz Gesetz
BBodSchV	Bundes-Bodenschutz- und Altlasten Verordnung
C	Carbon
Ca	Calcium
CAS	Enzyme b-cyanoalanine synthase
CEC	Cation exchange capacity
CN	Cyanide
CO	Carbon monoxide
gS	Coarse sand
CV	Cross validation
DB AG	Deutsche Bahn Aktiengesellschaft
df	Degrees of freedom
DRS	Diffuse reflectance spectroscopy
DW	Dry weight
EC	Electrical conductivity
Eh	Reduction-oxidation (redox) potential
Fe	Iron
Fe-CN	Iron-cyanide complex
FeS	Iron sulfide
FIA	Flow injection analysis
FP NIR	Field portable near infrared spectrometer
FP XRF	Field portable X-ray fluorescence
fS	Fine sand
FTIR	Fourier transform infrared
H	Hydrogen
HCN	Hydrogen cyanide
Hg	Mercury
HN_3	Ammonia
H_2S	Hydrogen sulfide
K	Potassium
k	Release rate coefficient
K_d	Apparent diffusion rate constant

Kr	Krypton
Ksp	Solubility product constant
LC_{50}	Median lethal concentration
LOD	Limit of detection
LOI	Loss on ignition
LOO-CV	Leave-one-out cross validation
M	Mole
Me	Metal
MG	Model generator
MIR	Mid-infrared
Mg	Magnesium
MGP	Manufactured gas plant
Mn	Manganese
mS	Medium sand
mS	Millisiemens
mV	Millivolt
N	Nitrogen
NIR	Near infrared
nm	Nanometer
O	Oxygen
p	Probability value
PAH	Polycyclic aromatic hydrocarbons
pE	Redox potential
pKa	Dissociation constant
PLS	Partial Least Square
ppm	Parts per million
q	Amount of released substance
q_1	Fast releasing pool
q_2	Stronger fixed pool
q_0	Amount of released substance at equilibrium
q_{tot}	Amount of released substance in time t
R	Reflectance
R^2	Correlation coefficient
rmp	Rotation per minute
RMSEP	Root mean square error of prediction
S	Sand
SE	Standard error

S Golay	Savitzky-Golay
SNV	Standard normal variation
SOM	Soil organic matter
SSQ_{resid}	Residual sum of squares
T	Clay
t	Reaction time
$t_{p,df}$	Limit of integration of the students distribution
TCN	Total cyanide
TCLP	Toxicity Characteristic Leaching Procedure
U	Silt
USEPA	United States Environmental Protection Agency
USGS	United States Geological Survey
UV	Ultraviolet
v	Constant
WAD	Weak acid dissociable
x	Number of ligand ions
XRG	X-ray granulometry
z	Metal's charge
α	Release constant

List of Figures

List of Pictures

List of Tables

1 General Introduction

When human kind learned how to control the fire and smelt the metals, a very long process, lasting till today, of anthropogenic soil pollution began. However, with a rise of civilization and industry, the nature and the distribution of contaminants have changed and evolved (Rhind, 2009). Nowadays, human activities related to industry, agriculture, waste disposal or oil spills, generate enormous input of diverse contaminants into the soils. According to the European Environment Agency (EEA, 2007) the number of sites in Europe where potentially polluting activities are occurring, or have taken place in the past, stands at about 3 million. As a consequence, advancement in soil remediation strategies, which involve contaminant detection, immobilization or removal, is of prominent importance (Vandegrift et al., 1992; Hester and Harrison, 1997).

Contaminants can be defined as substances that may cause potential harm to the environment including humans, animals, plants, waters, and soils. This potential often depends on the concentration of a substance (Rennert, 2002; Pierzynski et al., 2005). Soil contamination is either solid or liquid hazardous substances mixed with the naturally occurring soil. Once discharged to the soil environment, pollutants can undergo various chemical and biological reactions that influence the contaminants toxicity, as well as, transport through the soil profile and groundwater (Pfaff-Schley, 1996; Rennert, 2002). Investigating the stability of contaminants in the affected soil and advancing the knowledge concerning the detection methods helps implementing the remediation processes by saving the most precious and expensive factor, which is "time" (Wilson and Clarke, 1994). Iron-cyanide complexes are worldwide detected soil contaminants that create challenging site remediation projects.

1.1 Origin of iron-cyanide complexes contamination in soil

Cyanides are well recognized by the public due to their toxicity. In the past, HCN gas was frequently used as a chemical warfare agent. During the First World War, the USA and Italy used hydrogen cyanide against the Central Powers in 1918. In the 20th century, HCN gas was used in gas chambers in the World War II Holocaust and by Iraq in the war against Iran and against the Kurds in northern Iraq during the 1980s (Dzombak et al., 2006).

Cyanide-containing compounds are produced and used in commerce in large quantities,

but they are also introduced into the environment from several natural sources (Dzombak et al., 2006). They are produced by a variety of microorganisms like fungi, bacteria, actinomicetes and algae, and synthesized by over 800 species of plants (mainly in the form of cyanogenic glucosides) (Knowles, 1976). Cyanides from natural sources are degraded by soil microorganisms and converted to carbonate and ammonia so they do not persist in soil (Fuller, 1985).

Organisms do not produce iron-cyanide complexes, but their presence in soil is a result of anthropogenic activities (Mansfeldt et al., 1998; Dzombak et al., 2006). Iron-cyanide complexes have been observed at many industrial sites, either as an outcome of industrial processes or as an incident product. Road salts, purifier wastes, blast furnace sludge and paper de-inking sludge are examples of iron-cyanide containing materials (Smith and Mudder, 1991; Rennert, 2002). This work is focused on the iron-cyanide contaminated soils originating from the former the Manufactured Gas Plant (MGP) sites, where purifier wastes were deposited as a filling material.

From the early 1800s through the mid-1900s MGPs were operated nationwide to provide gas from the coal or oil for lighting, heating and cooking (EPA, 1999). Coal gas started to be widely used as a means for illumination in the United Kingdom in the early 19th century, initially in factories and subsequently for street lighting. The expansion of electric lighting in 1880s provided the incentive for the development of additional uses for coal gas, like heating and cooking. Due to the introduction of natural gas, town gas production declined and the MGPs were closed until the 1970s (DEIP, 1995). The USEPA and others estimate that from ca. 1815 to ca. 1960 over 50.000 manufactured gas plants were operated in the United States. According to Mansfeldt (2003), in Germany, the total number of former manufactured gas plants amounts to 1064.

The iron-cyanide contaminated purifier wastes material at the MGP sites originates from coal gas purification process (Young and Theis, 1991; Ghosh et al., 1999a). Gas production by coal gasification involved heating the coal in ovens with a limited supply of oxygen at high temperatures. Produced gas contained impure coal gas, ammoniacal liquor and tar. The liquid fractions were separated and the gas was purified to remove remaining hydrogen sulfide (H_2S), ammonia, (NH_3), hydrocarbons (PAH) and hydrogen cyanide (HCN) (DEIP, 1995). The primary purpose of the gas purification however was the H_2S removal, HCN was removed due to its corrosive effects on the pipe-lines rather than toxic effects. Hydrogen cyanide was not formed through coal pyrolysis, but from a reaction of ammonia with carbon (Mansfeldt, 2003):

$$NH_3 + C \longrightarrow HCN + H_2 \quad (1.1)$$

$$NH_3 + CO \longrightarrow HCN + H_2O \quad (1.2)$$

$$NH_3 + CH_4 \longrightarrow HCN + 3H_2 \quad (1.3)$$

$$2NH_3 + C_2H_4 \longrightarrow 2HCN + 4H_2 \quad (1.4)$$

The manufactured coal gas was conducted through boxes containing wood shavings, impregnated with ferric chloride, iron (III) hydroxide or crushed blast furnace slag mixed with a chemically active form of hydrated iron oxide to remove the impurities (Theis et al., 1994; Dimitrova, 2010). Hydrogen cyanide participated in a complex set of reactions, under reducing conditions with the sulfur and ammonia compounds in the manufactured gas, due to reactions with Fe^{2+} containing compounds:

$$3Fe(OH)_2 + 6HCN \longrightarrow Fe_2[Fe(CN)_6] + 6H_2O \quad (1.5)$$

$$3FeS + 6HCN \longrightarrow Fe_2[Fe(CN)_6] + 3H_2S \quad (1.6)$$

$$3Fe_2[Fe(CN)_6] + 1\,1/2\,O_2 + 3H_2O \longrightarrow Fe_4[Fe(CN)_6]_3 + 2Fe(OH)_3 \quad (1.7)$$

When the iron oxide lost its absorbing capacity, it had to be regenerated by being spread in the vicinity of the MGP in order to aerate them. The product of reactions 1.5 and 1.6 is the precipitate Berlin White, $Fe_2[Fe(CN)_6]$, which in the process of regeneration is oxidized to Prussian Blue (ferric ferrocyanide), $Fe_4[Fe(CN)_6]_3$ (reaction 1.7) (Mansfeldt, 2003). Ferric ferrocyanide is a common blue pigment and a final product of HCN removal from manufactured gas.

The source of iron-cyanide compounds in soil and groundwater at MGP sites is usually oxide-box residuals that were managed onsite as fill (Theis et al., 1994; Dzombak et al., 2006). Spent oxide waste, which typically contained high amounts of sulfur, tar, various complex iron-cyanides (formed by the dissolution of Prussian Blue), has been percolating for nearly 60 years into the soil and groundwater at the MGP sites. The management and remediation of cyanide contaminated water and soil can be very challenging because of the complexity of the chemistry and toxicology of cyanide compounds.

1.2 Speciation and toxicity of cyanides

Cyanide is present in the environment in many different organic and inorganic forms, which all contain a cyano group "-C≡N" as a part of their molecule. The most common, occurring in the soil and groundwater are (Meeussen, 1992):

- Free cyanides: like $HCN_{(aq)}$, $HCN_{(g)}$ and CN^- (volatile and toxic)
- Simple cyanides: like KCN and AgCN, (KCN readily dissolves in water to form CN^- and K^+, and AgCN is only slightly soluble)
- Complex cyanides: like $Fe(CN)_6^{3-}$, $Co(CN)_6^{2-}$, $Zn(CN)_4^{2-}$, $Fe_4[Fe(CN)_6]_3$ (dissociation to free cyanide depends on kinetic and thermodynamic stability)

An additional group of organic cyanide compounds, so-called nitriles, exists, which includes various pesticides containing cyanides, as well as naturally occurring nitriles, originating from plants and micro-organisms (Fuller, 1984; Kjeldsen, 1998). Furthermore, a group called thiocyanides containing the (-SCN) group occurs (Kjeldsen, 1998).
Free cyanides are considered to be the toxic species and are defined as the forms of molecular and ionic cyanide released into solution by the dissolution and dissociation of cyanide compounds and complexes (Smith and Mudder, 1991; Ghosh et al., 1999c). Therefore, the toxicity of the cyanide containing compounds mainly depends on the possibility of dissociation to free cyanide. Figure 1 shows the chemical classification of selected dissolved cyanide complexes that have been detected at MGP sites and their stability constant K, which is an indicative of the toxicity. Cyanide is extremely toxic to mammals, with a lethal dose (LC_{50} = 546 ppm for 10 min of inhalation) an adult person of ca. 1-2 mg kg^{-1} (Egekeze et al., 1980). It works by binding to an enzyme involved in respiration (cytochrome c oxidase), thus inhibiting the ability of cells to use oxygen (Shifrin et al., 1996).

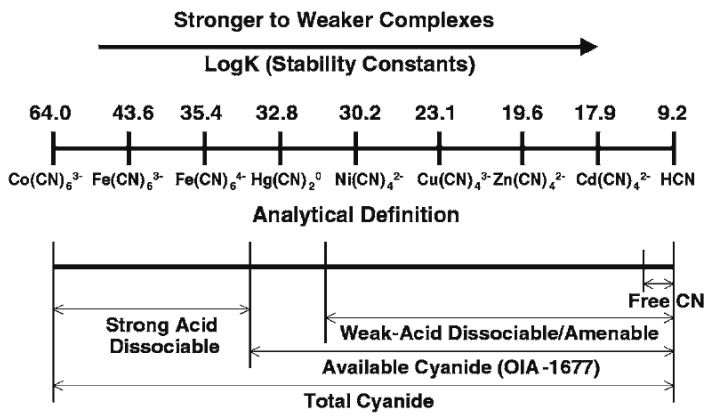

Figure 1: Chemical classification and the stability constant K of dissolved cyanide compounds (Ghosh et al., 2004).

Simple cyanides are defined as the salts of hydrocyanic acid, e.g. KCN. They dissolve completely in solution producing cyanide anions and free alkali, alkaline earth or heavy metal cations, e.g. K^+ or Hg^{2+} (Rennert, 2002). The released CN^- ions make the solutions of these complexes very toxic. Some of the heavy metal cyanides are almost insoluble (AuCN, $AgCN_2$, $Pt(CN)_2$) while others e.g. of lead, mercury and cadmium have a very good solubility. Therefore they can easily become mobile in soil solutions (Kjeldsen, 1998).

Cyanide complexes can be categorized as weak metal-cyanide complexes and strong metal-cyanide complexes, based on the strength of the bonding between the metal and the cyanide ion (Meeussen, 1992; Dzombak et al., 2006). The focus of this thesis are the iron-cyanide complexes, which belong to the group with strong metal bonding. Iron-cyanide compounds at MGP sites can be present in solid as well as in dissolved phase. The most abundant solid-phase cyanide compounds are Prussian Blue ($Fe_4[Fe(CN)_6]_3$) and Turnbulls Blue ($Fe_3[Fe(CN)_6]_2$), in which Fe^{3+} and Fe^{2+} are contained in different proportions (Meeussen, 1992). Berlin White ($Fe_2[Fe(CN)_6]$) is usually formed under extreme reducing conditions, but is very unstable and is oxidized to Prussian Blue (reaction 1.7) from very small amounts of oxygen (Theis at al., 1994; Proffit et al., 2001; Dimitrova, 2010).

The dissolved-phase complex cyanide species, in the soil and groundwater of MGP sites, can exist in a number of different chemical forms, but the most abundant are the iron-cyanide complexes: ferrocyanide $[Fe(CN)_6]^{4-}$,where iron is in the +II oxidation state, and ferricyanide $[Fe(CN)_6]^{3-}$, with iron in the +III oxidation state (Theis et al., 1994; Ghosh et al., 2004). According to Theis et al. (1994), more than 97 % of the cyanide complexes found at MGP sites are iron complexes. The rest were proved to be copper, nickel and thiocyanate. Iron-complexed cyanides are weakly toxic. The experiments revealed that dosages of up to 2 g ferrocyanide per day for an adult were not harmful, because they were not adsorbed by the human body (Nielsen et al., 1990). However, the toxicity of iron-cyanide complexes depends on their tendency to release toxic free cyanide, which is influenced by the kinetic stability of the complexes and by the presence of light (Kjeldsen, 1998).

Due to the complex chemistry, reactivity and toxicology of the cyanides, the management and regulation concerning cyanide in water and soil can be very challenging. Different cyanide compounds reveal different physical, chemical and toxicological properties, which are highly influencing fate and behavior of cyanide in the environment. Regardless of significant importance of cyanide speciation in conducting effective reclamation projects, until recently, the regulation of cyanide in soil and water was focused on the total (inorganic) cyanide content (Dzombak et al., 2006).

The regulations concerning cyanide concentration in soil and groundwater depend on the country. To present all the different values it would be necessary to create a separate chap-

ter dealing only with the regulations of cyanide in water and soil. Since this thesis focuses on one investigation site in Germany, the thresholds according to the Bundes-Bodenschutz Gesetz (BBodSchG) (1998) and the Bundes-Bodenschutz- und Altlastenverordnung (BBoSchAV) (1999) are presented. Table 1 shows the inspection values for cyanides in soil and groundwater according to the BBodSchG (1998) and BBodSchAV (1999).

Table 1: Thresholds for cyanide concentrations in direct contact (BBodSchG, 1998; BBodSchAV, 1999; Dimitrova, 2010).

Soil			
Children's playground	**Residential areas**	**Park and leisure facilities**	**Industrial areas**
50 mg kg^{-1} DW	50 mg kg^{-1} DW	50 mg kg^{-1} DW	100 mg kg^{-1} DW
Groundwater			
0.05 mg L^{-1} (TCN)		0.01 mg L^{-1}(WADCN)	

1.3 Chemistry of cyanides

Free cyanide refers to either soluble hydrogen cyanide, $HCN_{(aq)}$, or soluble cyanide anion (CN^-). $HCN_{(aq)}$ is a weak acid with a pKa of 9.24 at 25°C. Hydrogen cyanide has a very low boiling point (25.7°C) and thus is volatile in water under environmental conditions. Both liquid and gaseous forms dissolve easily in water, producing weak acid solutions. It can dissociate into cyanide ion according to the following dissociation reaction (Dzombak et al., 2006):

$$HCN_{(aq)} \longleftrightarrow H^+ + CN^- \qquad pKa = 9.24 \text{ at } 25°C \qquad (1.8)$$

At pH values less than 9.24, HCN is the dominant free cyanide species, while at greater pH values cyanide ion dominates free cyanide. In the natural systems the pH value is lower than the HCN dissociation constant, which makes it a dominant form (Meeussen et al., 1992c). The distribution of free cyanide in the aquatic solution and its dependence on the pH value is shown in Figure 2.

The simple cyanides group consist of alkali, alkaline earth or heavy metal cyanide salts of the form $Me(CN)_x$, where Me is the metal or an ammonium ion. Most of the simple cyanides are highly soluble in water and readily dissociate, releasing the cyanide ion (Kjeldsen, 1998; Dzombak et al., 2006):

$$Me(CN)_{x(s)} \longleftrightarrow Me^{x+} + xCN^- \qquad (1.9)$$

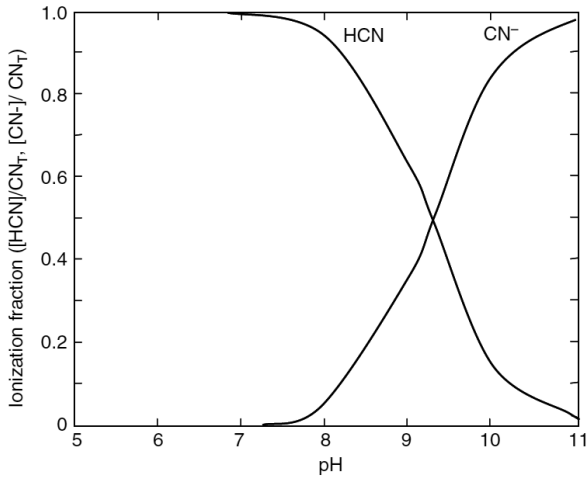

Figure 2: Distribution of free cyanide in the aquatic solution and its dependence on the pH value (Dzombak et al., 2006).

Only some of the heavy metal cyanides are almost insoluble like AuCN, $AgCN_2$ or $Pt(CN)_2$.

The cyanide ion acts as a strong ligand, where the C atom is a donor for many complex compounds (Rennert, 2002). In complex cyanides the cyanide ions are attached as ligands around a central metal ion. The formation of such complexes follows the reaction (Dzombak et al., 2006):

$$Me^{+z}_{(aq)} + nCN^{-}_{(aq)} \longrightarrow [Me(CN)_x]^{+z-x} \tag{1.10}$$

Where Me is a transition metal, z is its charge and x is the number of ligand ions. Most common at the MGP sites (and also the main focus of this thesis) are the iron-cyanide complexes. These octahedral iron-cyanide complexes are nearly inert due to the high stability and low dissociation (ferrocyanide: $pKa=10^{-36.9}$; ferricyanide: $pKa=10^{-43.9}$) (Meeussen et al., 1992c; Ghosh et al., 1999).

For ferrocyanide, each of the CN ligands donates its electron couple to the Fe^{2-} ion, while Fe^0 possesses 26 electrons ([Ar] $3d^8$). In ferrocyanide complex, iron atom has 24 electrons ([Ar] $3d^6$). From complexation with six cyanide ions it receives 12 additional electrons thus reaching the electron configuration of the noble gas krypton (Kr) ([Ar] $3d^{10}4s^24p^6$), which gives a relative high stability of the complex (Hollemann and Wiberg, 2001; Dimitrova, 2010).

For ferricyanide the iron ion (Fe^{3-}) possesses 23 electrons ([Ar] $3d^5$). Together with the

electrons donated from the CN ligands it obtains 35 electrons ([Ar] $3d^9 4s^2 4p^6$) thus, one electron less than the noble gas Kr, which makes the complex more kinetically unstable (Hollemann and Wiberg, 2001; Dimitrova, 2010).

Ferri and ferrocyanide form stable salts either with alkali or earth alkaline metals, or with transition metals without undergoing exchange of the cyanide ligand (Dzombak et al., 2006). The alkali and alkaline earth iron-cyanide complexes are all very soluble in water. The heavy metal and iron salts of iron-cyanide complexes are insoluble or sparingly soluble, but have the ability to dissociate into a heavy metal cation and a metal complex anion in alkaline solutions (pH > 6) (Rennert, 2002). An example of such a slightly soluble (solubility constant Ksp = $10^{-84.5}$) solid is Prussian Blue ($Fe_4[Fe(CN)_6]_3$) (Meeussen et al., 1994):

$$Fe_4[Fe(CN)_6]_{3\,(s)} \longleftrightarrow 4Fe^{3+} + 3Fe(CN)_6^{4-} \tag{1.11}$$

The stability of this complex is supported by the inorganic polymerization of the interacting, neighboring CN groups. Additionally, the charge transfer between Fe^{2+} and Fe^{3+} completely fills the inner *3d* orbital (Hollemann and Wiberg, 2001). Stability of Prussian Blue is very pH dependent:

$$Fe_4[Fe(CN)_6]_{3(s)} + 12H_2O \longleftrightarrow 4Fe(OH)_{3(s)} + 3[Fe(CN)_6]^{4-}_{(aq)} + 12H^+_{(aq)} \tag{1.12}$$

1.4 Behavior and processes of iron-cyanide complexes in soil

Cyanide can be detected in the soils and groundwater of many industrial sites (Kjeldsen, 1998). Cyanide-bearing wastes, at the sites of former Manufactured Gas Plants, are subjected to rain water percolation, which causes leaching of iron-cyanide solids that can yield detectable concentrations of dissolved cyanide in groundwater (Ghosh et al., 1999a; Proffit, 2001; Dzombak et al., 2006). Generally, the behavior of cyanides in soil and groundwater is extremely complex, due to the range of different potential chemical and physical transformations (Meeussen et al., 1994; Meeussen at al., 1995). Figure 3 shows the most significant cyanide compounds and reactions occurring at the gas purifiers waste contaminated sites. In order to design proper risk assessment or a remediation strategy for the cyanide contaminated former MGP sites, the fate and transport of these compounds in soil and groundwater must be investigated and understood.

Most of the cyanide at the gas work sites is originally in a solid form (e.g. Berlin White, Turnbulls Blue), therefore the fate of iron-cyanide complexes in the soil and groundwater can be discussed mainly in terms of dissolution and precipitation reactions (Meeussen et al., 1992; Ghosh et al., 1999c, Rennert, 2002). The dissolution behavior of Prussian Blue is mainly controlled by the joint effects of pH and pE (Meeussen et al., 1994).

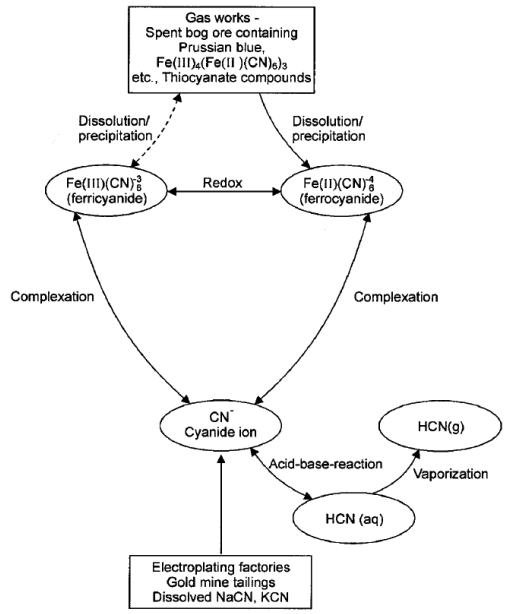

Figure 3: Overview of the cyanide compounds and their reactions at the MGP sites (Kjeldsen, 1998).

Figure 4 shows the different iron-cyanide solids, as a function of pH and pE, in a system with hydrous ferric oxide present. In Figure 4 it can be noticed that solid Prussian Blue can only exist under acidic pH and oxic conditions. As pH increases, Prussian Blue coexists with hydrous ferric oxide in the form of a solid solution (coprecipitant). At high pH, Prussian Blue dissolves (Dzombak et al., 2006). Prussian Blue is the more stable solid form of cyanide under oxidizing conditions e.g. with excess of Fe^{3+} over Fe^{2+} ions. Turnbull's Blue is found to exist under anoxic conditions (excess of Fe^{2+} over Fe^{3+} ions) under a wide range of pHs (Figure 4).

The change from a blue to a green color occurs when Turnbull's Blue forms a solid solution with hydrous ferric under neutral to alkaline pH conditions (Dzombak et al., 2006). According to Meeussen et al. (1992), Prussian Blue is stable at pH < 6, and dissolve with increasing alkaline conditions. Ghosh et al. (1999) stated that Prussian Blue is soluble under alkaline pHs (pH > 7) and oxic (pE > 5) conditions.

Dissolved iron-cyanide complexes predominate in soil and groundwater at the MGP sites. Their speciation is controlled by the redox potential (Figure 5). In moderately oxic to highly oxic conditions, the ferricyanide $[(Fe(CN)_6)^{3-}]$ complex dominates, while the ferrocyanide $[(Fe(CN)_6)^{4-}]$ dominates under anoxic conditions. However, equilibrium model calcula-

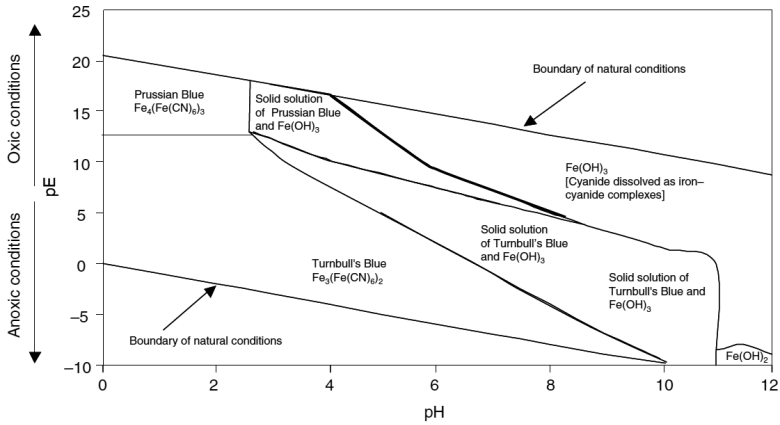

Figure 4: Presence of different iron-cyanide species as a function of pH and pE, in a system with hydrous ferric oxide present (Dzombak et al., 2006).

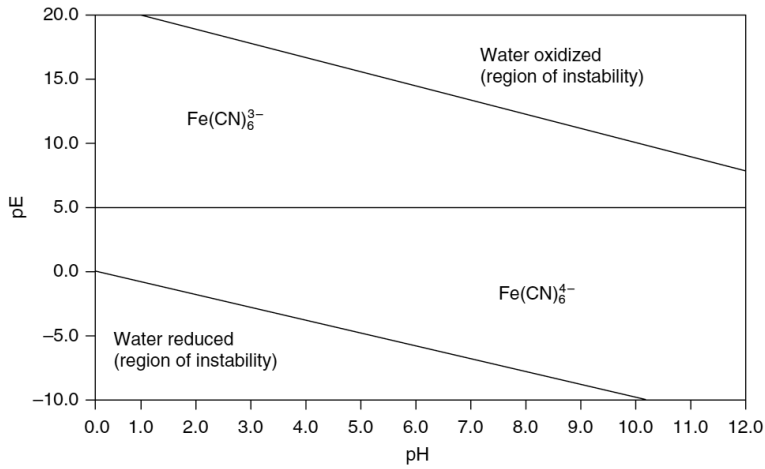

Figure 5: Presence of different dissolved iron-cyanide complexes as a function of pH and pE (Dzombak et al., 2006).

tions indicate that free cyanide should by the dominant species in soil and ground water at the MGP sites (Meeussen et al., 1992a). Adsorption-desorption phenomenon is another reaction that influences the iron-cyanide complexes behavior and mobility in soils of the MGP sites (Meeussen et al., 1995; Rennert and Mansfeldt, 2002; Kang et al., 2012). Gener-

ally, low soil pH (< 5), presence of iron and aluminum oxides, clay material with high anion exchange capacity, increases adsorption of negatively charged iron-cyanide complexes (Dzombak et al., 2006). These processes and the conducted studies will be discussed in the following chapters.

Iron-cyanide complexes when exposed to the UV or visible light radiation (up to 480 nm) can undergo the following reaction (Dzombak et al., 2006):

$$[Fe(CN)_6]^{3-}_{(aq)} + 6H_2O \longrightarrow [Fe(H_2O)_6]^{3+}_{(aq)} + 6CN_{(aq)} \quad (1.13)$$

According to reaction 1.13, the presence of light can produce toxic cyanide ion, but in the soil or groundwater where the light penetration is very limited, this process would continue for years (Meeussen et al., 1992). Nevertheless, theoretically, free cyanide can diffuse through the soil surface and escape in the atmosphere in form of $HCN_{(g)}$, however concentration of free cyanide at the MGP sites are low and often below the detection limit (Mansfeldt et al., 1998). Iron-cyanide complexes have relatively long persistence in soil and groundwater and their speciation at the MGP sites is rather influenced by the breakdown kinetics than by a thermodynamical equilibrium (Ghosh et al., 1999c; Dzombak et al., 2006).
Some plant species are efficient in degrading cyanide and can be employed in the recultivation of the MGP site in form of the phytoremediation strategy. According to the study made by Larsen et al. (2005), willow trees are capable of the uptake and metabolism of iron-cyanide complexes from solutions with different CN concentrations. Free cyanide can be also metabolized by microorganism and used as a nitrogen and carbon source (Knowles, 1976). However, the degradation of the iron-cyanide complexes proceeds much slower (Dzombak et al., 2006; Ebel, 2007).

1.5 Analytical determination of cyanide

Several different methods are available for determining cyanide. Some of the analysis methods provide for measurement of a group of species (Mansfeldt and Biernath, 2001; Dimitrova, 2010) are:

- total cyanide (TCN) in water including strong cyanide complexes dissolved in water as well as the WADCN fraction
- weak acid dissociable cyanide (WADCN) including weak cyanide compounds and free cyanide
- total cyanide (TCN) in sodium hydroxide extracts which includes the strong complexes (e.g. ferric ferrocyanide) which does not dissolve in water but under strong alkaline conditions

Analysis of cyanide in solids usually involves two processes: digestion and detection. Digestion procedure is performed to separate the analyte from disturbing matrixes and to liberate $HCN_{(g)}$ under controlled pH conditions (Mansfeldt and Biernath, 2001). In this study the micro dist (Figure 6) system was used (Dimitrova, 2010). The micro dist system refers to the method of the Hach Company, US QuickChem Method 10-204-00-1-X approved by the USEPA (2008). The amount of the HCN liberated during the digestion is dependent on the pH applied during the distillation procedure. This enables to distinguish among the three cyanide species.

The micro dist system is designed to digest water samples. Cyanide from soil, plant material needs to be extracted prior to distillation step. Different approaches available for cyanide extraction from solid samples will be discussed in the following chapters.

Free cyanide trapped during the digestion process can be measured titrimetrically or colorimetricaly. For the purposes of this thesis, an automated spectrophotometrical flow injection system (FIA) Compact (MLE, Dresden) was used. Injection Analyzer applied for cyanide detection refers to the DIN EN ISO 14 403 D (2002) standard for determination of total and free cyanide with continuous flow analysis.

The available analytical methods aimed at measuring individual species of cyanide are free cyanide by gas chromatography, gas-liquid diffusion (including microdiffusion), ion - selective electrode, direct colorimetric analysis and ion chromatography (Dzombak et al., 2006). Fourier transform infrared spectroscopy (FTIR) in the mid-infrared (MIR) range has been frequently applied to characterize Fe-CN complexes in soils (Proffit et al., 2001; Jannusch et al., 2002; Rennert et al., 2007).

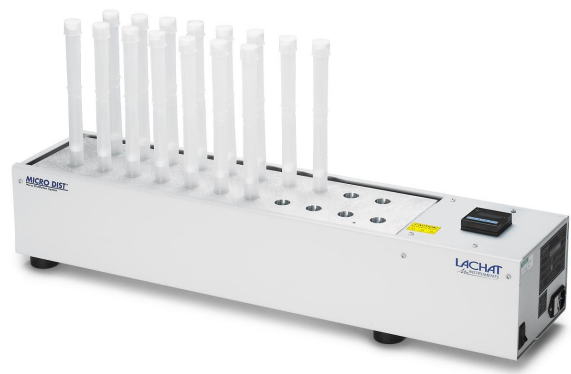

Figure 6: Micro dist Rapid Distillation Unit (ATS Scientific INC).

2 Scope of the thesis

2.1 Project summary

This thesis is partially founded by the Deutsche Bahn AG and is developed within the project "Stabilisierung des DB AG-Standortes ehem. Leuchtgasanstalt Cottbus durch Verfahren der Bioremediation (Phytoremediation)" ("Stabilization of the DB AG locations of a former Manufactured Gas Plant in Cottbus using the Bioremediation (Phytoremediation)"). The main aim of the project is to stabilize the contamination, in the form of cyanide, at the MGP Cottbus site using different plants (willow, poplar, locust, sunflower, mustard etc.) The effectiveness of the remediation strategy applied during the project was verified by a number of field, laboratory and greenhouse experiments, which started in year 2010 and are still in progress. According to Maruyama et al. (2001), cyanide in plants is rapidly metabolized by the enzyme b-cyanoalanine synthase (CAS). Phytoremediation of cyanide has been widely studied by many scientists for a number of plants (Ebbs et al., 2003; Larsen et al., 2004 and 2006; Trapp et al., 2001), where the biological transport and metabolisms processes were demonstrated and investigated. The literature overview supports the hypothesis that phytoremediation is an effective approach to stabilize the cyanide contamination at the MGP sites and to reduce the negative impact of the contamination on the groundwater.

The remediation activities started in year 2010 with removal of old MGP buildings from the site (Picture 2). On the basis of the cyanide contamination spatial distribution, gathered during the site screening, 2 m of the highly contaminated top soil (Picture 3) was removed and replaced with clean sandy material. In the beginning of the year 2011, the planting scheme was developed and performed in the middle of April 2011. The site was planted with poplar, willow and black locust trees according to the arrangement presented in Figure 7. The vegetation development on the MGP site in Cottbus is presented in Picture 1.

Additionally, in the year 2012, the free space in the eastern part and the embankment in the southern part of the site, were planted with sunflower and mustard according to the schedule presented in Figure 7. Annual harvesting of the plants and collection of the trees leafs and tissues revealed cyanide accumulation in the measured plant samples.

Picture 1: Development of the vegetation in year 2011 at the MGP investigation site in Cottbus (Repmann et al., 2012).

2.2 Site description

The investigation site is located in the central south-western part of Cottbus (51°45,161'N; 14°18,529'E), in the south of Brandenburg State, in Germany. The available historical information about the former Manufactured Gas Plant is very limited. Accessible data comment that the MGP in Cottbus started operation in 1861 and produced gas mainly for the owner's purposes, not for the public supply. The site is owned by the German Railways (Deutsch Bahn AG). The production of the manufactured gas was stopped in the middle of 20th century, which caused the cessation of the MGP in Cottbus. Until 2010, the old buildings belonging to the former MGP had still existed (Picture 2). Prior to the remediation activities on the site, the old constructions were removed and 2 m of the highly contaminated top soil was replaced (Picture 3).

The site covers an area of approximately 2500 m^2 and is abundantly covered with the vegetation. The groundwater table is at a depth of 7 m and the water flows in the north-west direction. According to the Köppen classification system, Cottbus has a humid continental climate (Peel et al., 2007) with a mean annual temperature of 8.8°C and an average annual precipitation sum of 589 mm (Linder et al., 1997).

Top soil is composed of sand containing coal, slag, gas purification wastes and organic matter (up to 0.5 m deep). The deeper soil (0.5 - 7.0 m) has a sandy texture (texture classes according to German classification system). At the depth of approximately 1 m a layer of coherent structured soil occurs, which unevenly covers the whole investigation field (up to 2 m deep). The soil pH varies between 3.2 and 7.7 (Sut et al., 2012). Spatial distribution of the cyanide concentration was provided by the site screening, where the investigation field was divided in 6 separate surface transects (A, B, C, E, G, I) (Figure 8). Soil was collected

Picture 2: Former Manufactured Gas Plant site in Cottbus: picture taken prior to remediation activities (photo made by Dr. Repmann).

Picture 3: Remediation operations: removal of the contaminated top soil (photo made by Dr. Repmann).

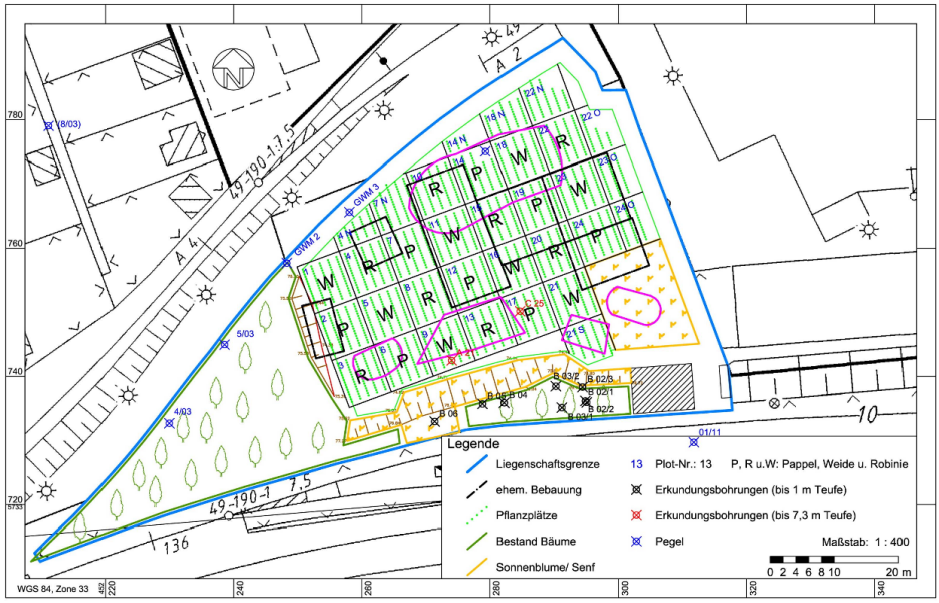

Figure 7: Planting scheme applied at the MGP Cottbus (Repmann et al., 2012).

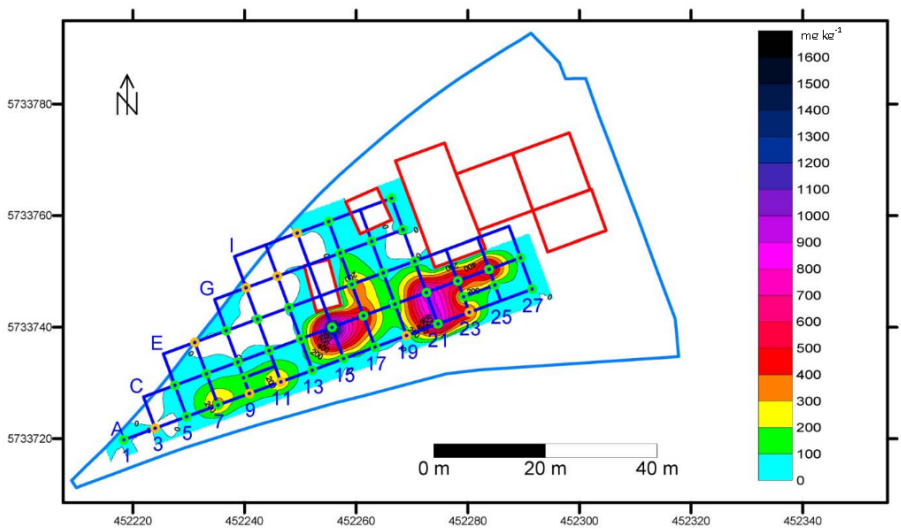

Figure 8: Distribution of the cyanide contamination at the MGP Cottbus (Dimitrova, 2010).

within a sampling grid of 6 x 6 m spacing at a depth of 0.5 m. The highest cyanide contents where measured along the C profile in the central part of the site (up to 1600 mg kg^{-1}). During the successive project activities, the highest detected cyanide concentration (at the depth different then 0.5 m) was about 18000 mg kg^{-1}.

2.3 Outline of the thesis, aims and objectives

Contamination in the form of iron-cyanide complexes is a common problem at thousands of the former Manufactured Gas Plant sites that are spread worldwide (Mansfeldt et al., 1998; Proffit, 2001). Due to the high number of those facilities, toxicity of the by-products or risk of soil and groundwater contamination, negative environmental impact becomes obvious (Pfaff-Schley, 1996). The main aim of this thesis was to investigate the detection and behavior of iron-cyanide complexes in the soil at the MGP Cottbus. This was done to enable developing in-situ method for cyanide site screening, advancing the knowledge concerning the stability of Prussian Blue in order to improve the efficiency of phytoremediation processes and to understand the fate of iron-cyanide complexes in soil to better evaluate (qualitatively and quantitatively) possible environmental hazards. As indicated in the section above (Chapter 1), many issues, concerning the nature of iron-cyanide complexes, have been previously studied. However, in the course of thesis development, some aspects of the cyanide behavior turned out to be contrasting with results reported in the literature. Prussian Blue is documented in the literature as a relatively stable compound, but prior to evaluating its behavior, one should not forget that it is a complex substance that is stored in a very heterogeneous environment (soil mixed with gas purification wastes). Thus, more research with the field material, instead of synthetic iron-cyanide solutions, is required to advance the knowledge concerning the potential environmental hazard in the vicinities of former MGP sites.

Firstly, the feasibility of Field Portable Near Infrared Spectroscopy (FP NIR) to determine the cyanide concentration in soil was investigated. Diffuse reflectance spectroscopy in the region (NIR DRS) has become a very popular and widely used technique for many industries due to its rapid and non-destructive analysis of bulk material (Shenk et al., 1992; Malay and Williams, 1997; Siebielec et al., 2004; Viscarra Rossel et al., 2006; Stenberg et al., 2010; Sut et al., 2012) that saves time and resources and allows immediate assessment of site contamination. Available methods for cyanide determination are usually time consuming and fixed in laboratory settings. This part of the thesis presents a novel use of the FP NIR to determine cyanide concentrations in soil. The objective of this study was to evaluate NIR spectrometer responses with respect to the field situation and to elucidate the limits of detection after performing different sample preparation methods (Siebielec et al., 2004; Viscarra Rossel et al., 2006; Sut et al., 2012).

Secondly, the stability of Prussian Blue in a soil collected at the MGP Cottbus was investigated in a column and batch experiments, since, according to the literature, the mobility of iron-cyanide complexes depends mainly on the dissolution of the ferric ferrocyanide (Ghosh et al., 1999a; Meeussen et al., 1992; Meeussen et al., 1995). Lack of a standard leaching method to determine the water soluble (plant available) cyanide fraction generates potential limitations for implementing remediation strategies like phytoremediation (Sut et al., 2013). The objectives of this study were to: (i) investigate the solubility of iron-cyanide complexes from the MGP soil containing Prussian Blue, under circum-neutral pH, oxic, unsaturated water conditions in a column leaching experiment, in order to assess the potential of cyanide leaching from the soils with varying pH and total cyanide concentration; (ii) study the stability of iron-cyanide complexes in the MGP soils, under circum-neutral pH, oxic, saturated water conditions in a sequential batch extraction; (iii) evaluate the comparability of the column and the batch experiments in terms of qualitative and quantitative determination of cyanide contamination; (iv) study the applicability of neutral solution extraction (distilled water) to determine the water soluble cyanide fraction and to advance the understanding of cyanide behavior in MGP site soils (Sut et al., 2013).

Subsequently, the results obtained in the column leaching experiment have been used to model the long-term release of iron-cyanide complexes from the soil of the MGP site in Cottbus. Generally, column experiments simulate the discharge of contaminants in soils and aquifers more closely than batch experiment (Rennert, 2002), therefore to investigate the mechanism and to model the release rate of iron-cyanide complexes from the MGP soils the leaching under unsaturated flow conditions approach was chosen. In order to design effective remediation strategies, it is relevant to understand contaminant fate and transport in soil, and to quantify and mathematically model the release rate (Sut et al., 2013). The objective of this study was to apply different isotherm and kinetic equations to the column experimental data in order to investigate the driving mechanisms for the ferric ferrocyanide release, and to study the influence of soils parameters such as pH, texture, OM content, initial CN concentrations.

Previous research, conducted for the purposes of this thesis, revealed instability of Prussian Blue in the soil of a former MGP in Cottbus, implying a likely threat of groundwater contamination. Slightly elevated cyanide concentrations, measured in the groundwater at the MGP site in Cottbus, are relatively low considering the high release rates and constant dissolution of the ferric ferrocyanide obtained in the column leaching experiment. To investigate the behavior and potential retention mechanisms of the iron-cyanide complexes in the soil of a MGP in Cottbus, samples from two long boreholes (up to 7 m long) were analyzed in the laboratory. Ultimately, the influence of the sandy loam soil material (collected at the MGP Cottbus) and synthetic iron sulfide on the retention of the iron-cyanide complexes

transport was investigated in the batch and column experiments, due to i) vertical distribution of cyanide concentration in the investigated soil profiles, indicating the highest total cyanide concentration in the layer of gas purification wastes and sandy loam underneath it; ii) high contents of iron and sulfur in the wastes material, implying iron sulfide as potential source of iron excess required to form solid iron-cyanide complex.

2.4 Organization of the thesis

This thesis begins with the literature review presented in Chapter 1. In this chapter general information and basic facts concerning cyanide's origin, toxicity, chemistry, behavior and analytics are discussed. In Chapter 2, information concerning the project, site description, thesis outline and organization are supplied.

The following chapters (Chapter 3 through 6) are organized as self-contained papers. They present the articles that were published (chapter 3 through 5) or submitted (chapter 6) to peer reviewed journals. Each chapter is composed from a separate abstract, introduction, results, discussion and conclusions, except of chapter 4, where the results and discussion part is written together. In Chapter 7, additional discussion regarding supplementary data obtained for the studies, presented in Chapters 3-5, is given. In Chapter 8, the main results of the research reported in this thesis are presented and recommendations for the future research are elaborated.

3 Feasibility of field portable near infrared (NIR) spectroscopy to determine cyanide concentrations in soil

The study presented in this chapter was published as: M. Sut, T. Fischer, F. Repmann, T. Raab and T. Dimitrova, "Feasibility of Field Portable Near Infrared (NIR) Spectroscopy to Determine Cyanide Concentrations in Soil," Water, Air & Soil Pollution, Vol. 223, No. 8, 2012, pp. 5495-5504. doi:10.1007/s11270-012-1298-y.

3.1 Abstract

Vicinities of Manufactured Gas Plants were often contaminated with solid iron-cyanide complexes as a result of the coal gasification process. During the remediation of affected soils, knowledge about contaminant concentrations is crucial, but laboratory methods are often expensive and time consuming. Rapid and non-destructive field methods for contaminant determination permit an analysis of large sample numbers and hence, facilitate identification of 'hot spots' of contamination. Diffuse near infrared reflectance spectroscopy has proven to be a reliable analytical tool in soil investigation. In order to determine the feasibility of a Polychromix Handheld Field Portable Near-Infrared Analyzer (FP NIR), various sample preparation methods were examined, including homogenizing, sieving, drying and grinding. Partial least squares (PLS) calibration models were developed to determine near infrared (NIR) spectral responses to the cyanide concentration in the soil samples. As a control, the contaminant concentration was determined using conventional Flow Injection Analysis (FIA). The experiments revealed that portable near-infrared spectrometers could be a reliable device for detecting cyanide concentrations >2400 mg kg^{-1} in the field and >1750 mg kg^{-1} after sample preparation in the laboratory. We found that portable NIR spectrometry cannot replace traditional laboratory analyses due to high limits of detection, but that it could be used for identification of contamination 'hot spots'.

3.2 Introduction

Cyanide compounds usually colligate as extremely poisonous substances, but their toxicity highly depends on the form and stability of the compound (Kjeldsen, 1998). Their occurrence in water and soil is mostly caused by manmade activities, like the process of gas purification after coal gasification. Hence, cyanides are most commonly found as solid iron cyanide complexes (Prussian Blue) in the vicinities of the Manufactured Gas Plants (MGPs). In the past, when plants were still in active operation, the manufactured gas was conducted through wood shavings mixed with an active form of hydrated iron oxide in order to remove H_2S (g), which additionally eliminated hydrogen cyanide (HCN). When the iron oxide lost its capacity, the material was deposited and used mainly as a filling material, which contained double-iron-cyanide compounds formed due to the reacting of free cyanide with iron (Dzombak et al., 2006). These activities led to high concentrations of a variety of different cyanide complexes in the uppermost soil layers at these sites.

The toxicity of cyanide containing compounds strongly depends on the chemical form in which it is present (Meeussen et al., 1992; Meeussen et al., 1994). Daylight induced decomposition of iron-cyanide (Fe-CN) complexes can lead to release of poisonous hydrogen cyanide (HCN) (Kjeldsen, 1998). Ferric ferrocyanide (Prussian Blue) forms stable precipitates under acidic to neutral pH and excess metal (Fe) conditions (Dzombak et al., 2006).

Diffuse reflectance spectroscopy in the near infrared region (NIR DRS) has become a very popular and widely used technique for many industries due to its rapid and non-destructive analysis of bulk material. Near infrared spectroscopy is used to investigate the vibrational properties of a sample (Bokobza, 2002). In soil analysis, spectral features of the near infrared (NIR) region (780-2500 nm) are associated with molecular overtones and combination vibrations of light atoms that have strong molecular bonds, for example, chemical bonds that contain H attached to atoms such as N, O, or C (Confalonieri et al., 2001). The absorbance of NIR bands is mostly determined by the composition of the soil surface, so chemical properties that depend on the soil matrix (like carbon content) can be predicted better than those that rely on soil solution (Janik et al., 1998).

Chang et at. (2001) noticed that NIR spectroscopy can be used to estimate several soil properties, such as total C, total N, moisture content, particle size, cation exchange capacity (CEC), extractable Ca, K, and Mn, respiration rate, and potentially mineralizable N. Near infrared diffuse reflection spectroscopy showed that this method is feasible for assessing soil N and organic matter content (McCarty and Reeves, 2001; Slaughter et al., 2001; He et al., 2005; Viscarra Rossel et al., 2006). Cozzolino and Moro´n (2006) have stated that NIR spectroscopy has great potential to predict soil organic C with respect to different particle-size fractions with the best calibrations obtained for clay and silt. The study suggested that

increased accuracy from NIR spectroscopy predictions of matrix properties might have an origin in decreased variability in particle size and in the fact that small particles absorb much less energy than large particles.

Malley and Williams (1997) and Siebielec et al. (2004) examined the NIR DRS prediction of soil heavy metals concentration. Malley and Williams (1997) stated that the correlation between heavy metals and the NIR detectable absorbencies of organic matter - containing protein, cellulose and oil - is the major mechanism by which the trace metals can be predicted. Siebielec et al. (2004) found a clear relationship between soil texture and accuracy in metal prediction, with the exception of Fe, which was predicted well over the entire range of clay content. Sandy soils are low in metals, which produce less accurate predictions. A good correlation of inorganic components can be explained by the relation of the inorganic material to the organic constituents (Shenk et al., 1992).

At the present time, several methods for determining cyanide concentration in soil are available. Cyanide quantification usually requires a two step process: digestion of the sample (e.g. micro distillation system) and its analytical detection performed e.g. by automated spectrophotometrical flow injection analysis (FIA) (Dimitrova, 2010). Fourier Transform Infrared Spectroscopy (FTIR) in the mid-infrared (MIR) range has been frequently applied to characterize Fe-CN complexes in soils, due to its strong C≡N stretching vibration in the range of 2200-2000 cm^{-1} (Proffit et al., 2001; Jannusch et al., 2002; Rennert et al., 2007).

Nowadays, soil remediation is of prominent importance (Dzombak et al., 2006) and the knowledge about potential contaminants - like Fe-CN compounds - is crucial in order to determine likely environmental hazards. Laboratory methods are usually time consuming, so there is a need to develop rapid and non-destructive methods, which are capable of determining the contaminant concentration in the field. The study conducted by Hürkamp et al. (2009) showed that field portable X-ray fluorescence (FP XRF) is able to characterize the distribution of lead concentrations in alluvial soils on a large scale. Field portable analyzers save time and resources, and allow immediate assessment of site contamination. In order to evaluate the feasibility of the Polychromix Handheld Near-Infrared Analyzer in determining the cyanide concentration in soil, a set of soil samples from a former MGP in Cottbus was chosen. The objective of this study was to evaluate NIR spectrometer responses with respect to the field situation and to elucidate the limits of detection after performing different sample preparation methods.

3.3 Materials and Methods

Sampling strategy and experimental design

The description of the investigation site is presented in Chapter 2 (2.2). The samples (n=100) were collected using a hand driller. They were taken up to 190 cm in depth. The fresh field samples were homogenized for further analysis. As a reference, for the FP NIR spectrometer response, the total cyanide concentration (TCN) was determined with the automated spectrophotometrical flow injection system FIA Compact (MLE, Dresden). To extract cyanide, 20 g of soil (n=100) were weighted and extracted in 200 mL 1 M sodium hydroxide (1:10 ratio) for 12 h in an end-over-end shaker at 16 rpm. In order to force settling of soil particles, the extracts were centrifuged for 10 min at 3000 rpm. According to micro distillation procedure, 5 mL of extract were digested in an acidic environment using a micro distillation system (Dimitrova, 2010). After distillation cyanide was determined with the flow injection analyzer (FIA Compact, MLE) (Dimitrova, 2010).

In order to determine the concentration of water soluble cyanide complexes, 20 g of each sample was extracted in 50 mL of distilled water (2:5 ratio) for 1 h with an end-over-end shaker at 16 rpm. Afterwards, the water extracts were introduced in a centrifuge at 3000 rpm for 20 min, 20-30 mL were filtered through 0.45 µm syringe filters, which were conserved with 200 - 300 µL of 1 M NaOH in order to preclude the loss of cyanide. Consequent procedures were consistent with microdistillation procedure (Dimitrova, 2010) and with the sodium hydroxide extracts. The detection limit for both extractions is 0.02 mg L^{-1} of cyanide in analyte.

Organic matter (OM) was determined with the Loss on Ignition method (LOI). Approximately 10 g of each sample were sieved (< 2 mm), placed in a porcelain beaker and heated up overnight at 105°C. This procedure was repeated until the change of mass was lower than 0.1 %. After recording the weight, samples were heated up at 450°C for 12 h. The organic matter was calculated as the percentage of the dry weight of a sample. Allen and Bonnette (1974) stated that ferric ferrocyanide decomposes at 450°C to ferric oxide. The obtained OM values were recalculated according to the loss of CN after LOI.

Additionally, spectra of few soil samples as well as commercial cyanide compound Prussian Blue (Fe_4 $[Fe(CN)_6]_3$) (SIGMA-ALDRICH), were recorded using FTIR spectroscopy (Impact 410 Nicolet, resolution 4 cm^{-1}, 8 scans per sample)

Iron and calcium concentrations were determined with a Portable X Ray Fluorescence (XRF NITON XL3t) in a laboratory setting. The samples were air dried, sieved (< 2 mm) and ground to fine powder using a vibrating tube mil (15 min each sample). Approximately 5 to 10 g of material was introduced in plastic sample caps (Spex Industries Inc.), covered with

thin film for XRF (Mylar). The measurements were performed using the built in procedure for soil analysis.

For NIR spectroscopy, the samples (n=100) were air dried, sieved (< 2 mm) and introduced into a glass flask (5 g per sample so that the height of each sample equaled 2 cm). For each sample, the diffuse reflectance spectra were recorded with a Polychromix Handheld Near-Infrared Analyzer (resolution 11 nm) in the range from 1600 to 2400 nm. Scans were averaged (5 scans per sample) using Microsoft Excel to obtain one representative scan for each sample. The reflectance (R) was converted to apparent absorbance spectra log(1/*R*) units. Prior to the calibration step, spectra were preprocessed by using a smoothing algorithm and the first derivative (Savitzky and Golay, 1964).

Multivariate data analysis and model development were performed with the R software suite. The sample set (n=100) was randomly divided into calibration (n=80) and validation sets (n=20). A multivariate calibration model was developed, on the calibration data set, using the Partial Least Squares (PLS) method (Geladi and Kowalski, 1986; Martens and Næs, 1989) is a common modeling technique that selects successive orthogonal factors that maximize the covariance between predictor (spectra) and response variables (laboratory data) (Viscarra Rossel et al., 2006). In order to determine the number of factors of the respective models, leave-one-out cross validation (LOO-CV) was used (Efron and Tibshirani, 1993). The PLS components were estimated by the root mean square error of prediction (RMSEP) as functions of the number of components. Primarily, the model response was validated for each parameter and each sample pretreatment. The validation included predicting the soil property of the sample removed by estimating each m-factor PLS model using n-1 soil sample.

The predictive ability of a calibration model in estimating the cyanide concentrations was validated using a validation data set (n=20). The prediction errors were evaluated by robustly estimating the regression parameters of the linear model and by abbreviating the largest prediction errors. The predictive performance of the developed model was assessed by the adjusted correlation coefficient (R^2), RMSEP and the probability value (p), using the analysis of variance (ANOVA).

An analogous scanning and validation procedure was employed in order to examine the model response to sample grinding. The previously sieved and dried sample set (n=100), was additionally ground, using an agate mortar, in order to evaluate FP NIR response to different sample preparation procedures.

In order to calculate the limits of detection (LOD) for different sample pretreatments, the PLS CV was performed of the complete data set (n=100). This validation approach was applied due to nonuniform spreading of cyanide concentrations values in the data set (n=100).

Soil sample represented a range of cyanide concentration up to 17860 mg kg^{-1}, where only 15 samples (out of 100) indicated very high values (>1000 mg kg^{-1}). The number of PLS components was determined empirically by the minimum error. The standard deviation of the spectroscopically measured vs. NIR predicted concentrations regression function was assumed to be the background noise. The limit of detection was calculated according to equation 3.1.

$$LOD = t_{p,df}\sqrt{\frac{SSQ_{resid}}{df}} \tag{3.1}$$

LOD is the limit of detection, $t_{p,df}$ is the limit of integration of the Students distribution, p is the probability (0.95, two-sided), and residual sum of squares (SSQ_{resid}) and df is the sum of squares and the degrees of freedom of the residuals of the spectroscopically measured vs. NIR predicted concentrations regression function, respectively. LOD was calculated both: for the non-ground and for ground samples.

3.4 Results

Cyanide detection with FIA revealed that water soluble cyanide is a small fraction (1-10 %) depending on the borehole. The concentration of water soluble cyanide spans from below LOD to 39 mg kg^{-1}, where the alkaline soluble fraction ranged from below LOD to 17860 mg kg^{-1}. The low cyanide concentration in the water soluble fraction supports the assumption that the investigated soil is contaminated with ferric ferrocyanide (Mansfeldt and Biernath, 2001; Dimitrova, 2010).

Figure 9 shows a comparison of spectra measured by a) FP NIR spectrometer and b) FTIR spectrometer. The NIR spectrum of the commercial compound Prussian Blue (SIGMA-ALDRICH) shows the absorption band at 4215 cm^{-1}, which is assumed to be caused by a single C≡N stretching vibration. The same peak (4215 cm^{-1}) is visible in soil from MGP where the total CN concentration (NaOH extractable) was equal to 1780 mg kg^{-1}. Comparing the NIR and FTIR spectra of the same soil sample, it is noticeable that the mid-infrared region contains more information about the soil constituents. Absorption bands in the 1100-850 cm^{-1} region appear due to the Si-O asymmetric stretching mode (Haberhauer et al., 1998; Ellerbrock et al., 2005; Fischer et al., 2010) and those of Si-O bending vibrations are between 600 and 150 cm^{-1} (Farmer, 1974). The broad absorption band at 3400 cm^{-1} is caused by the vibration of OH (Haberhauer et al., 1998; Chapman et al., 2001; Fischer et al., 2010). The 950-600 cm^{-1} region corresponds to water librations and vibrations of H-bond bridges; bending vibration of H_2O occurs at ca. 1628 cm^{-1} (Durig, 2002; George and Lewis, 2002; Nakamoto, 2002). The absorbance peak situated between 1490 and 1340 cm^{-1} might be as-

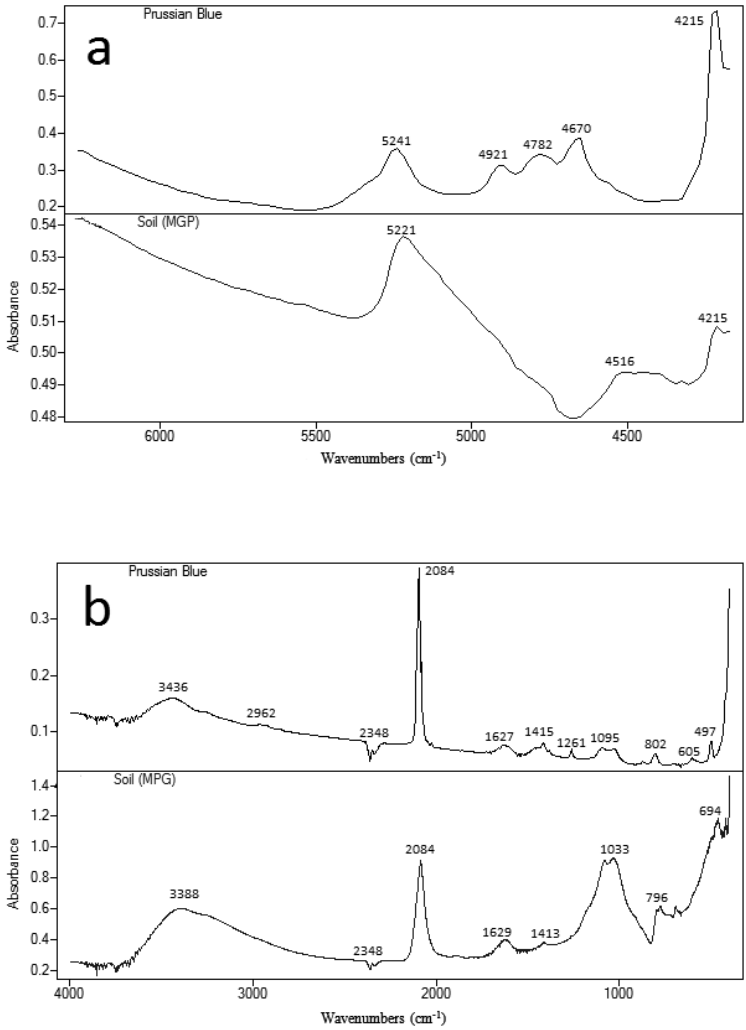

Figure 9: Examples of a) near infrared and b) fourier transform infrared smoothed spectra of soil containing Fe-CN compound (MGP) and commercial compound $Fe_4[Fe(CN)_6]_3$ (Prussian Blue).

sociated with bending vibration of aliphatic, OH deformations, symmetric COO-stretch as well as stretching of phenolic OH (Haberhauer et al., 1998; Madari et al., 2006). Wavenumbers ranging from 2200 to 2000 cm^{-1} are relevant regarding the C≡N stretching vibration. Both FTIR scans from soil (MPG) and commercial compound (Prussian Bule) indicate the absorbance peak at 2084 cm^{-1}, which according to the literature demonstrate the presence of $Fe_4[Fe(CN)_6]_3$ (Proffit et al., 2001; Jannusch et al., 2002). The PLS method was used to develop a model for the non-ground set of samples (n=100). Minimal noise was achieved

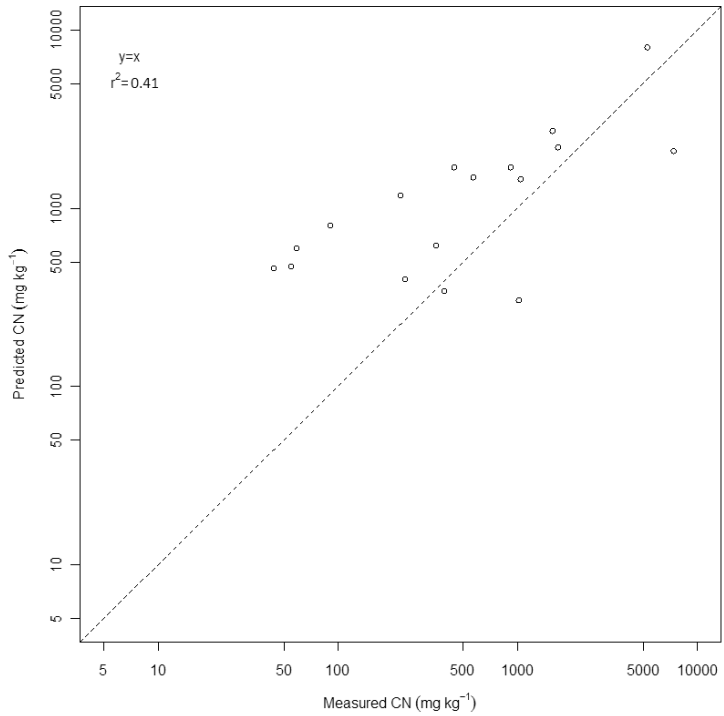

Figure 10: Cyanide measured to predicted concentrations (mg kg^{-1}); score plot obtained after PLS/CV on smoothed and first derivative spectra of non-ground set of samples.

when 4 components were used, which explained 90 % of data variation. This number of components allowed us to model as much of the complexity of the system as possible without overfitting the concentration data (Haaland and Thomas, 1988). Figure 10 represents the correlation of measured versus predicted values of cyanide concentration using validation data set (n=20). The model gave a RMSEP of 1503 and R^2 of 0.41 ($p < 0.01$). In Figure 10, a large scatter of the points can be observed, both in low and high concentrations.

The results presented in Figure 11 are the best obtained from the ground set of samples. The PLS scores plot represents the relation of measured versus predicted cyanide concentrations using 4 components. The same sample preparation (plus grinding) and validation process were applied. Several different models were tested, ranging in spectra preprocessing and number of components selection, before the most appropriate was chosen. Final result gave a RMSEP of 838 and a R2 of 0.86 ($p < 0.0001$). Figure 11 shows a large scatter of the points in the concentration lower than 1000 mg kg^{-1}, where the relation above this value is linear.

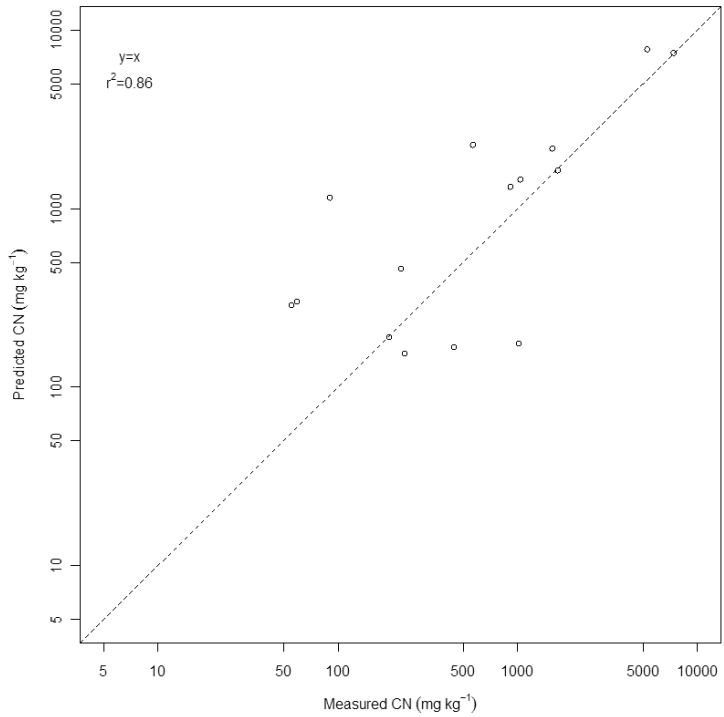

Figure 11: Cyanide measured to predicted concentrations (mg kg^{-1}); score plot obtained after PLS/CV on smoothed and first derivative of ground set of samples.

Figure 12 represents the model regression coefficient response in the NIR region. The right side of the spectrum points high values (≈ 4215 cm^{-1}), indicating the response of the cyanide signal in the NIR spectrum. Positive peaks are due to the component of interest, while negative peaks correspond to interfering components (Haaland and Thomas, 1988), possibly -OH, N-H and C-H from soil organic matter (Fidencio et al., 2002; Cozzolino and Moron, 2003, Zornoza et al., 2008). Thus the correlation coefficients can be considered as indicators of the correlation between the infrared frequencies and the soil constituents of interest. Calculations for FP NIR according to equation 3.1 revealed that the limit of detection for non-ground samples was equal to 2400 mg kg^{-1} and for the ground samples 1750 mg kg^{-1}.

Table 2 represents the correlation coefficients for different soil constituents (calcium, iron, cyanide, organic matter) indicating a relation of iron to cyanide and organic matter. Results also pointed a correlation of calcium to OM.

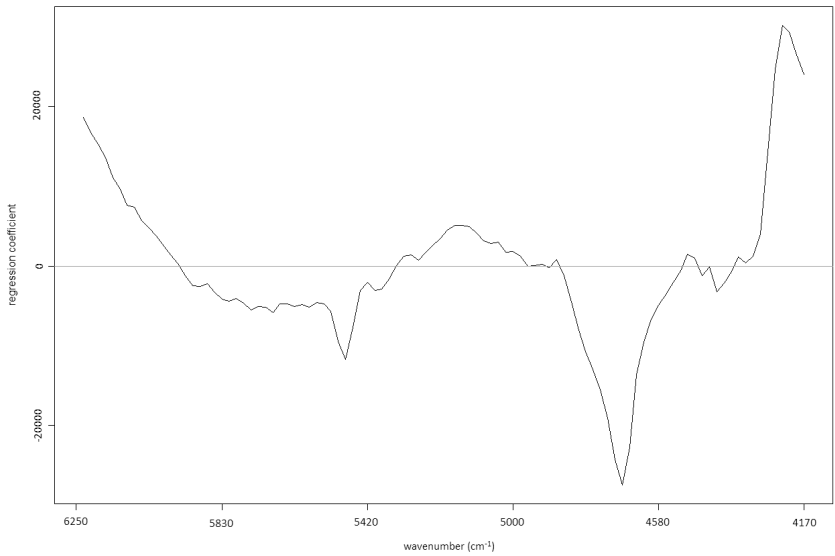

Figure 12: Regression coefficients for the cyanide model in the NIR region.

Table 2: Correlation coefficients for different soil constituents including calcium, iron, cyanide, and organic matter.

Correlation coefficients			
Ca	-0.03	0.18	0.63
	CN	0.88	0.48
		Fe	0.6
			OM

3.5 Discussion

The purpose of this paper is to evaluate the feasibility of FP NIR spectrometry in determining the cyanide concentrations in soil. Near infrared spectra typically consist of broad, weak, non-specific, extensively overlapped bands (Blanco et al., 1999). The intensity of these bands depends on the change in dipole moment and change of anharmonicity of the bond. Therefore, hydrogen, as a light atom, reveals the largest vibration and the greatest deviation from the harmonic behavior. The NIR region corresponds to bonds containing light atoms with single bonding, whereas the bands for bonds such as C=O, C≡N are much weaker or absent (Blanco and Villarroya, 2002).

The MIR region in FTIR spectroscopy has been successfully applied to specify iron-cyanide complexes in soil (Proffit et al., 2001; Jannusch et al., 2002; Rennert et al., 2007). It was also observed that scans provided by FTIR contained more information about soil constituents than FP NIR (Figure 9). In the near-infrared region, spectra obtained from samples with high cyanide concentration (>1000 mg kg^{-1}), revealed an absorption band at 4215 cm^{-1} (Figure 9a), which we assume to be an overtone of the C≡N stretching vibration. Cyanide NIR absorption bands were not reported in the literature, so this assumption is pioneer. This supposition can be proven by Figure 12. Moreover, in the MIR range, the first overtone of the CN stretching vibration is at 2084 cm^{-1} (Figure 9b), which, according to the unharmonicity of the CN vibration group, should appear in NIR range at wavenumbers lower than 2084 x 2 = 4168 cm^{-1}. Hence, the peak at 4215 cm^{-1}, obtained in NIR region, is most probably induced by the combination band of the [2γ(CN) + (some low energy vibration)] type.

From the NIR spectra, it could be noticed that scans of the samples with cyanide concentrations <1000 mg kg^{-1}, showed no absorption at 4215 cm^{-1}. A chemometrical approach was used for cyanide calibration. Although the samples were dried, water caused an intense absorption band at 5241 cm^{-1}. However, this broad OH-band did not interfere with the CN-band at 4215 cm^{-1} (Figure 9a). Coating of sand particles with organic matter, Fe and cyanides, which possibly resulted in higher variability of the predicted results, can be circumvented by grinding of the samples. The samples represented a wide range of cyanide concentrations (up to 17860 mg kg^{-1}) in order to maximize the correlation coefficient in the study of feasibility of FP NIR for prediction of this soil contaminant.

Developed calibration models as well as calculated LOD pointed to good response of FP NIR spectrometer to cyanide concentrations exceeding 1750 mg kg^{-1}. Unfortunately, the number of samples with such a high concentration was not enough to assess the method performance when only values exceeding 1750 mg kg^{-1} were used.

Flow injection analysis (FIA) was used as a reference method for FP NIR. Soil samples (n=100) were tested for NaOH extractable cyanide. Additionally, water extractable cyanide was determined. Comparison of these extracts revealed that the soil from MGP in Cottbus is mainly contaminated with ferric ferrocyanide ($Fe_4[Fe(CN)_6]_3$), whereas the water soluble fraction was rather small (ranging from 0.3-39 mg kg^{-1}) and most probably indicated the presence of hexacyanoferrates [$Fe(CN)_6^{3-}$] and [$Fe(CN)_6^{4-}$] (Meeussen et al., 1992).

3.6 Conclusions

Our study revealed that direct in situ measurements of cyanide in soil using NIR spectrometry yield high LODs, which can be improved by including sample preparation. Water, particle size and coating phenomena could be reduced by drying, sieving and grinding of the

samples, respectively. Prediction of cyanide concentrations of dried and sieved samples ($R^2 = 0.41$, $p < 0.01$) was improved after grinding ($R^2 = 0.86$, $p < 0.0001$). FP NIR may be applicable for the estimation of cyanide concentrations in soil >1750 mg kg^{-1}. However, our investigations were limited to one study site and the calibration model should be adapted to differing site conditions. We found that portable NIR spectrometry cannot replace traditional laboratory analyses due to high limits of detection, but that it could be used for identification of contamination 'hot spots'.

4 Stability of Prussian Blue in soils of a former Manufactured Gas Plant site

The study presented in this chapter was published as: M. Sut, F. Repmann and T. Raab, "Stability of Prussian Blue in Soils of a Former Manufactured Gas Plant Site", Soil and Sediments Contamination an International Journal, Vol. 23, 2013, pp. 504-522. doi:10.1080/15320383.-2014.839626.

4.1 Abstract

Soil contamination with iron-cyanide complexes is a common problem at former manufactured gas plant (MGP) sites. Dissolution of the cyanide, from Prussian Blue (ferric ferrocyanide), creates environmental hazard, whereas the risk of groundwater contamination depends on the stability of dissolved iron-cyanide complexes. Lack of a standard leaching method to determine the water soluble (plant available) cyanide fraction generates potential limitations for implementing remediation strategies like phytoremediation. Applicability of neutral solution extraction to determine the water soluble cyanide fraction and the stability of Prussian Blue in surface and near-surface soils of an MGP site in Cottbus, under saturated and unsaturated water conditions, was studied in column leaching and batch extraction experiments. MGP soils used in the long-term tests varied according to the pH (5.0-7.7) and to the total cyanide content (40-1718 mg kg^{-1}).

Column leaching, after 4 months of percolation, still yielded effluent concentrations exceeding German drinking water limit (> 50 µg L^{-1}) and the solubility of Prussian Blue reported in the literature (< 1 mg L^{-1}) from both alkaline and acidic soils. Long-term (1344 h) extraction of MGP soils with distilled water was sufficient to dissolve 97 % of the total cyanide from the slightly alkaline soils and up to 78 % from the acidic soils.

Both experiments revealed that dissolution of ferric ferrocyanide under circum-neutral pH and oxic water conditions is a function of time, where the released amount is dependent on the soil pH and total cyanide content. Unexpectedly high and continuous solubility of Prussian Blue, both in acidic and slightly alkaline MGP soils, implies the need to introduce an additional cyanide fraction ("readily soluble fraction") to improve and specify cyanide

leaching methods. Long-term extraction, of cyanide contaminated soil, in neutral solution seems to be a promising approach to evaluate the potential hazard of groundwater pollution at the MGP sites.

4.2 Introduction

Contamination in the form of iron-cyanide compounds is commonly found in the vicinities of former manufactured gas plants (MPG). The process of gas manufacturing (coal gasification) involved gas purification based on inorganic chemical reactions of hydrogen sulfide and hydrogen cyanide in the gas with iron oxides. Gas was conducted through boxes containing wood shavings impregnated with hydrated iron oxide. When the iron oxide lost its absorbing capacity, it was often disposed on the site and used as a filling material (Kjeldsen, 1998). The spent oxide wastes typically contained high amounts of sulfur, tar and various complex iron-cyanides, which are often found as a Prussian Blue coloration in the soil (ferric ferrocyanide $Fe_4[Fe(CN)_6]_3$ and other iron-complexed cyanides like ferricyanides $[Fe(CN)_6^{3-}]$ and ferrocyanides $[Fe(CN)_6^{4-}]$ (Meeussen et al., 1990; Meeussen et al., 1992; Meeussen et al., 1994; Theis et al., 1994).

Rainwater infiltration causes leaching of spent oxide box wastes into the groundwater and the presence of dissolved cyanide in the soil (Ghosh et al., 1999c; Meeussen et al., 1994; Theis et al., 1994; Weigand et al., 2001). The actual risk of groundwater contamination from the cyanide contaminated MGP soils depends mainly on the solubility and mobility of the iron-cyanide complexes (Mansfeldt et al., 2004). For the ferric ferrocyanide, the principal interaction between the solid phase and the soil solution is the dissolution and precipitation reaction (Meeussen et al., 1995):

$$Fe_4\left[Fe(CN)_6\right]_{3(s)} + 12H_2O \longleftrightarrow 4Fe(OH)_{3(s)} + 3Fe(CN)_{6\,(aq)}^{-3} + 3e^- + 12H^+ \qquad (4.1)$$

According to Meeussen et al. (1992), Prussian Blue is stable at pH less than 6, and tends to dissociate readily under alkaline conditions. Extended study on iron-cyanide solids dissolution was presented by Ghosh et al. (1999c), who stated that based on batch experiments and MINEQL$^+$ chemical equilibrium model calculations Prussian Blue has low solubility at pH less than 4. However, solubility of iron-cyanide solids increases with increasing pH (> 4). Meeussen et al. (1990) investigated leaching of soils contaminated with iron-cyanide minerals in a column experiment and a batch experiment under different pH conditions (pH 3 - 9). They stated that the cyanide concentrations in the leachates and extracts were dependent on the soil pH, but were not related to the total cyanide content of the soils. Weigand et al. (2001) used column experiments to study the release and mobility of iron-cyanide complexes in soils from a former MGP site. They stated that flow regime, especially

residence time of pore water, plays a key role for contaminant seepage i.e. increasing its concentration. Weigand et al. (2001) conducted a batch experiment where 2.25 mg of cyanide was extracted from 7 g of soil (containing totally 29 mg of cyanide). Extraction was not exhaustive, but indicated relative stability of iron-cyanide complexes under experimental conditions.

Concerning environmental impact assessment, contaminant concentration in groundwater (EC, 2006) as well as in soils is taken under consideration (BBodSchG, 1998; NEPC, 1999). Hence, it is of great importance to study the contaminants dissolution from the soil material, in order to evaluate potential groundwater pollution. As indicated above, the solubility of iron-cyanide complexes has been previously studied. However, more than 60 years after cessation of the MGP in Cottbus, cyanide concentration in groundwater is still exceeding German drinking water limits. Monitoring of the groundwater offstream resulted in varying cyanide concentration reaching up to 1.5 mg L^{-1} (Kurzbericht DB-AG, 2011). Several open questions arise, regarding the on-site stability of Prussian Blue, and therefore more experiments with the MGP soils itself (instead of synthetic solutions) are required.

To advance the knowledge about the stability of Prussian Blue in surface and near-surface soils in order to design and implement remediation strategies like phytoremediation, the objectives of the approach presented here were to: (i) investigate the solubility of iron-cyanide complexes from the MGP soil containing Prussian Blue, under circum-neutral pH, oxic, unsaturated water conditions in a column leaching experiment, in order to assess the potential of cyanide leaching from the soils with varying pH and total cyanide concentration; (ii) study the stability of iron-cyanide complexes in the MGP soils, under circum-neutral pH, oxic, saturated water conditions in a sequential batch extraction; (iii) evaluate the comparability of the column and the batch experiments in terms of qualitative and quantitative determination of cyanide contamination; (iv) study the applicability of neutral solution extraction (distilled water) to determine the water soluble cyanide fraction and to advance the understanding of cyanide behavior in MGP site soils.

4.3 Materials and Methods

4.3.1 Column leaching experiment

Dzombak et al. (2006) presented a range of leaching approaches available for cyanide contaminated soils. When leaching under acidic environment is desired, extraction with acid solution can be conducted, but it can result in low liberation of metal-complexed cyanides existing within solids in adsorbed or precipitated form (Dzombak et al., 2006). According to Dzombak et al. (2006), the Method 1311 in Toxicity Characteristic Leaching Procedure

(TCLP) (USEPA, 1998) employs a weak (acetic) acid extract solution, but cyanide is not one of the leachate constituents included in the TCLP methods development and is not specified as a TCLP extract solution analyte.

Another available approach for cyanide leaching is extraction with alkaline solution, which is conducted when the total amount of cyanide, including water insoluble, is desired. According to Dzombak et al. (2006) the Method 9010B (USEPA, 1998) provides for alkaline solution extraction (NaOH) when methods for analysis of cyanide in solids are required. Method 4500-CN in Standard Methods (APHA/AWWA/WEF, 1998) suggests procedure where cyanide-bearing solids are mixed for 12 h to 16 h with 10 % (2.5 mol L^{-1}) NaOH solution. These methods have been implemented and altered by a number of scientists (Mansfeldt and Biernath, 2001; Meeussen et al., 1992).

In order to assess the extractable cyanides simulating contact with rainwater extraction with neutral solution (like distilled water) is conducted (Dzombak et al, 2006). According to Method 4500-CN (APHA/AWWA/WEF, 1998), 500 mg of solids should be extracted for one hour in 500 mL of distilled water in order to liberate "soluble cyanide". There is no specific method developed for determining the water soluble fraction of cyanide, but the description of the Method 1312 in Synthetic Leaching Procedure (USEPA, 1998) indicates that this test can be used to measure water extractable cyanide. There are no standard procedures developed for near-neutral pH, oxic water leaching of soils.

To implement a remediation technique like phytoremediation, the water soluble fraction of the contaminant needs to be evaluated, in order to determine the plant available cyanide under experimental conditions. Soils (labeled A, B, C and D), originating from the former MGP site in Cottbus, were leached with distilled water to assess the iron-cyanide solubility from contaminated substrate and to study the amount of extractable cyanide from solids simulating contact with rainwater.

Investigated soils were selected to study cyanide leaching from the MGP soils with varying pH and total cyanide content. Soils A, C and D are top soils (up to 0.5 m deep), whereas soil B was the lower sandy layer (0.5 - 1.5 m deep) of soil A. The properties of the investigated soils are presented in Table 3.

Leaching of iron-cyanide complexes from soil under circum-neutral pH, oxic conditions was determined by conducting laboratory column experiments at controlled flow rates under unsaturated conditions. Eight percolation columns (two replicates for each soil) were constructed from Plexiglas® (ID 5.4 cm, height 30 cm) to allow visual inspection of likely changes in the soil during the experiment. The tubes were positioned perpendicular to each other. The soil was homogenized by hand and each column was loaded with ≈ 700 g of field fresh soil. While packing procedure, layers of about 1 cm thickness were

Table 3: Soil properties based on the fresh mass of the sample.

Soil	Soil characteristic	OM (%)	Water content (%)	Tot. CN (mg kg^{-1})	Tot. water soluble CN (mg kg^{-1})	pH	EC (µS cm^{-1})	Clay (%)	Silt (%)	Sand (%)
A	top soil	3.4	12.6	875	148	7.6	1455	9.0	14.1	76.9
B	0.5 - 1.5 m deep	1.2	6.4	401	26	5.9	2041	11.8	17.6	70.6
C	top soil	3.1	12.9	1718	21	5.0	2253	7.4	15.2	77.4
D	top soil	4.2	10.6	40	0.6	7.7	780	8.0	14.1	77.9

filled into the column and compacted by weak pressing with a pestle to ensure hydraulic connectivity between the layers and to avoid preferential flow paths (Lewis and Sjöstrom, 2010). The columns were assembled in an extractor hood, which was wrapped with aluminum foil to minimize light interference. All collected soil leachates containing cyanide compounds were stored in darkness prior to subsequent analysis. The experiment was conducted at a room temperature.

A peristaltic pump fed 20 mL of distilled water to each column per day. After 2 months the amount of water was increased to 50 mL per day (applying the same flow rate). The distilled water was introduced to the system 4 days in a week (every 24 hours) for 4 months. Every week percolation was interrupted by a 96 h draught interval (during the weekend). After 4 months of water percolation, a flow interruption of 2 months was performed. Resuming the flow resulted in additional 250 mL (5 days) leaching through the columns.

4.3.2 Batch experiment

After 4 months, the column leaching experiment was terminated due to technical reasons, but the leachates cyanide concentrations were still quite prominent (cyanide concentrations up to 26.5 mg L^{-1}). Batch experiments were conducted to investigate the stability of iron-cyanide complexes in the MGP soil when longer contact time with water is provided. For the batch experiment the same soil (A, B, C and D) as for the column experiment was used. Soil material (40 g) was homogenized, sieved (< 2 mm) and introduced to polyethylene bottles, where 100 mL of distilled water was added. The samples were shaken in an end-over-end shaker at 16 rpm. Each sample was extracted in three replicates for 1344 h. In defined time intervals (1 h, 24 h, 72 h, 96 h, 168 h, 216 h, 336 h, 505 h, 677 h, 840 h and after 1344 h) soil-water suspensions were centrifuged for 10 min at 3000 rpm in order to separate the phases. 2 mL of centrifuged sample was used for further analysis.

4.3.3 Soil and extracts analysis

The description of the investigation site is presented in Chapter 2 (2.2).

Soil columns leachates & batch extracts were analyzed for cyanide content with the automated spectrophotometrical flow injection system FIA Compact (MLE, Dresden). Injection Analyzer applied for cyanide detection refers to the DIN EN ISO 14 403 D (2002) standard for determination of total and free cyanide with continuous flow analysis. pH and EC were studied with a bench pH/mV meter MultiLab 540 (WTW). Cations were analyzed with an ICP Optical Emission Spectrometer icap 6000 series (Thermo Electron Corporation). For the anions analysis ion chromatography was used (ICS DIONEX DX 500). All the investigated samples were filtered through 0.45 µm syringe filters prior to analysis. Results of the soil column leachates are presented in Table 4.

Total cyanide in the investigated soils (Table 3) was determined with the FIA. To extract cyanide, 20 g of each soil type (3 replicates) were weighted and extracted in 200 mL 1 mol L^{-1} sodium hydroxide (1:10 ratio) for 12 h in an end-over-end shaker at 16 rpm. The extraction with sodium hydroxide (1 mol L^{-1}) provides an effective means for the determination of water insoluble cyanide species (Mansfeldt and Biernath, 2001). In order to force settling of soil particles, the extracts were centrifuged for 10 min at 3000 rpm. To liberate HCN from complexed cyanide, 5 mL of extract were digested in an acidic environment using the micro dist system (Dimitrova, 2010). The micro dist system refers to the method of the Hach Company, US QuickChem Method 10-204-00-1-X approved by the USEPA (2008).

Water soluble cyanide in the investigated soil (Table 3) was determined using 20 g of each soil type (3 replicates) and extracted in 50 mL of distilled water (1:2.5 ratio) for 1 h with an end-over-end shaker at 16 rpm. Afterwards, the water extracts were centrifuged at 3000 rpm for 20 min, 20 - 30 mL were filtered through 0.45 µm syringe filters, which were conserved with 200 - 300 µl of 1 mol L^{-1} NaOH in order to preclude the loss of analyte. 5 mL of filtered extracts were distilled, according to the Method 10-204-00-1-X approved by USEPA (2008), and subsequently analyzed with FIA (DIN EN ISO 14 403 D, 2002). The detection limit for both extractions is 0.02 mg L^{-1} of cyanide in the analyte.

Organic matter was determined with Loss on Ignition method (LOI). 10 g of each soil sample were sieved (< 2 mm), placed in a porcelain beaker and heated up during the night at 105° C. This procedure was repeated until the change of mass was lower than 0.1 %. After recording the weight, samples were heated up at 450° C for 12 h. The LOI, hence the organic matter, was calculated as the percentage of the dry weight of the respective sample.

Table 4: Column leachates characteristics: values determined in the beginning (22/06/11) and in the end (11/11/11) of the experiment.

Column	Leachate (mL)	Cyanide (mg L^{-1})		EC (mS cm^{-1})		pH		Nitrate (mg L^{-1})		Sulfate (mg L^{-1})		Chloride (mg L^{-1})	
		22/06/11	11/11/11	22/06/11	11/11/11	22/06/11	11/11/11	22/06/11	11/11/11	22/06/11	11/11/11	22/06/11	11/11/11
A1	1992	2015	20	5.4	2.2	7.5	8.1	365	3.7	1373	1030	23.5	3
A2	1914	1865	26	6	2.8	7.8	8.1	370	6	1364	813	23	2.5
B1	1947	720	9	3.1	0.2	8	7.7	0	1.2	1461	36	3.3	0.9
B2	1893	620	8	3.1	0.2	6.9	7.7	1	5.3	1506	30	3.9	0.7
C1	1526	168	22	2.8	2.2	7	6.8	143	3.8	1312	1288	6.3	1.4
C2	1880	175	31	2.8	2.2	6.6	6.4	174	9.8	1487	1299	7	0.7
D1	2029	25.6	0.4	3.7	0.6	7.6	8.1	260	2.2	1679	32	15.9	1
D2	1850	29.6	0.4	3.7	0.6	8	8.3	211	5.3	1561	39	13.3	1

Column	Ca (mg L^{-1})		Mg (mg L^{-1})		Mn (mg L^{-1})		K (mg L^{-1})		Fe (mg L^{-1})	
	22/06/11	11/11/11	22/06/11	11/11/11	22/06/11	11/11/11	22/06/11	11/11/11	22/06/11	11/11/11
A1	1100	510	67.7	1.9	1.1	0.04	21.6	7.8	386	9.4
A2	1066	442	65.8	3.1	0.2	0.01	14.6	6.9	344	12.9
B1	708	49	21.9	0.3	3.4	0.12	3.2	0.6	49.2	4.2
B2	738	40	22.6	0.3	2.7	0.11	2.9	1.1	65.2	5.4
C1	653	628	53	6.6	3.4	0.11	6.7	4.8	41	11.5
C2	660	597	53.8	1.2	2.7	0.58	7.3	2.6	53	12.3
D1	662	104	66.3	8.8	0	0	63.5	13.1	1.8	0
D2	657	98	67.2	8.2	0	0	65.6	13.9	1.6	0

Grain size analysis was performed by sieving (> 20 μm) and X-ray granulometry (XRG) using the SediGraph 5120™ particle-size analyzer (Müller et al., 2009).

Additionally, spectra of the investigated soils (A, B, C and D) were recorded using FTIR spectroscopy (Impact 410 Nicolet, resolution 4 cm^{-1}, 8 scans per sample), which is a commonly used technique for iron-cyanide complexes speciation (Mansfeldt et al., 2004; Rennert et al., 2007). Concentrations of selected heavy metals (lead, copper, zinc, nickel, chrome), were determined by an X-ray fluorescence (XRF) analyzer (Niton XL3t 900, soil model, powder samples with 120 s of measurement) (Shefsky, 1997).

4.4 Results and Discussion

4.4.1 Soil analysis

Properties of the MGP soils are listed in Table 3. The soil pH varies between 5.0 and 7.7. According to Bodenkundliche Kartieranleitung (2005), soil A and B are medium loamy sand soils (SI3), whereas soils C and D are characterized as weak loamy sand soils (SI2). Water soluble cyanide fraction ranged from 0.6 mg kg^{-1} to 148 mg kg^{-1}. Total cyanide content for the investigated soils deviate from 40 mg kg^{-1} to 1718 mg kg^{-1}.

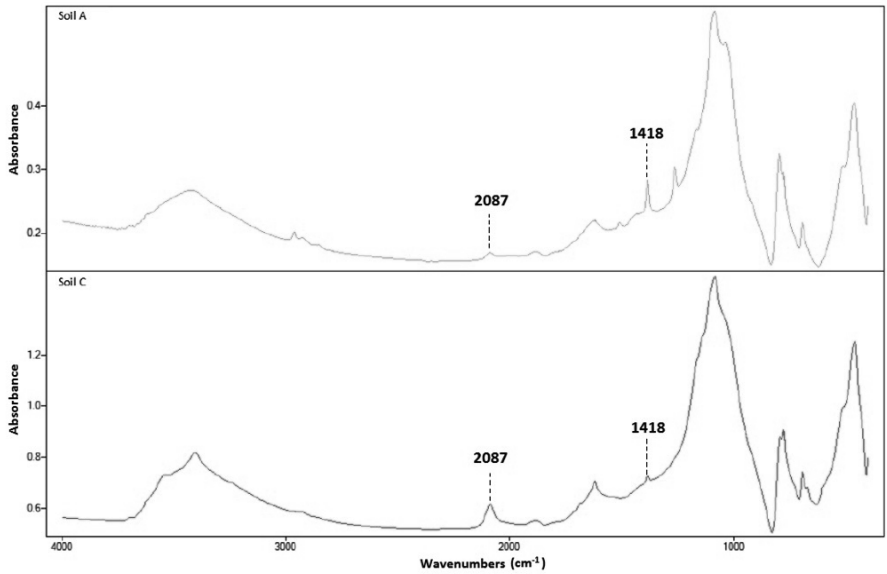

Figure 13: FTIR spectra of the cyanide contaminated soil from the MGP Cottbus, indicating presence of ferric ferrocyanide (2087 cm^{-1} and 1418 cm^{-1}).

In order to determine which form of iron-cyanide complex is present in the soils used for the column leaching experiment, FTIR spectrometry was used. The FTIR absorption spectra of two chosen soils (A and C) are illustrated in Figure 13. The soils exhibit infrared absorption bands at wavenumbers 2087 cm^{-1} and 1418 cm^{-1}, which according to Rennert et al. (2007) and Mansfeldt et al. (2004) indicate CN stretching and NH bending vibrations of ferric ferrocyanide, respectively.

XRF analysis revealed no elevated levels of heavy metals in the investigated MGP soils.

4.4.2 Column leaching experiment

Results obtained from the column leaching experiment indicated cyanide release exceeding the German drinking water limit of 50 µg L^{-1} cyanide. The experimental data are given in Table 4, where cyanide concentrations in the columns leachates, after 4 months of water percolation, are listed. In acidic environment of soil B and C, after the period of 4 months, cyanide concentration in the leachates was approximately at 8.5 mg L^{-1} and 26.5 mg L^{-1}, respectively. For the slightly alkaline soils A and D, leachates concentrations amounted for 23 mg L^{-1} and 0.4 mg L^{-1}, respectively. According to Meeussen et al. (1992), Prussian Blue is stable at pH less than 6. Ghosh et al. (1999a) reported the solubility of Prussian Blue at

the pH range 6.8 - 8.0 to be approximately at 6 mg L^{-1}. Dzombak et al. (2006) stated that iron-iron cyanide solids in the form of Prussian Blue exhibit low solubility (< 1 mg L^{-1}) in acidic to neutral pH regimes and under moderately oxic to anoxic conditions. Leaching of columns filled with MGP soil, revealed higher instability of ferric ferrocyanide, under the experimental conditions, as reported in the literature.

For all investigated columns, it was noticed, that the release of cyanide from the MGP soil can be described by two phases (Figure 14). Phase I, which is characterized by the sharp drop in cyanide concentration and strong increase in cyanide accumulated mass respectively, releases readily water soluble cyanide species like alkali metal complexes (e.g. $[Fe(CN)_6]^{3-}$, $[Fe(CN)_6]^{4-}$, $[CaFe(CN)_6]^{-}$, $[CaFe(CN)_6]^{2-}$). Meeussen et al. (1990) stated that higher initial cyanide concentrations were associated with small particles washed out from the columns. Leachates preparation (filtering and distillation) and analysis (FIA) conducted in the column experiment was applied to measure only water soluble cyanide fraction. Hence, we assume, that the initially high cyanide concentrations (up to 1800 mg L^{-1}), measured in our leachates, are the result of solution transport. Phase II, characterized by the continuous release on low concentration level and moderate increase in accumulated mass, originates from constant/continuous dissolution, possibly controlled by the solubility of ferric ferrocyanide.

Percolation was weekly split by a 96 h flow interruption, which seldom caused an increase in effluent concentrations, suggesting that the residence time of the pore water was too short to reach the equilibrium between the solid and the solution phase. The final drought interval (starting at ≈ 2000 mL) led to an increase of the cyanide concentration in all investigated leachates, reaching in column C1 concentrations even four times higher than the base level (Figure 14). This result suggests that the mobility of iron-cyanide complexes (in phase II) under unsaturated water percolation is constrained by non-equilibrium release.

Our findings are consistent with the study made by Weigand et al. (2001), were the increase of the cyanide concentration was observed after the flow interruption (180 h) in the unsaturated column experiment. The increase of the percolating water amount didn't reduce the cyanide concentrations in the produced leachates. The experiment showed that the more water we percolated the more cyanide we leached, which implies that water regime plays an influential role in the movement of iron-cyanide complexes in soil.

Experiments revealed the highest obtained cyanide content (1319 mg) in column C, whereas column A indicated noticeable fraction of water soluble cyanide (103 mg) (Table 5). The highest leached cyanide mass was obtained from column A (269 mg), which surpassed more than twice the amount of water soluble cyanide. The slightly alkaline character of soil A (Table 3) suggests the increased solubility of ferric ferrocyanide (Dzombak et al., 2006).

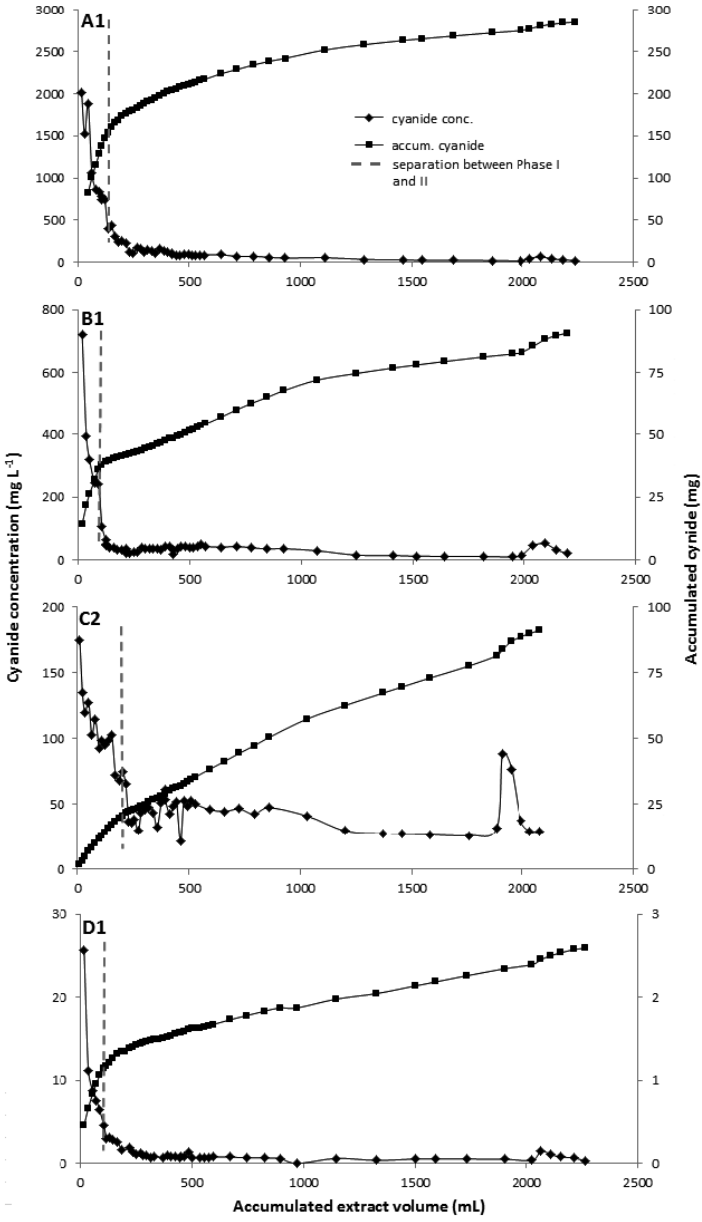

Figure 14: Results obtained from the column percolation for the A1, B1, C2 and D1 columns with distilled water under circum-neutral pH, where the cyanide concentration is the value measured in the column leachates; volume of water refers to the accumulated amount of the collected leachates; accumulated cyanide stands for the collected mass of pollutant, during the experiment, plotted cumulatively.

Table 5: Cyanide balance obtained from the column experiment, where the total and the water soluble cyanide content was measured by sodium hydroxide and water extraction respectively, according to the procedure described in ''Soil and extract analysis'' section; data presented are mean values obtained from 2 replicates.

Column	Cyanide						
	Content		Measured in leachates				
	total (mg)	water soluble (mg)	accum. (mg)	accum./total (%)	accum./water soluble (%)	Phase I (mg)	Phase I/accum. (%)
A	608	103	269	44	262	149	55
B	348	19	75	22	389	36	48
C	1319	16	73	5	446	17	24
D	26	0.4	3	10	650	1	50

From column C, we were able to leach only 5 % (73 mg) of the total cyanide mass, which was still 4.5 folds higher than the water soluble fraction (Table 5). According to Meeussen et al. (1990), total cyanide contents of soils are of limited relevance in assessing possible hazards of contaminated sites. In contrast, our experiments revealed higher released cyanide amount than present in the water soluble fraction, especially for acidic soil C, which points to instability of Prussian Blue. Moreover, the linear shape of accumulated cyanide mass for column C1 in Figure 14 implies further dissolution of ferric ferrocyanide, as well as the contamination hazard potential, under these conditions.

4.4.3 Batch experiment

Once the results of the column experiment suggested potential hazard, due to solubility of ferric ferrocyanide, a series of a batch experiments were performed to verify the leaching data. Soils used in the column (A, B, C and D) experiment were additionally extracted with distilled water.

Longer contact time (1344 h) between the cyanide contaminated soils and water solution resulted in almost complete dissolution of iron-cyanide complexes in alkaline soil A (97 %) (Table 6). However, for alkaline soil D (pH = 7.7) dissolved cyanide mass amounted only to 38 % of the total cyanide. Since the properties of soil A and D are analogous (Table 3), we suggest that different cyanide dissolution rate is a result of varying total cyanide content.

Acidic character of soil B (pH = 5.9) only slightly reduced the dissolution of ferric ferrocyanide, resulting in 78 % of dissolved cyanide with respect to the total amount. The lowest accumulated cyanide mass was measured in the soil-water solution of acidic soil C (28 %). Within the extracting period, none of the soil-water extracts reached equilibrium, suggesting that dissolution of ferric ferrocyanide under experimental conditions (pH = 5.0 - 7.7) was only a matter of time.

Table 6: Cyanide balance obtained from the batch experiment, where cyanide content and measured values correspond to the cyanide balance obtained for the column experiment; data presented are mean values obtained from 3 replicates.

Soil	Cyanide				
	Content	Measured			
	total	accum.	accum./total	Phase I	Phase I/total
	(mg)	(mg)	(%)	1 hour (mg)	(%)
A	24.50	23.84	97.31	5.40	22.04
B	22.28	17.43	78.24	2.72	12.21
C	61.92	17.31	27.96	1.17	1.90
D	1.20	0.45	37.60	0.07	5.48

Figure 15 shows the relation of accumulated cyanide mass to the extraction (shaking) time in the batch experiment. Linear character of the curves obtained (especially for soil C) supports the assumption that dissolution of ferric ferrocyanide in the investigated soils is a function of time. Our results imply the instability of Prussian Blue under the experimental conditions. Our results are contradictory with the study made by Weigand et al. (2001) where soil contaminated with cyanide (total cyanide mass equal to 29 mg) was extracted for 72 h. Higher solution phase concentrations were observed in the first extract (24 h) followed by the release on the low concentration level, indicating relative stability of iron-cyanide complexes.

The batch experiment revealed an analogues trend compared to the one found in the column leaching experiment (Figure 14). Initially sharp increase in the cyanide accumulated mass within the first 24 hours of extraction is noticed (phase I), followed by the constant dissolution (phase II). However, in the batch experiment, the increase of the accumulated iron-cyanide mass is prominent through the whole experiment, which might be related to the shaking procedure that promotes breakdown of aggregates. In the first two extractions (1 h and 24 h) an increase in the accumulated cyanide mass can be noticed in all the investigated soils. The iron-cyanide release rates in further sampling intervals were not considerably different, which can be noticed in Figure 16. Analogous to the column leaching experiment we assign phase I to the readily dissolved iron-cyanide complexes and phase II to slow dissolution of ferric ferrocyanide.

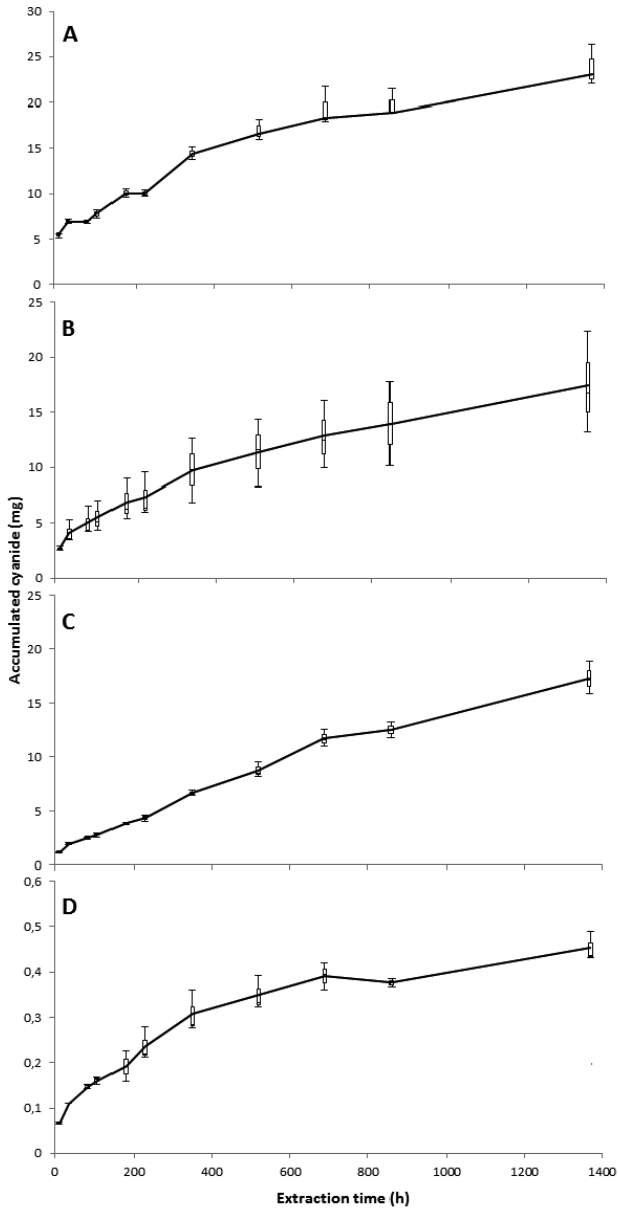

Figure 15: Mean cumulative cyanide quantities v/s extraction time for A, B, C and D soils in the batch experiment, where plotted curves indicate maximum, minimum and average accumulated cyanide mass measured for each soil type in 3 replicates. The experiment was conducted under oxic water conditions with pH ranging from 5.0 to 7.7.

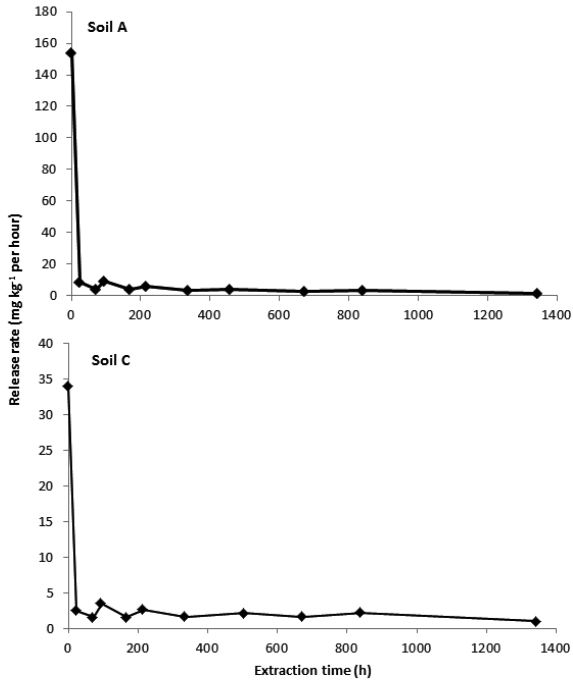

Figure 16: Relation of cyanide release rate per hour to the extraction time for soil A (pH = 7.6) and C (pH = 5.0).

4.4.4 Correlation of column and batch experiments

Studying contaminants release and behavior in soil columns experiments is a prevalent practice (Loch et al., 1981; Morillo et al., 2000; Kamra et al., 2001; Wang et al., 2009), especially with respect to the water soluble phase. The opportunity of evaluating readily dissolved amount of contaminant is essential for implementing recultivation techniques like phytoremediation, where the capacity of plant uptake plays a crucial role.

Once it was noticed that both experiments (column and batch) revealed analogues releases of the iron-cyanide complexes, characterized by the phase I and II, an attempt to quantitatively compare readily soluble fraction (phase I) was performed. Our aim was to investigate whether we can quantitatively predict phase I in the column leaching experiment on the basis of the batch experiment. The values used in the correlation are presented in Table 7. For the column experiment, cyanide concentrations in phase I were visually obtained from the graphs (Figure 14). Cyanide concentrations, measured after 1 h of extraction (Figure 16), were assigned to represent phase I in the batch experiment.

Table 7: Cyanide concentrations (mg kg^{-1}) in the column and the batch experiment (calculated on the soil dry mass) in phase I.

Soil	Phase I	
	Column (mg kg^{-1})	Batch (1 h)(mg kg^{-1})
A	255	169
B	50	27
C	33	24
D	2	1

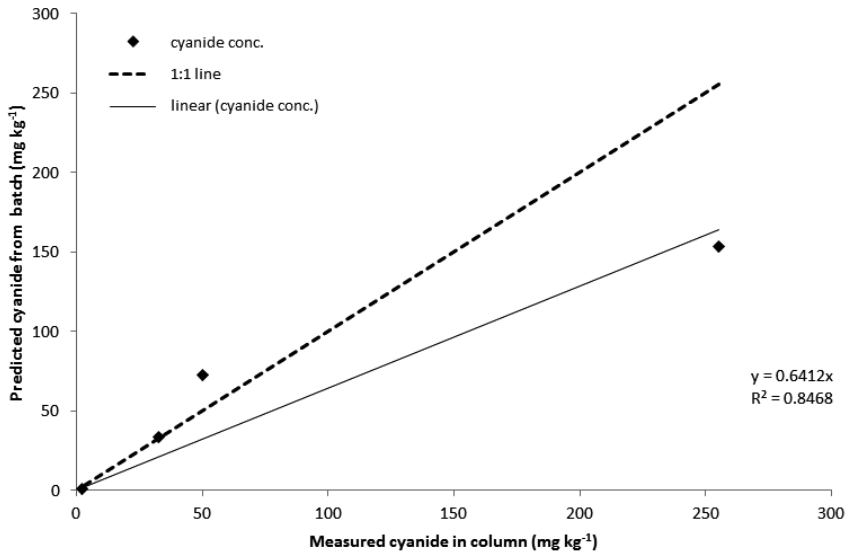

Figure 17: Columns v/s batch cyanide concentrations (phase I).

Values obtained for 1 h of extraction in the batch experiment indicate positive linear correlation (R^2=0.8468) with phase I cyanide concentrations measured in the column experiment (Figure 17). The sequence of the predicted values corresponds to the measured ones (cyanide conc. in the batch increases with the increasing cyanide conc. in the column). Slope of the regression line lies below the ideal line indicating that the quantification of phase I in the column, on the basis of experimental data from batch, is underestimated. Nevertheless, as indicated above, batch experiments can serve as a preliminary prediction of what can be expected in the column experiment. Conducted prior to the column leaching experiments, batch analysis provides rough estimation concerning the concentration of readily mobile fraction of iron-cyanide complexes.

Regardless of the positive correlation of phase I in both experiments, an attempt to quantitatively compare phase II needs to be further investigated. Even though the FTIR scans, as well as the blue color of the MGP soil, pointed to the presence of Prussian Blue, cyanide release rates varied with respect to material (soil A, B, C or D) and experiment. Higher release rates were obtained for the batch experiments. Up to 97 % of cyanide was extracted for soil A within 1344 h, whereas in the column experiment, percolation evolved 44 % of the total cyanide content (Table 5 and Table 6). Breaking of aggregates, due to the shaking procedure, can lead to faster ferric ferrocyanide dissolution. In the column experiment, re-precipitation of Prussian Blue in the bottom was observed, which could have retarded the dissolution. It was assumed that dissolved iron-cyanide complexes are transported through the column and, presumably, due to the presence of available iron and low redox conditions (water saturation) they precipitate in the form of ferric ferrocyanide. The retardation of solid iron-cyanide complexes dissolution due to reaction with iron is consistent with the study made by Ghosh et al. (1999b), where the effectiveness of elemental iron, to attenuate the transport of cyanides, was investigated in column and batch experiments.

To implement remediation strategies, like phytoremediation, for any contaminated site, two contaminants fractions are crucial: water soluble (plant available) and total concentration. The Method 9010B used by Dimitrova (2010), which was applied in this study, provides effective determination of the total amount of cyanide, approved by the USEPA (1998). In order to determine the water soluble cyanide fraction, the approach specified in Standard Methods in Method 4500-CN (APHA/AWWA/WEF, 1998) was used, where investigated MGP soils were shaken for 1 h in distilled water. According to this procedure, the water soluble cyanide in Table 3 and Table 5 was determined. Also Young and Theis (1991) applied the approach specified in Method 4500-CN (APHA/AWWA/WEF, 1998) to soils from MGP sites, but the water extraction yielded no detectable cyanide.

In Table 5, where the cyanide balance for the column leaching experiment was obtained, it can be noticed that the water soluble cyanide fraction, defined by the 1 h extraction, is lower than the cyanide amount released in phase I. Moreover, the accumulated cyanide mass was still increasing (Figure 14) after 4 months of water percolation. Corresponding results were obtained from the batch experiment, where the shaking period of 1344 h revealed continuously increasing cyanide concentrations in the soil-water extracts (Figure 15). 24 h extraction in NaOH of soil A, in order to determine total cyanide content, indicates comparable cyanide amount to the one obtained after 1344 h of water extraction. Both experiments resulted in continuous dissolution of ferric ferrocyanide, under the experimental conditions, but the released amounts are dependent on the soil solution pH (cyanide release increases with increasing pH for soil A, B and C) and on the total cyanide content (despite of alkaline character of soil D).

Continuous dissolution of Prussian Blue, demonstrated in the column leaching and the batch experiments, for both alkaline and acidic soils, initiate a question whether the procedure suggested in Standard Methods in Method 4500-CN (APHA/AWWA/WEF, 1998) and implemented in this study, is appropriate for defining water soluble cyanide fraction. Dzombak et al. (2006) stated that there is no specific method developed for neutral solution extraction of cyanide. Since we can conclude that dissolution of ferric ferrocyanide under circum-neutral pH, oxic conditions is a function of time and only the released amount is soil pH dependent, we would suggest introducing one more fraction to specify cyanide release. 1 h of water extraction can specify "readily soluble fraction". The rest of the liberated cyanide can be determined as the "long-term water available fraction", which is difficult to be defined in time. Depending mainly on the soil chemistry, "long-term water available fraction" can be as high as the "total content".

Many scientists have studied cyanide release using synthetic solutions (Ghosh et al., 1999a; Ghosh et al., 1999c), MGP soils (Young and Theis, 1991; Weigand et al., 2001; Ghosh et al., 2004) or cyanide-bearing wastes (Theis and West, 1986) by conducting leaching tests under varying pH conditions. Results presented in these studies do not correspond with the high solubility of Prussian Blue in the investigations conducted on the soils from the MGP in Cottbus. Long-term extraction or leaching of surface and near-surface, cyanide-contaminated soils with distilled water simulates the environmental conditions, where the rainwater infiltration enhances the dissolution of ferric ferrocyanide. This approach of leaching method for circum-neutral pH, oxic water conditions provides a reliable tool for assessing the potential environmental hazard and corresponds with the elevated cyanide concentration measured in the groundwater at the Cottbus MGP site.

4.5 Conclusions

Column leaching and batch experiments with distilled water were conducted to assess the extractable cyanide from surface and near-surface soils and to simulate the dissolution behavior of Prussian Blue from contact with rainwater. The study revealed instability of Prussian Blue under circum-neutral pH, oxic water conditions. Leached effluent concentrations were exceeding German drinking water limit and solubility reported in the literature, but corresponding with the elevated cyanide concentration measured in the groundwater at the MGP in Cottbus.

The concentration of cyanide in the column leachates and batch extracts is influenced by the rapid mobilization of readily soluble hexacyanoferrats and the slow dissolution of ferric ferrocyanide under circum-neutral pH, oxic water conditions. The approach of leaching with neutral solution seems to provide a promising method to simulate the Prussian Blue

behavior in the soils, to assess the water extractable cyanide and to predict the readily soluble amount (phase I).

Both experiments indicated high solubility of Prussian Blue, implying that complete dissolution of solid iron-cyanide complexes, from acidic and slightly alkaline soils, is a matter of time. The study revealed that the released amounts of ferric ferrocyanide, under oxic conditions, differ with respect to the soil pH and the total cyanide content. Generally, the solubility of Prussian Blue increases with increasing soil pH, but is however relatively low in alkaline soils with minor total cyanide content. 1 h extraction of the MGP soils with distilled water failed to assess the total extractable cyanide in the column and batch experiments. Unexpectedly high and continuous dissolution of ferric ferrocyanide, under neutral solution extraction, implies introduction of "readily soluble fraction", which combined with "long-term water available fraction" and "total content" yields a more detailed description of the cyanide release.

Water regime seems to play an important role in cyanide dissolution, hence the increased cyanide concentrations, originating from ultimate flow interruption, sustain the non - equilibrium release as a probable constrain for the iron-cyanide mobility under unsaturated flow conditions. The amount of dissolved cyanide is dependent on the amount of water introduced to the columns, the more water is percolated, the more cyanide is leached, which suggests that when evaluating the potential hazard of groundwater contamination, total cyanide concentrations should be taken under consideration.

5 Long-Term Release of Iron-Cyanide Complexes from the Soils of a Manufactured Gas Plant Site

The study presented in this chapter was published as: M. Sut, T. Fischer, F. Repmann and T. Raab, "Long-term release of iron-cyanide complexes from the soils of a former Manufactured Gas Plant site", Journal of Environmental Protection, Vol. 4 No. 11B, 2013, pp. 8-19. doi: 10.4236/jep.2013.411B002.

5.1 Abstract

Iron-cyanide (Fe-CN) complexes have been detected at Manufactured Gas Plant sites (MGP) worldwide. The risk of groundwater contamination depends mainly on the dissolution of ferric ferrocyanide. In order to design effective remediation strategies, it is relevant to understand the contaminant's fate and transport in soil, and to quantify and mathematically model a release rate. The release of iron-cyanide complexes from four contaminated soils, originating from the former MGP in Cottbus, has been studied by using a column experiment. Results indicated that long-term cyanide (CN) release is governed by two phases: one readily dissolved and one strongly fixed. Different isotherm and kinetic equations were used to investigate the driving mechanisms for the ferric ferrocyanide release. Applying the isotherm equations assumed an approach where two phases were separate in time, whereas the multiple first order equation considered simultaneous occurrence of both cyanide pools. Results indicated varying CN release rates according to the phase and soil. According to isotherm and kinetic models the long-term iron cyanide release from the MGP soils is a complex phenomenon driven by various mechanisms parallely involving desorption, diffusion and transport processes. Phase I (rapid release) is presumably mainly constrained by the transport process of readily dissolved iron-cyanide complexes combined with desorption of CN bound to reactive heterogeneous surfaces that are in direct contact with the aqueous phase (outer-sphere complexation). Phase II (limited rate) is presumably driven by the diffusion controlled processes involving dissolution of precipitated ferric ferrocyanide

from the mineral or inner-sphere complexation of ferricyanides. CN release rates in phase I and II were mainly influenced by the pH, organic matter (OM) and the total CN content. The cyanide release rates increased with increasing pH, decreased with low initial CN concentration and were retarded by the increase in OM content.

5.2 Introduction

Cyanide in the form of iron-cyanide (Fe-CN) complexes is a potentially toxic compound that once exposed to UV or visible light radiation, in solution, can be broken down to free cyanide (CN^- and HCN) (Kjeldsen, 1998). Anthropogenic activities, like the process of gas purification after coal gasification in Manufactured Gas Plants (MGPs), yielded side products in the form of ferric ferrocyanide (Prussian Blue), leading possibly to the contamination of soil and groundwater. The manufactured gas was conducted through wood shavings, impregnated with hydrated iron oxide, in order to remove hydrogen sulfide (H_2S) and hydrogen cyanide (HCN). When the iron oxide lost its absorbing capacity it was often deposited in the vicinities of MGP, which generated a potential environmental pollution due to high amounts of sulfur, tar and various complex iron-cyanides.

Knowledge concerning the behavior, particularly dissolution and desorption, of contaminants can help in reducing the extent of cleanup technologies. In order to design effective remediation strategies, it is relevant to understand contaminant fate and transport in soil, and to quantify and mathematically model the release rate (Saffron et al., 2006). The mobility of iron-cyanide complexes in soil is mainly governed by the characteristics of the soil solution (pH, pE), the presence of complexing cations (K^+, Mn^{2+}, Fe^{2+}, etc.), the presence of UV light as well as the substrate composition and stratigraphy (e.g. clay content, hydrological barriers) of the site. Fe-cyanide complexes are negatively charged and can form inner-sphere complexes on positively charged surfaces, which makes adsorption on the soil particles a possible Fe-CN retention mechanism (Rennert and Mansfeldt, 2002). With decreasing pH the adsorption of iron-cyanide complexes on iron and aluminum oxides surfaces, which are positively charged under acidic conditions, increases. Hence, neutral and alkaline soils sorb CN anions to a lower extent than acidic soils. Depending on the pH, Fe-CN complexes can be adsorbed on the soil organic matter (SOM). According to Mansfeldt (2003), the adsorption takes place through hydrogen bonds under acidic conditions and through charge transfers complexes under neutral to caustic conditions. Fuller (1985) stated that the sorption of ferricyanide in soil is driven by the pH, iron-oxides and clay mineral content. According to Ohno (1990) sorption of ferrocyanide was increased, when the pH of the soil decreased. Rennert and Mansfeldt (2002) found that ferrocyanides adsorb on goethite surfaces rather than ferricyanides. Rennert and Mansfeldt (2001) pre-

dicted that ferricyanide form outer-sphere and weak inner-sphere surface complexes on goethite. According to them, ferrocyanide was sorbed inner-spherically and by precipitation of a Prussian Blue-like phase. Cheng and Huang (1996) found that the adsorption of either ferrocyanide or ferricyanide complexes onto aluminum oxide is achieved through outer-sphere complexation. Gosh et al. (1999) carried out a column experiment, where both ferricyanide and ferrocyanide were not restrained by the sandy aquifer material.

Sorption of iron-cyanide complexes by soils, as shown above, is a subject that is studied in soil chemistry, but the reverse process (release/desorption) should be of an equal environmental interest, due to its practical importance. Column studies can provide key information concerning the mechanism of the iron-cyanide complexes dissolution or desorption. Release rate parameters can be estimated from the isotherms of the time dependent data using various mathematical models. The aim of this study was to use different isotherm and kinetic equations to investigate the phenomena of iron-cyanide complexes release from the MGP soils. Applying various models to the column experimental data, was believed to provide the knowledge whether the contaminant discharge is driven by the kinetics of desorption from the heterogeneous substrates (Elovich, Freundlich), the diffusion-controlled phenomena (Parabolic Diffusion Equation) or by the transport following Multiple First Order Equation. Additionally the influence of soils parameters such as pH, texture, OM content, initial CN concentrations on the iron-cyanide complexes release rate was studied.

5.3 Materials and Methods

5.3.1 Field data

The description of the investigation site is presented in Chapter 2 (2.2). Gas works produced a variety of largely hazardous waste products (like iron-cyanide complexes) that were used as a filling material contaminating the surrounding field. Soils (labeled A, B, C and D) used in the column experiment originate from the former MGP site in Cottbus. Soils A, C and D are the top soils (up to 0.5 m deep), whereas soil B was the lower sandy layer (0.5 - 1.5 m deep) of soil A. Selected chemical and physical properties of the investigated soils are presented in Table 3.

Grain size analysis was performed by sieving (> 20 μm) and X-ray granulometry (XRG) using the SediGraph 5120™ particle-size analyzer (Müller et al., 2009). Organic matter was determined with the Loss on Ignition method (LOI). pH and EC were studied with a bench pH/mV meter MultiLab 540 (WTW). Total and water soluble cyanide (Table 3) determination was performed according to the micro dist procedure US QuickChem Method 10-204-00-1-X (USEPA, 2008). After distillation cyanide was determined with the flow injection

analyzer (FIA Compact, MLE) (DIN EN ISO 14 403, 2002). The detection limit for both (total and water soluble CN) extractions is 0.02 mg L^{-1} of cyanide in analyte.

5.3.2 Column experiment (dissolution/desorption)

The release of iron-cyanide complexes from the MGP soils (A, B, C and D) was studied by conducting laboratory column experiments at constant flow rates under unsaturated conditions (Sut et al., 2013). Eight percolation columns (two replicates for each soil) were constructed from Plexiglas® (ID 5.4 cm, height 30 cm) and positioned perpendicular to each other. A peristaltic pump fed distilled water to each column, in the beginning of the experiment at a flow rate of 20 ml h^{-1} once per day. Introduced soil was homogenized by hand and each column was loaded with ≈ 700 g of field fresh soil. The system was daily percolated with distilled water and the obtained leachate was subsequently analyzed with the FIA. The experimental set up is shown in Figure 18.

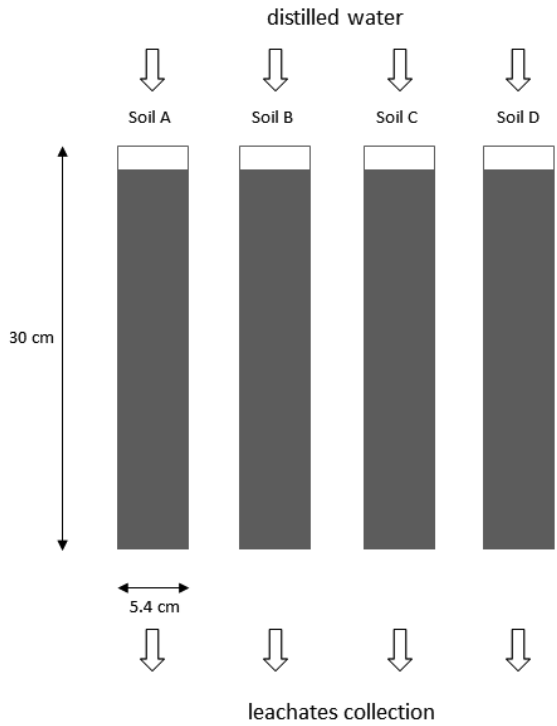

Figure 18: Scheme of the column experiment set-up.

5.3.3 Isotherm Equations

Three isotherm models were applied to the CN experimental data in order to better understand the release process of iron-cyanide complexes from the MGP soils with the varying pH, OM content, CN concentration and soil texture. The gathered data were computed according to the following equations that often describe time - dependent data sufficiently (Chien et al., 1980).

5.3.3.1 Elovich Equation (Chien et al., 1980)

The Elovich equation is generally considered an empirical equation. It has been used in the soil chemistry to describe the kinetics of sorption and desorption of various inorganic materials on the soil (Atkinson et al., 1970), and the soil chemical reaction rates (Chien and W. R. Clayton, 1980; Torrent, 1987).

$$q = (1/\alpha) \cdot \ln(a \cdot \alpha) + (1/\alpha) \cdot \ln t \tag{5.1}$$

where:

- q - the amount of released CN in time t (mg CN kg^{-1});
- α - a release constant (mg CN kg^{-1} day^{-1}); and
- a - a constant related to the initial velocity of the reaction (mg CN kg^{-1}).

Plot of "q" vs. "ln t" gives a linear relationship with the slope of $(1/\alpha)$ and the intercept of $(1/\alpha)$ ln $(a\ \alpha)$.

5.3.3.2 Parabolic Diffusion Equation (Laidler, 1965)

The parabolic diffusion equation is often used to indicate that diffusion-controlled phenomena are rate limited. The diffusion models have been developed to predict the dynamic character of release and have been successfully used to describe for example metal reactions on soil and soil constituents (Jardine and Sparks, 1984).

$$q = a + K_d \cdot t^{1/2} \tag{5.2}$$

where:

- q - the amount of released CN in time t (mg CN kg^{-1});
- a - constant (mg CN kg^{-1}); and
- K_d - apparent diffusion rate constant (mg CN $kg^{-1}day^{-1/2}$).

Plot of "q" vs. "$t^{1/2}$" gives linear relationship if the reaction confirms the parabolic diffusion law. The "a" and "K_d" parameters are determined from the intercept and the slope of the function respectively.

5.3.3.3 Freundlich Equation (Aharoni et al., 1991)

Freundlich equation is generally considered an empirical relationship describing the adsorption of solutes from a liquid to a solid surface, and have been widely applied to experimental data. Elkhatib et al. (1992) used a modified Freundlich equation to describe the kinetics of lead and copper desorption (Elkhatib et al., 2007) from soils.

$$q = k \cdot t^{v} \tag{5.3}$$

where:

- q - the amount of released CN in time t (mg CN kg^{-1}) ;
- k - release rate coefficient (day^{-1});
- t - reaction time (day); and
- v - a constant.

The Freundlich isotherm is a power function, where "k" and "v" are constants that can be determined from the coefficient and the exponent respectively.

5.3.4 Kinetic Equation

Transport models assuming chemically controlled non-equilibrium, which describes the kinetic of a release or dissociation reactions is often defined as a first order reaction (Nederlof et al., 1994). The heterogeneity of a system as well as the controlling mechanism of the release process (such as mass transfer or chemical reaction) determines the rate constants that are required to describe the experimental data.

5.3.4.1 First Order Equation (Van der Zee and Van Riemsdijk, 1998)

Release kinetics based on the first order equation, where the total released amount (q) within a certain time (t), is expressed by the following equation:

$$q = q_o \cdot (1 - e^{-kt}) \tag{5.4}$$

where:

- q - the amount of released CN in time t (mg CN kg^{-1});

- q_o - the amount of CN released at equilibrium (mg CN kg^{-1}); and
- k - apparent release rate coefficient (day^{-1}).

Assuming that CN release is constrained by more than one pool, total released CN amount should be expressed as:

$$q_{tot} = q_1 + q_2 \tag{5.5}$$

where:

- q_{tot} - is the total amount of released CN in time t (mg CN kg^{-1});
- q_1 - is the fast releasing CN pool (mg CN kg^{-1}); and
- q_2 - is the stronger fixed CN pool (mg CN kg^{-1}).

The release kinetics for two pools concept (one readily and one slowly liberating) can be expressed using the multiple first order rate equation, where each pool has its capacity and rate constant:

$$q = q_1 \cdot (1 - e^{-k_1 t}) + q_2 \cdot (1 - e^{-k_2 t}) \tag{5.6}$$

Numerical parameters (k) fit was based on least sum of squares.

5.3.5 Statistical analysis

The predictive performances of the developed models were assessed by adjusted correlation coefficient (R^2), standard error (SE) and the probability value (p), using the analysis of variance (ANOVA).

5.4 Results

5.4.1 Column Experiment

Release of cyanide from MGP soils (A, B, C and D), was investigated with the soil column experiment. The CN release rate was studied for four soils with different pH's and textures (Table 3). According to Bodenkundliche Kartieranleitung (2005), soil A and B are medium loamy sand soils (SI3), whereas soils C and D are characterized as weak loamy sand soils (SI2). Figure 19 represents the relation of the released cyanide, plotted cumulatively, vs. release time. Figure 19 indicates that long-term CN release from soil can be described using two separate cyanide pools: one available and one strongly fixed. The amount of released cyanide representing each pool was visually obtained from the graph (Figure 19).

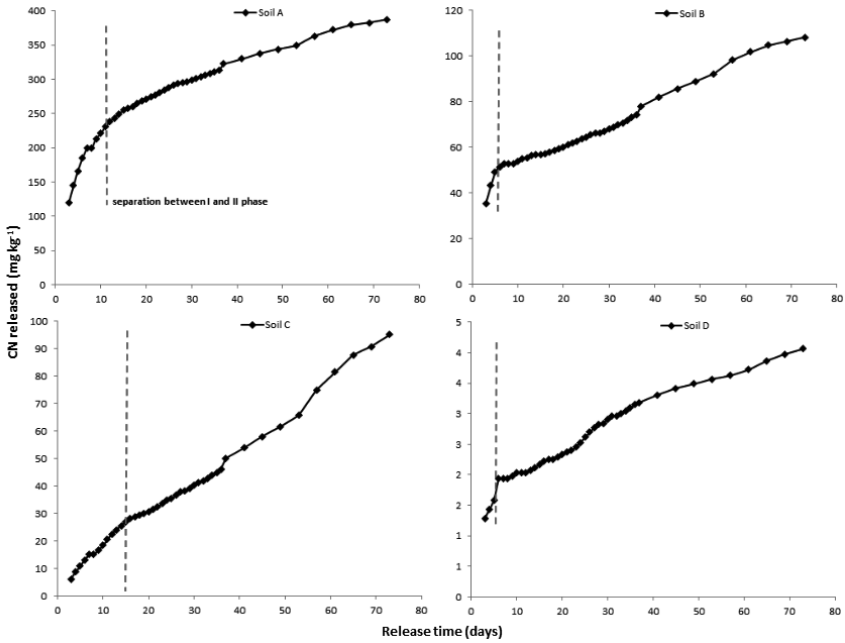

Figure 19: Cumulative CN release curves for the four investigated soils (Sut et al., 2013).

It is assumed that amount of cyanide in the column leachates is influenced by mobilization of readily soluble hexacyanoferrats (phase I) and slow dissolution of ferric ferrocyanide (phase II) (Hingston et al., 1974). The kinetics of CN release will be based on deriving a constant release rate for each phase, based on the continuously measured CN rerelease as a function of time.

5.4.2 Isotherm Models

Modeling of the CN release experimental data using isotherm equations assumes that the above mentioned two phase approach is separate in time and that phase I precedes phase II. Treating the processes separately, intent to derive the cyanide release rates for each phase.

5.4.2.1 Elovich Equation

The empirical equation (Chien and Clayton, 1980) was used to describe the CN release rate from the MGP soils (A, B, C and D) in the column experiment. Figure 20 demonstrates the Elovich equation plots of released CN vs. ln of reaction time obtained for phase I and phase II. In Figure 20 it can be noticed that a linear relationship exists between the released CN "q" and ln of release time "ln (release time)" for both phases in all investigated soils.

The Elovich equation parameters, determined from the slope and intercept of the linear plots, are given in Tables 8 and 9. In the Elovich equation a decrease in "α" values and increase in "a" values would increase the reaction rates (Low, 1960; Jardine and Sparks, 1984). Regression analysis (Table 8) indicated significant (<0.01) correlation in all investigated soil.

The Elovich equation parameters for phase II are listed in Table 9. Regression analysis (Table 9) indicated significant (<0.01) correlation in all investigated soils. As indicated by the regression analysis, the Elovich equation resulted to be adequate for describing the kinetics of CN release from contaminated soils in a column experiment. Moreover, the Elovich equation provides a very good fit ($R^2 > 0.95$) for phase I and a good fit ($R^2 > 0.84$) for phase II of CN release.

Table 8: The Elovich equation parameters and correlation coefficients for phase I CN release in the MGP soils.

	Phase I				
Soil	α mg CN $kg^{-1}day^{-1}$	a mg CN kg^{-1}	R^2	SE	p
A	0.01	125.00	0.99	3.29	<0.01
B	0.05	39.92	0.96	1.54	<0.01
C	0.07	5.82	0.98	1.37	<0.01
D	2.02	2.21	0.98	0.03	<0.01

Table 9: The Elovich equation parameters and correlation coefficients for phase II CN release in the MGP soils.

	Phase II				
Soil	α mg CN $kg^{-1}day^{-1}$	a mg CN kg^{-1}	R^2	SE	p
A	0.01	88.99	0.98	4.46	<0.01
B	0.04	15.77	0.85	5.72	<0.01
C	0.02	3.79	0.96	3.81	<0.01
D	1.27	0.58	0.93	0.08	<0.01

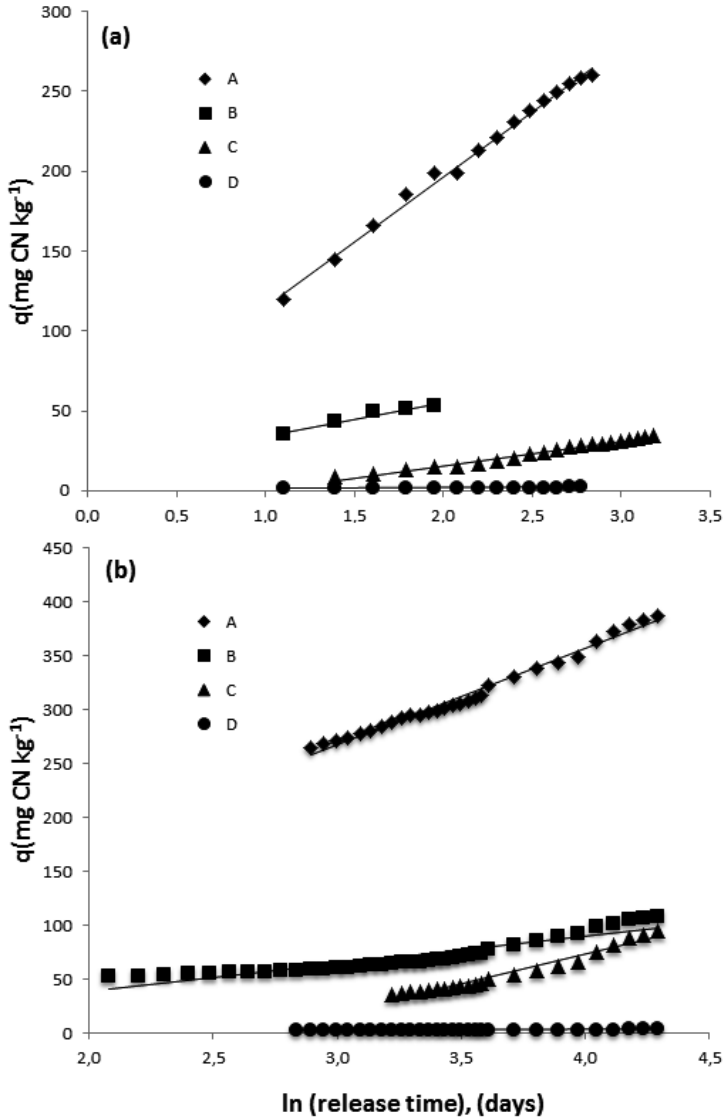

Figure 20: The Elovich equation plots for CN release from the MGP soils in (a) phase I and (b) phase II.

5.4.2.2 Parabolic Diffusion

The parabolic diffusion equation was subsequently used to describe the CN release from the contaminated soils (A, B, C and D) in the column experiment. A parabolic diffusion plot of CN release vs. $t^{1/2}$ is shown in Figure 21. The parabolic diffusion equation parameters, determined from the slope and intercept of the linear plots, are given in Tables 10 and 11.

Regression analysis for phase I (Table 10) indicated significant (<0.01) correlation and high correlation coefficient (>0.91) in all investigated soil. In phase II (Table 11), regression analysis demonstrates significant (<0.01) correlation in all investigated soil, as well as high correlation coefficient (>0.97) and low SE.

Table 10: The parabolic diffusion equation parameters and correlation coefficients for phase I CN release in the MGP soils.

	Phase I				
Soil	K_d mg CN $kg^{-1}day^{-1}$	a mg CN kg^{-1}	R^2	SE	p
A	83.00	69.63	0.94	4.96	<0.01
B	32.18	35.81	0.99	0.81	<0.01
C	10.03	5.57	0.99	0.77	<0.01
D	0.54	0.02	0.92	0.11	<0.01

Table 11: The parabolic diffusion equation parameters and correlation coefficients for phase II CN release in the MGP soils.

	Phase II				
Soil	K_d mg CN $kg^{-1}day^{-1}$	a mg CN kg^{-1}	R^2	SE	p
A	29.30	139.92	0.99	2.26	<0.01
B	10.29	15.98	0.94	3.60	<0.01
C	17.12	53.96	0.98	2.60	<0.01
D	0.26	0.95	0.97	0.05	<0.01

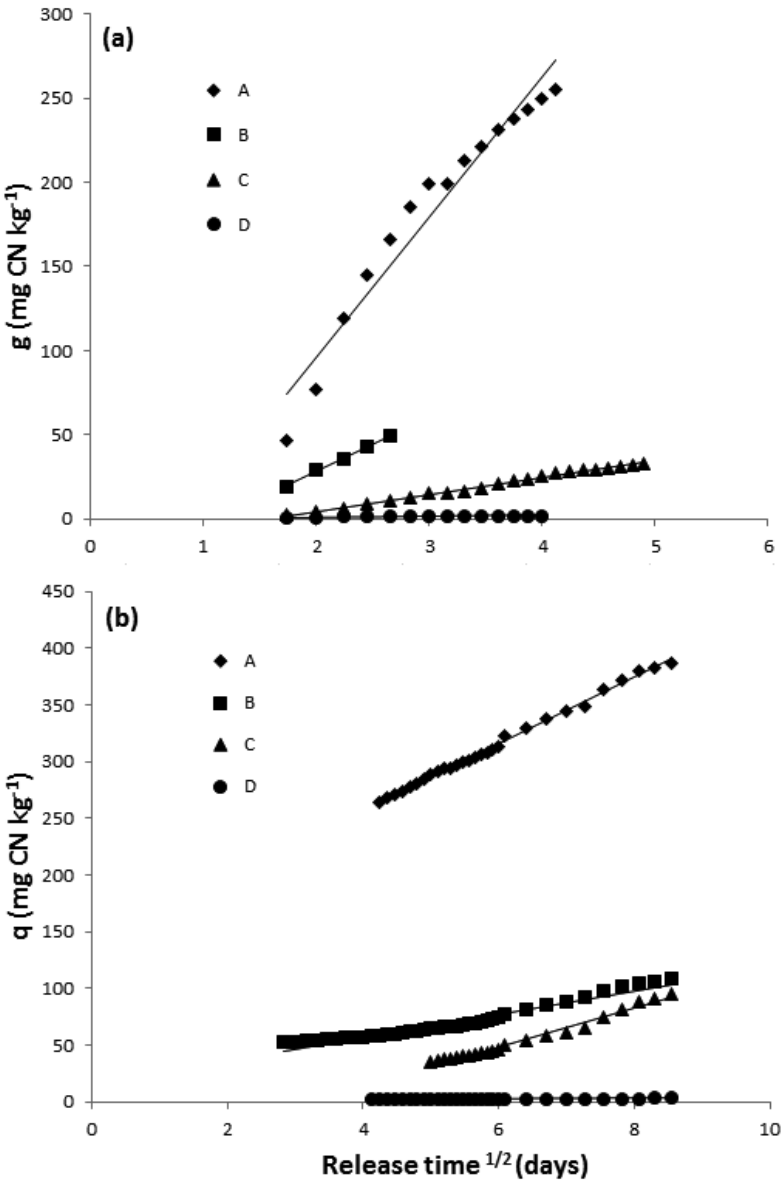

Figure 21: The parabolic diffusion equation plots for CN release from the MGP soils in (a) phase I and (b) phase II.

5.4.2.3 Freundlich Equation

The Freundlich equation was also used to describe the CN release from the MGP soils in a column experiment. The Freundlich isotherm is a power function, where "*v*" and "*k*" are constants. Isotherms of this form have been observed for a wide range of heterogeneous surfaces, including activated carbon, silica, clays, metals, and polymers (Umpleby et al., 2001). The release of CN in phase I and II was well modeled by the Freundlich equation (Figure 22).

In both phases (I and II), a power function was able to fit the data with a high degree of correlation: $R^2 > 0.93$ and $R^2 > 0.90$ respectively. Regression analysis (Tables 12 and 13) indicated significant (<0.01) correlation in all investigated soil. The Freundlich equation proved to be successful in describing both phases in CN release from the MGP soils.

Table 12: The Freundlich equation parameters and correlation coefficients for phase I CN release in the MGP soils.

	Phase I				
Soil	$v \times 10^{-3}$	k (day^{-1})	R^2	SE	p
A	427.60	81.40	0.97	7.30	<0.01
B	477.30	21.77	0.94	2.00	<0.01
C	596.50	5.58	0.98	0.70	<0.01
D	295.40	0.94	0.97	0.04	<0.01

Table 13: The Freundlich equation parameters and correlation coefficients for phase II CN release in the MGP soils.

	Phase II				
Soil	$v \times 10^{-3}$	k (day^{-1})	R^2	SE	p
A	278.40	117.00	0.99	3.60	<0.01
B	345.90	22.37	0.91	3.80	<0.01
C	948.70	1.60	0.99	2.70	<0.01
D	300.30	0.87	0.95	0.06	<0.01

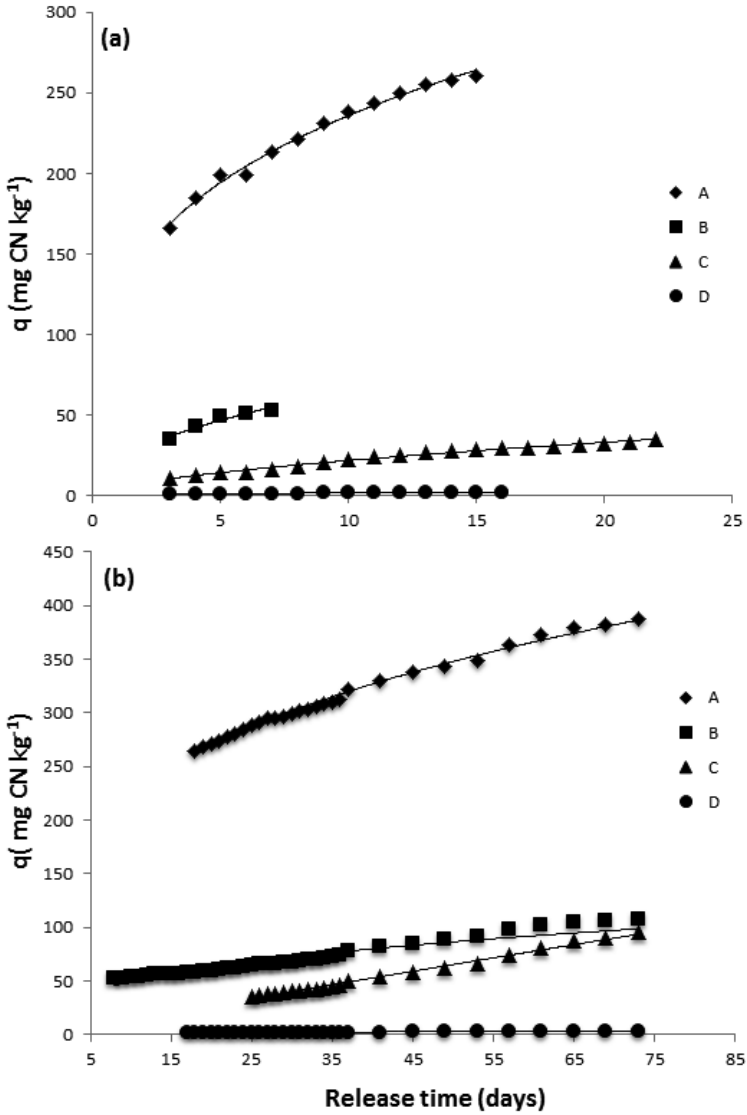

Figure 22: The Freundlich equation plots for CN release from the MGP soils in (a) phase I and (b) phase II.

5.4.3 Kinetic Model

Another consideration assumes that release of iron-cyanide complexes is constrained by two phases that occur simultaneously, which would suggest non-equilibrium liberation. In this approach transport phenomena of phase I is not considered separately from the slow chemical reaction of phase II. For this approach, a modified first order equation was used. The total released CN amount was determined as a sum of phase I and phase II (Equation 5.6), where each phase had its capacity and rate constant.

5.4.3.1 Multiple First Order Equation

A multiple, two-component first-order equation was used to describe the CN release form the MGP soils in a column experiment. Figure 23 represents fitted release curves for the investigated soils, the measured CN and the released quantities form both phases. Figure 23 shows that the two-component first order model provides a good fit of the experimental data for soil A, B and D. The multiple first order equation parameters and correlation coefficients are listed in Table 14. Applying this kinetic approach, it was assumed that each phase has its release rate (k), which is proportional to the amount present in a specific pool.

Regression analysis (Table 14) indicated significant (<0.01) correlation in all investigated soil. According to the correlation coefficient and standard error, a modified two-component first-order equation was successful in describing the experimental data from soil A, B and D. Slightly worse correlation was obtained for soil C (R^2 = 0.89; SE = 7.42).

Table 14: The multiple first order equation parameters and correlation coefficients for CN release in the MGP soils.

Soil	Phase I k_1 (day^{-1})	Phase II k_2 (day^{-1})	R^2	SE	p
A	0.17	0.53×10^{-2}	0.97	9.28	<0.01
B	0.37	0.01	0.92	4.14	<0.01
C	0.08	0.01	0.89	7.42	<0.01
D	0.5×10^{-2}	0.25	0.94	0.10	<0.01

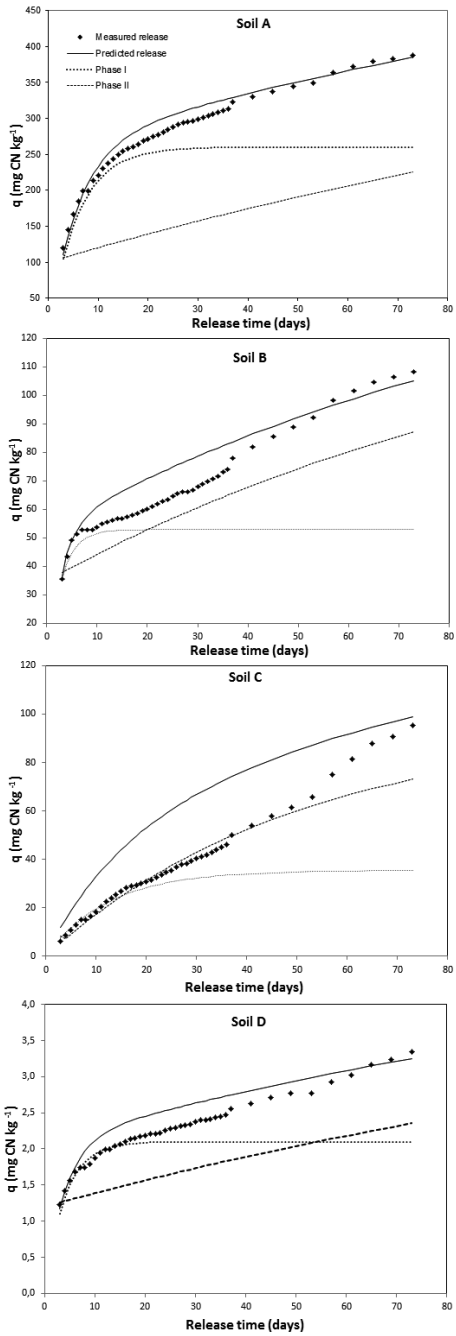

Figure 23: Cumulative measured CN release plots with predicted CN release, phase I and phase II, using the modified first order equation, for the MGP soils.

5.5 Discussion

In contaminated soils, on the sites of former MGPs, the mobility of iron-cyanide complexes is mainly governed by the dissolution and precipitation of ferric ferrocyanide and adsorption on soil minerals (Meeussen et al., 1992). The purpose of our work was to gain better knowledge concerning the iron-cyanide complexes release from the MGP soils by applying various isotherm and kinetic equations. The column experiment simulated the experimental conditions relevant to anthropogenically altered soils. The approach presented here assumes that the release of iron-cyanide complexes is constrained by two phases. According to Aharoni et al. (1991), the rate of release is rapid, when it is governed by the transport process taking place in the liquid phase, or diffusion in the bulk of the liquid, at the film adjacent to the solid particle, in liquid-filled pores, etc. Theis et al. (1986) attributed quick and complete desorption of ferricyanide from goethite to outer-sphere complexation.

If the release rate is slow, it is probably limited by the process taking place in the solid phase. It can be constrained by the constant dissolution of the ferric ferrocyanide like precipitate, which according to Mansfeldt and Dohrmann (2001) may originate from coprecipitation on the soil surface or from precipitation of iron-cyanide complexes with alkali and alkaline earth cations. Rennert and Mansfeldt (2001; 2002) proposed that slow and incomplete desorption of ferrocyanide was attributed to inner-sphere surface complexation, which occurs through the formation of direct chemical bonds with the mineral surface, (typically with surface oxygen atoms), and by precipitation of a Prussian Blue-like phase on the goethite surface.

Pursuant to the results obtained in the column experiment (Figure 19), it is believed that the release of iron-cyanide complexes from the contaminated soils can be described using two separate cyanide pools: one available (like transport of readily dissolved hexacyanoferrats or desorption of weak outer-sphere complexation) and one strongly fixed (like dissolution of precipitate in from of ferric ferrocyanide or desorption of inner-sphere complexation). Applying the isotherm models to the column experimental data required handling the phases separately in order to derive the release rate constants. Implementing the equations to the complete data set (Figure 19) resulted in very low correlations, which proves the hypothesis that the release of iron-cyanide complexes from the MGP soils is constrained by two phases.

The Elovich equation has been frequently used to study the chemical release processes and is suitable for systems with heterogeneous adsorbing surfaces (Wu et al., 2009). The kinetic behavior of inorganic materials like metals (Pb and Cu) has been successfully described by the Elovich equation (Aharoni et al., 1991; Jardine Sparks et al., 1984). Mathematical analysis of the CN release data indicated that the Elovich equation is suitable to describe the kinetic behavior of iron-cyanide complexes in the MGP soils (Figure 20). In the Elovich

equation, a decrease in "α" increases the reaction rate. In phase I (Table 8), the CN release rate increases with the increasing soil pH (Table 3), except for the soil D, where release rate is very low according to soil pH (7.7). The low release rate of soil D is most probably caused by the low total CN concentration (Table 3) hence, the cyanide release rate in phase I is influenced by the soil pH as well as the initial CN concentration in soil. Generally, in the desorption processes, one of the most important parameter is the initial pH value of the solution, which influences both the contaminant surface binding sites and the contaminant chemistry in water. Our findings are consistent with the study made by Ohno (1990), who investigated sorption of ferrocyanide by five soils, where increasing sorption was observed with decreasing soil pH. In phase II, the relation of "α" and "a" values are analogous with the ones obtained for phase I, where the release rates for phase I are higher than for phase II. Low pH of the soil C (pH = 5) most probably reduces the amount of readily dissolved iron-cyanide complexes in the phase I, which results in only slightly higher "α" values for the phase II. Lower, but still significant, was the correlation in soil B ($R^2 = 0.85$), which may be affected by the low OM content (Table 3). On the other hand, depending on pH, the overall charge of SOM is either neutral or negative, hence the anion adsorption cannot be expected. However, Rennert and Mansfeltd (2002) state that SOM promotes the sorption, hence the content of C_{org} is possibly enhancing the sorption of iron-cyanide complexes on soils. The suggested reaction for this process was the charge transfer complexes, formed by cyanide ion (CN^-), via cyanide-N with quinone groups of humic acids (Schenk and Wilke, 1984).

Simultaneously, the parabolic diffusion equation was used to describe the CN release from the MGP soils. This model has been used by many scientists to characterize the diffusion-controlled phenomena in soil constituents and the release of ion in soil and soil minerals (Evans and Jurinak, 1976). It assumes that described CN release is determined by the sum of various diffusion processes with different diffusion coefficients and various particle sizes. Linear relationship visible in phase II indicates (Figure 21) that the parabolic equation adequately describes the CN release process, suggesting that phase II is driven by the diffusion of CN out of the mineral matrix. On the other hand, in phase I, the regression line for the soil A doesn't pass through the origin, suggesting that the diffusion is not the main driving mechanisms. Additionally, in phase I, the "a" value was determined from the y-intercept (t = 0). The intercept is most probably affected by the rapid CN release, which would be much slower if not influenced by the transport of already dissolved phase. The apparent CN diffusion rate coefficient "K_d" in the parabolic diffusion law is considered the measure of the relative rate of CN release (Aharoni et al., 1991). The difference between the "K_d" values indicates that the release power of the soils is different. In phase I (Table 10), the "K_d" values for the studied soils were increasing with the increasing soil pH, except for the soil D,

which despite of the alkaline character, indicated low CN release, most probably induced by low initial CN concentration. Soil B, despite of acidic character, indicated comparably high CN release rate, which can be attributed to the low OM content. The diffusion coefficient "K_d" is higher in sandy soils with lower organic matter. More heterogenic soils are more likely to have an increase in transport-limited process (Aharoni et al., 1991). In phase II, the relative rate of CN release (K_d) seems to be affected by the CN concentration. Major decrease in "K_d" value can be noticed in soil A, despite of basic soil pH. Release rate in soil B also decreased, whereas in soil C, continuous release, comparable to the one obtained in phase I, can be observed (Table 11). Based on correlation coefficient it can be stated that the parabolic diffusion law effectively describes the phase II of CN release from the MGP soils. For the phase I, the results revealed ("*a*" value determined from the y-intercept) that the diffusion phenomena is not the driving mechanisms, however it doesn't imply that CN release does not include a slow diffusion reaction. It may rather indicate that the kinetics of this process shouldn't be considered separately from the transport phenomena. More study need to be done to determine whether CN release is driven by intraparticle diffusion, external-film diffusion or internal-pore diffusion.

Subsequently, the release of CN from the MGP soil was described using the Freundlich equation. This power function exhibits increasing release rate with increasing time, but decreasing positive slope as time increases (Figure 22). The Freundlich equation is often used for heterogeneous surfaces and describes desorption from solid to the solutes in liquid and assumes that different sites with several adsorption energies are involved. Many organics and inorganics follow this type of behavior (Chien and Clayton, 1980; Aharoni et al., 1991). According to mathematical analysis (Tables 12 and 13), the Freundlich reaction based model was successful in describing, both phase I and phase II, CN release from the MGP soils. The exception is phase I in soil A, where the regression line doesn't pass through the origin (Figure 22), suggesting that desorption is not the driving mechanism. Soil A is alkaline (pH = 7.6) and has high CN content, which would explain high amount of dissolved cyanide in the pore water and imply that the CN release in phase I is mainly constrained by the transport of readily dissolved compounds rather than desorption. The values of release rate coefficient "*k*", in phase I and II, decrease with the decreasing soil pH, except for the soil D, where low "*k*" value might be a result of low CN concentration in soil.

Applying the isotherm equations to the column data was aimed at better understanding the mechanisms of the CN release that, prior to the kinetic study, was divided in two phases. This modeling approach assumed that phase I and phase II are separated in time. Results revealed various release rates in both phases, implying that the driving mechanisms are different. The column experimental data for phase II showed good correlation with the Elovich, Freundlich and Parabolic Diffusion Equations leading to inconclusive results about

the driving mechanisms of the CN release. For the phase I, poor fitting of the regression line (Freundlich) and the negative intercept values (Parabolic diffusion), implied the transport of dissolved iron-cyanide complexes as the main process.

The First order equation was previously used by many researchers to describe time - dependent data (Nederlof et al., 1994; Freese, 1994). This modeling approach assumes that both CN release phases occur simultaneously. The modified first order model well described the CN release data (Table 14), which is supported by the graphical test presented in Figure 23. This result suggests that the release of CN from the MGP soils followed the multiple first order kinetics. Worst graphical and regressional correlation was obtained for soil C. The release of CN from soil C is almost linear, most probably due to low soil pH, constrained mainly by one strongly fixed pool. According to Meeussen et al. (1994) the mobility of cyanide in the soil largely depends on pH. Under acidic conditions, solid iron-cyanide complexes in the form of precipitated Prussian Blue are likely to be expected. It could explain why the two-component approach didn't manage to describe the kinetics of CN release from the soil C. Due to the low pH, the amount of dissolved iron-cyanide complexes is relatively low, so the difference in the release rates for phase I and phase II is relatively small (Table 14).

Rate constants for each soil vary (Table 14), indicating the highest release rate in soil B for phase I and in soil D for phase II. The low initial release rate in phase I for soil C is consistent with the study made by Meeussen et al. (1994). They stated that acidic character of soil will considerably decrease the CN concentration in groundwater and reduce the mobility of iron-cyanide complexes in such soils. High initial release rate (k_1) in soil B can be constrained by the low OM content, despite of a slightly acidic character of the soil. Using the multiple first order kinetic equation for modeling of the long-term cyanide release probably closer reflects the phenomena that occur in the MGP soils. It is more probable that the release of phase I and phase II appear simultaneously rather than completely separate in time.

5.6 Conclusions

The study of iron-cyanide complex release, in a column experiment, was conducted to investigate the long-term desorption or dissolution mechanisms. The research revealed that the cyanide liberation from the investigated MGP soils is driven by two phases. From the kinetic studies, it was observed that the cyanide release was initially rapid (phase I) followed by a much slower release rate (phase II). Most probably, one more fraction exists (an amount that is not released), but our experimental time scale didn't allow for that observation.

Modeling with isotherm equations, assuming that both phases are separate in time, delivered inconclusive results concerning the driving mechanisms for the cyanide release in phase II. The Elovich equation was in good agreement to describe the CN release in phase I and II, suggesting desorption from the heterogeneous surfaces to the liquid. Analogously good correlation was obtained by using the Freundlich equation, except for phase I in soil A, where too high CN content and alkaline pH imply transport of readily dissolved cyanide as a main driving release mechanism. The parabolic diffusion adequately describes the rate-limiting CN release (phase II), implying that it's driven by the diffusion of CN out of the mineral matrix. For phase I, obtained results imply that transport of dissolved cyanide is the main mechanisms. Indefinite results for phase II, obtained from applying the isotherm equations, most probably indicate that the long-term iron cyanide release from the MGP soils is a complex phenomenon driven by various mechanisms parallely involving desorption, diffusion and dissolution processes.

The multiple first order equation assumed simultaneous occurrence of both phases and adequately described the CN release from soil A, B and D, except for the soil C, where due to its acidic character, the CN mobility is most probably constrained by one strongly fixed pool. This non-equilibrium approach is considered to closer reflect the probable cyanide release mechanisms from the MGP soils.

Based on conducted isotherm and kinetic modeling, we attribute the fast release rate (phase I) to the transport process of readily dissolved iron-cyanide complexes (hexacyanoferrats) that is taking place in the liquid phase combined with the desorption of CN bound to heterogeneous surfaces that are in direct contact with aqueous phase (outer-sphere complexation).

Mobility governed on the low release level (phase II) is probably controlled by the desorption, dissolution or diffusion processes, like the dissolution of precipitated ferric ferrocyanide or of inner-sphere complexed ferricyanides.

The iron-cyanide release rates for phase I and II, obtained in the kinetic modeling, revealed that the CN mobility is mainly influenced by the pH (which affects both the contaminant surface binding sites and the contaminant chemistry in water), by the initial CN concentration and by the possible sorption on soil organic matter. The cyanide release rates increased with the increasing pH, decreased with low initial CN concentration and was retarded by the increase in OM content (Appendix III.2; Figures 38, 39, 40, 41).

6 Retardation of the iron-cyanide complexes in the soil of a former Manufactured Gas Plant site

The study presented in this chapter is being prepared for publication as: M. Sut, F. Repmann and T. Raab "Retardation of the iron-cyanide complexes in the soil of a former Manufactured Gas Plant site".

6.1 Abstract

The soil in the vicinities of former Manufactured Gas Plant (MGP) sites is commonly contaminated with cyanide, which primarily occurs in form of solid Prussian Blue (ferric ferrocyanide) and its dissolution products - iron-cyanide complexes ferri and ferrocyanide. The phenomenon of cyanide mobility in the soil has been intensively studied and according to the literature is mainly governed by the dissolution and precipitation of ferric ferrocyanide, which is only slightly soluble (< 1 mg L^{-1}) under acidic conditions. This paper suggests vertical transport of a colloidal ferric ferrocyanide, in the excess of iron and circum-neutral pH conditions, as an alternative process that influences the retardation of the pollutant movement through the soil profile.

Investigations of the two boreholes from a former MGP site revealed the highest cyanide contamination in the wastes layer (up to 824 mg kg^{-1}) that was partially vertically transported through the soil profile and retarded by a layer of soil material with coherent structure (CN concentrations up to 222 mg kg^{-1}). The acidic character of the wastes and the accumulation of the blue patches along the sandy soil layer revealed the potential sink function of a sandy loam material due to colloidal transport of the ferric ferricyanide.

Batch and column experiments were applied to investigate the retardation of iron-cyanide complexes by the sandy loam soil. In this study a colloidal vertical transport of the Prussian Blue particles along the column profiles, imitating the boreholes conducted on the former MGP site, was demonstrated as a potential alternative process influencing the cyanide mobility in the circum-neutral pH and under the excess of available iron conditions. Physical

and chemical properties of the investigated sandy loam material reduced the CN concentration in the percolation solution. Precipitated solid iron-cyanide complexes were mechanically filtered by the coherent structure of the investigated soil. Additionally, the reduction of the CN concentration of the percolation solution by the sandy loam soil was presumably induced due to formation of potassium manganese iron-cyanide ($K_2Mn[Fe(CN)_6]$).

6.2 Introduction

Until the discovery of the natural gas reserves in the middle of 20th century, all over the world Manufactured Gas Plants (MGPs) were producing gas for lighting and heating. Soils on the sites of the former MGPs are contaminated with the gas purification by-products, which contained high amounts of sulfur, tar and various complex iron-cyanides, mainly present in form of Prussian Blue (ferric ferrocyanide, $Fe_4[Fe(CN)_6]_3$) and its dissolution products.

During coal gasification hydrogen cyanide (HCN) was produced and hydrogen sulfide (H_2S) was formed from sulfur compounds in the coal. HCN and H_2S needed to be removed from the gas, prior to its distribution, due to their toxic and corrosive character (Mansfeldt et al., 2004). The raw gas was conducted through boxes containing wood shavings impregnated with hydrated iron oxide. By the reaction of HCN with the Fe-rich purifier material, iron-cyanide complexes, $[Fe(CN)_6]$, were formed, mostly in form of solid Prussian Blue. Additionally, the impurity in form of H_2S was removed from the raw gas, by the transformation into iron sulfides, which lowered the absorbing capacity of the iron oxide. Low content of the oxide in the purifier had to be restored by regeneration, which was based on the aerial oxidation producing reactivated iron oxide and sulfuric acid (Mansfeldt et al., 2004). When the absorbing capacity was entirely drained, it was often disposed on the site and used as a filling material (Kjeldsen, 1998). Both activities (regeneration and disposal) led to soil and groundwater contamination in form of iron-cyanide complexes, iron sulfide and elemental sulfur.

In the area of the former MGPs, the risk of groundwater contamination depends - besides site controlling factors such as geology and hydrology - mainly on the dissolution and precipitation of ferric ferrocyanide and the potential retention mechanism of its solid form as well as its dissolution products. Despite of the low solubility of Prussian Blue (solubility product constant Ksp = $10^{-84.5}$; Meeussen et al., 1992), dissolved iron-cyanide complexes are detected in the ground water (Meeussen et al., 1995; Rennert, 2002):

$$3\,Fe_4[FeCN)_6]_{3(s)} + 32\,H_2O \longrightarrow 4\,Fe_3(OH)_{8(s)} + 4\,[Fe(CN)_6]^{3-}_{(aq)} + 5\,[Fe(CN)_6]^{4-}_{(aq)} + 32\,H^+ \qquad (6.1)$$

According to the reaction above, in soils and groundwater at the former MGP sites, dissolved CN occurs mainly in form of iron-cyanide complexes: ferri ($[Fe(CN)_6]^{3-}$) and ferro ($[Fe(CN)_6]^{4-}$) cyanide. These cyanide compounds are not hazardous, but can be converted to extremely toxic free cyanide (CN^- and $HCN_{(g)}$) when exposed to sunlight (Meeussen et al., 1992).

The mobility of the dissolved iron - cyanide complexes can be influenced by a variety of chemical processes involving precipitation - dissolution, sorption - desorption, oxidation - reduction, microbial decomposition and complexation with inorganic ions (Theis et al., 1986; Meeussen et al., 1994; Mansfeldt et al., 2004). Generally, the solubility of ferric ferrocyanide increases with an increasing soil pH and with an increasing redox potential (Meeussen et al., 1994). Adsorption is a possible retention mechanism for iron - cyanide complexes transport in the soil profile. With decreasing pH the adsorption of iron - cyanide complexes on iron, aluminum oxides and clay minerals, which are positively charged under acidic conditions, increases. As a consequence, neutral and alkaline soils can retain the iron-cyanide species to a lower extent than acidic soils (Sut et al., 2013).

The purifier wastes supposed to contain large amounts of amorphous iron sulfide (FeS) and elemental sulfur, which amounted for 60 % of the purifier (Environmental Resources Limited, 1987). According to Rennert (2002), due to oxidation of sulfur species in soil, sulfuric acid is produced, which has an acidifying influence of the surrounding soils causing protonation of the soil particles surfaces. Dissolved anions in form of iron-cyanide complexes can be absorbed on these surfaces (Rennert, 2002). Another possible retention mechanisms, is the precipitation of the dissolved iron-cyanide complexes due to the availability of the iron generated by the oxidation of iron sulfide. The formed ferric ferrocyanide can be retained in the solid form due to low pH of the surrounding environment (due to the sulfuric acid production) and can be transported through the soil profile or filtered by the pore system. Ghosh et al. (1999b) studied the feasibility of using a reactive barrier, in form of sand mixed with elemental iron fillings, to attenuate the movement of iron-cyanide complexes in groundwater. The removal of dissolved cyanides was studied by conducting a column experiment where various cyanide containing solutions under various flow rates and sand to iron ratios were examined. The study indicated that using a reactive barrier, in form of elementary iron, decreases the cyanide concentration in the solution. According to Ghosh et al. (1999b), both ferro and ferricyanide in the neutral pH range do not adsorb onto sand and gravel material. As a consequence, the observed decrease in dissolved iron-cyanide complexes concentration was attributed to precipitation reactions (Ghosh et al., 1999c). According to Mansfeldt et al. (1998), Rennert and Mansfeldt (2002) and Wehrer et al. (2011), in the subsoils of former MGP sites, especially in acidic soils, a fraction of iron-cyanide complexes exists which has been transported as Prussian Blue colloids due to vertical migration.

However, this phenomenon was not proven yet, since it was not directly demonstrated.

As indicated above, the mobility of the iron-cyanide complexes in soil is reported to be mainly governed by the dissolution and precipitation reactions. The phenomenon of the possible vertical colloidal movement of the solid iron-cyanide compounds needs to be further investigated. Soil analysis of a two ≈ 7 m long boreholes, drilled on a former MGP site in Cottbus, revealed likely migration of the CN from the MGP wastes, through the sandy layer towards the coherent sandy loam material, which acted like a sink for the vertically transported iron-cyanide complexes. The acidic character of the MGP wastes and the soil would imply a colloidal transport rather than dissolution and precipitation reactions.

The objective of this study was to test whether the presence of the coherent sandy loam soil can affect the movement of the iron-cyanide complexes and to advance the knowledge concerning the potential of the Prussian Blue vertical colloidal transport in the soils of a former MGP site in Cottbus (Germany), using synthetic iron sulfide. Laboratory batch and column experiments were conducted to study the effectiveness of this approach for the cyanide reduction from the synthetic solution. Knowledge concerning the possible colloidal vertical transport of iron-cyanide complexes is of importance for better risk assessment of a groundwater contamination.

6.3 Materials and Methods

6.3.1 Sampling strategy and soil analysis

The description of the investigation site is presented in Chapter 2 (2.2). Own pre-studies showed that at the depth of about 1 m a layer of coherent soil, with a varying thickness (0.6 - 2.0 m) exists, which is characterized by high moisture and dense structure. The groundwater table is situated at a depth of about 7 m below the surface. The soil pH varies between 3.2 and 7.7 (Sut et al., 2012).

The sample material of 2 boreholes (A-21 and C-25) was collected using a hand driller. The locations of boreholes A-21 and C-25 are shown in Figure 7. The boreholes were about 7 m deep, reaching the groundwater table. Each 0.1 m, a soil sample was collected. Every second soil sample (every 0.2 m) was homogenized for the further analysis.

Uncontaminated coherent soil material was collected using a hand driller at the depth of 1 -2 m. The sampling point was located in the south-western part of the site. Grain size analysis of the uncontaminated coherent soil material was performed by sieving (> 20 μm) and X-ray granulometry (XRG) using the SediGraph 5120™ particle-size analyzer (Müller et al., 2009).

Total cyanide was determined using 20 g of soil that were extracted in 200 mL of 1 mol L^{-1} sodium hydroxide (1:10 ratio) for 12 h in an end-over-end shaker at 16 rpm. The extraction with sodium hydroxide (1 mol L^{-1}) provides an effective means for the determination of total cyanide species (Mansfeldt and Biernath, 2001). In order to force settling of soil particles, the extracts were centrifuged for 10 min at 3000 rpm. To liberate HCN from complexed cyanide, 5 mL of the extract were digested in an acidic environment using the micro dist system (Dimitrova, 2010). The micro dist system refers to the method of the Hach Company, US QuickChem Method 10-204-00-1-X approved by the USEPA (2008) (Sut et al., 2013).

Water soluble cyanide in the investigated soil was determined using 20 g soil sample extracted in 50 mL of distilled water (1:2.5 ratio) for 1 h with an end-over- end shaker at 16 rpm. Afterwards, the water extracts were centrifuged at 3000 rpm for 20 min, 20-30 mL were filtered through 0.45 µm syringe filters, which were conserved with 200 - 300 µL of 1 mol L^{-1} NaOH in order to preclude the loss of analyte. 5 mL of filtered extracts were distilled, according to the Method 10-204-00-1-X approved by USEPA (2008), and subsequently analyzed with FIA (DIN EN ISO 14 403 D, 2002). The detection limit for both extractions is 0.02 mg L^{-1} of cyanide in the analyte (Sut et al., 2013).

pH and EC of water extracts were studied with a bench pH/mV meter MultiLab 540 (WTW). Redox potential was measured with an Ag/AgCL HANNA HI 9025 electrode. Cations in water extracts were analyzed with an ICP Optical Emission Spectrometer icap 6000 series (Thermo Electron Corporation). For the anions analysis in the water extracts ion chromatography was used (ICS DIONEX DX 500). All the investigated samples were filtered through 0.45 µm syringe filters prior to analysis.

Organic matter was determined with Loss on Ignition method (LOI). 10 g of each soil sample were sieved (< 2 mm), placed in a porcelain beaker and heated up during the night at 105°C. This procedure was repeated until the change of mass was lower than 0.1 %. After recording the weight, samples were heated up at 450°C for 12 h. The LOI, hence the organic matter, was calculated as the percentage of the dry weight of the respective sample.

Concentrations of selected elements in soil (like heavy metals), were determined by an X-ray fluorescence (XRF) analyzer (Niton XL3t 900, soil model, powder samples with 120s of measurement) (Shefsky, 1997).

Soil spectra were recorded using FTIR spectrometer (Impact 410 Nicolet, resolution 4 cm^{-1}, 8 scans per sample (Mansfeldt et al., 2004).

6.3.2 Batch experiments

Uncontaminated coherent soil material (40 g) was homogenized, dried (40°C), sieved (< 2mm) and introduced to polyethylene bottles. 100 mL of the potassium hexacyanoferrate (III) and (II) (MERCK) solutions were added, with the CN concentration equal to 100 and 1000 mg L^{-1} respectively. The samples were shaken in an end-over-end shaker at 16 rpm. The experiment, where the solution with CN concentration equal to 100 mg L^{-1} was used, lasted for 216 h during which in defined time intervals (24 h; 72 h; 216 h) soil-water suspensions were centrifuged for 10 min at 3000 rpm in order to separate the phases. 2 mL of centrifuged sample was used for further analysis. The same procedure was repeated for the solution with the 1000 mg L^{-1} CN concentration, but the time range differed: the experiment lasted for 360 h and the measuring intervals were: 24; 48; 120; 192; 360 h. Both batch experiments were conducted in 2 replicates.

6.3.3 Column experiment: 1st trial

Two percolation columns were constructed from Plexiglas®(I.D. 5.4 cm; height 30 cm) to allow visual observations of the soil during the experiment. The tubes were positioned perpendicular to each other. First column was filled with quartz (MERCK; particle size 0.2-0.8 mm) up to 22 cm. In the second column, a 9 cm layer of coherent soil material mixed with quartz was added (1:1 ratio). Prior to implementing, the soil material was homogenized, dried (40°C), and sieved (< 2 mm). The experimental set up of the column experiment is shown in Figure 24a. The experiment was conducted at room temperature.

A peristaltic pump fed 1000 mL of potassium hexacyanoferrat (III) (MERCK) solution, to each column, per day in a continuous circular flow. The starting cyanide concentration in the percolated solutions was 1100 mg L^{-1}. Collected column leachates were analyzed for CN, pH and EC.

After two months of infiltrating the columns with potassium hexacyanoferrat (III) solutions, a layer of iron (II) sulfide (FeS) (Alfa Aesar; powder) was added at the top of existing quartz material in each column. The layer was composed of 500 mg FeS mixed with 25 g of quartz. The layer was additionally covered with a thin layer of pure quartz (Figure 24b). Column percolation was resumed and lasted for 2 weeks.

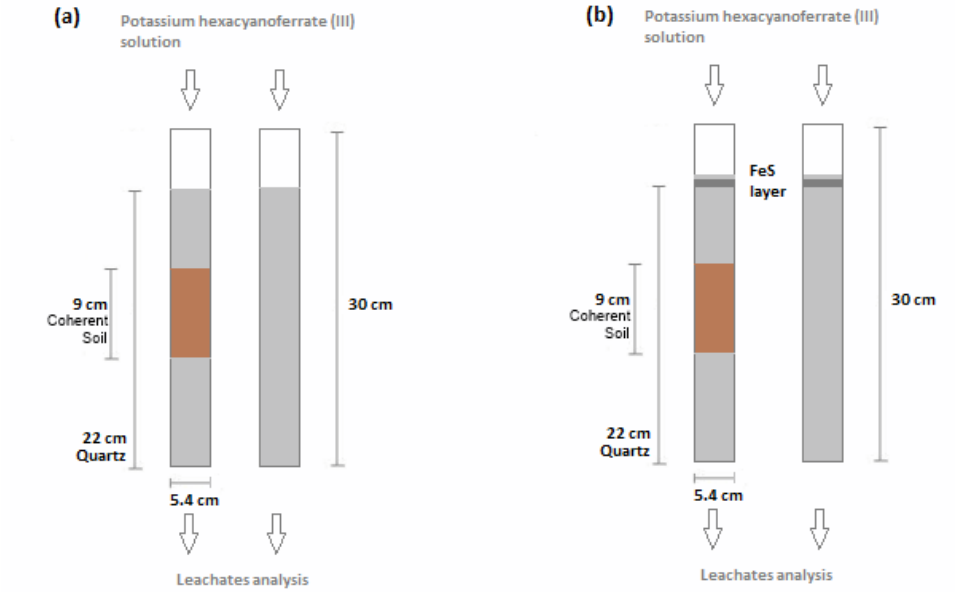

Figure 24: Set up scheme of the 1st column experiment, where: a) columns are filled with quartz and coherent soil material; b) columns are filled with quartz, coherent soil material and iron (II) sulfide.

6.3.4 Column experiment: 2nd trial

Five percolation columns were constructed from Plexiglas®(I. D. 5.4 cm; height 30 cm) and positioned perpendicular to each other. The experimental set up of the 2nd column study is shown in Figure 25. In first 3 columns from the left, coherent soil material mixed with the quartz (1:3; 1:1 and 3:1 ratio) was inserted (column no 1, 2 and 3 respectively). Two columns were completely filled with quartz (up to 22 cm) (column 4 and 5). In one of the quartz columns (column 4), two filter papers (Sartorius stedim biotech; 0.2 µm) were additionally built in (Figure 25). At the top of the quartz material, a layer composed of 0.84 g FeS and 25 g quartz, was inserted.

A peristaltic pump was percolating the potassium hexacyanoferrat (III) (MERCK) solution, with the starting CN concentration equal to 500 mg L^{-1} at the continuous circular flow, with a flow rate of 0.3 mL min^{-1}. Obtained column leachates were analyzed for pH, EC and CN concentration. The infiltration lasted for 47 days.

Subsequently, the columns were disassembled in order to conduct visual investigation of the filling material. The sample material was collected at the columns height of 3-5 cm (representing the upper layer of the quartz material), 7-9 cm (representing the upper layer of

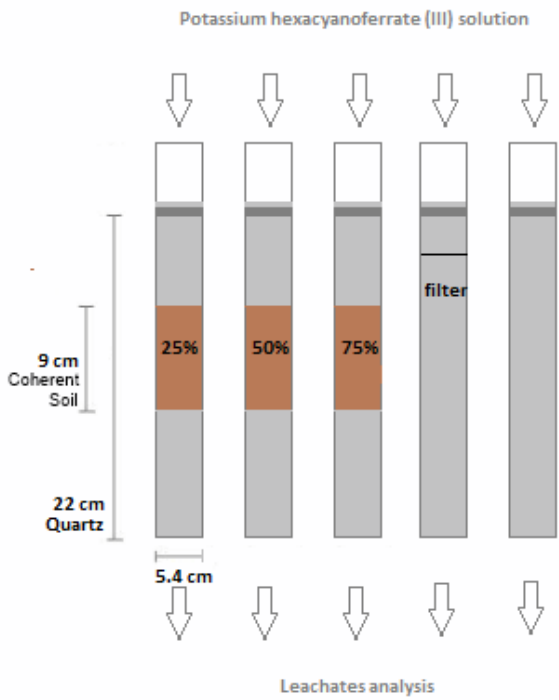

Figure 25: Set up scheme of the 2nd column experiment.

coherent soil material), 9-11 cm (representing the middle layer of the coherent soil material) and 15-17 cm (representing the quartz layer below the coherent soil material). In the column 4 and 5, the samples were collected at the bottom and at the top of the column. Collected samples were analyzed with the FIA for the water soluble and total cyanide, and additionally scanned with the FTIR.

During the experiment, blue precipitate in the bottom of the bottles containing percolation solution appeared. In order to determine the amount of CN precipitated in the bottles, the solutions were filtered (0.2 µm paper filters), the obtained precipitate was weighted and the CN mass was calculated. It was assumed that all the cyanide present in the blue precipitate, deposited in the bottom of the bottles, is in form of ferric ferrocyanide. The results of the cyanide balance are presented in Table 44 in Appendix IV.5.

6.4 Results

6.4.1 Uncontaminated coherent soil material analysis

The properties of the coherent soil are listed in Table 15. Material was collected at the depth of 1.0-1.9 m, every 0.1 cm a sample was collected for further analysis. In Table 15, range values of the investigated soil properties are provided due to similar results obtained in each sample. The soil pH is about 7. EC varies from 0.7 to 0.3 mS cm^{-1}. According to AG Boden (2005), the soil material is sandy loam (S13) (Table 16).

Table 15: Properties of the coherent soil material based on the fresh mass of the sample.

Depth (m)	pH	EC (mS cm^{-1})	Water content (%)	OM content (%)
1.0-1.9	6.84-7.25	0.7-0.3	9.26-12.69	0.29-1.07

Table 16: Particle size distribution analysis for the coherent soil material.

S	U	T	gS	mS	fS
		(%)			
72.4	18.1	9.9	4.8	32.1	35.5

6.4.2 Borehole A-21

The properties of the soil collected in the borehole A-21 are listed in Table 28 (Appendix IV.1). The material was collected up to 7.3 m (the level of groundwater table) and every second 0.1 m was subjected to analysis. Visual observation of the collected material revealed that up to 0.3 m depth, dark brown top soil occurs. At the depth between 0.4 to 1.0 m a layer of MGP wastes exist, characterized by the blue color and strong smell of heavy hydrocarbons. At the depth of about 1.0 to 1.4 m a sandy soil layer occurs, which is followed by a highly moist and coherent sandy loam layer (1.5-2.0 m) with intensive blue color patches. Rest of the soil profile (below 2.0 m) is composed of reddish sandy material. The soil pH varies between 4.4 and 7.4. Elevated EC values were measured in the depth between 1.5 and 1.7 m (coherent structure), which correlates with the high sulfate and calcium concentrations (Table 29 in Appendix IV.1). Water soluble cyanide fraction ranged from 0.3 to 23.7 mg kg^{-1}, with the highest concentration measured in the MGP wastes layer (Figure 26). Total cyanide concentrations ranged from 2.3 to 824.0 mg kg^{-1}, with the highest total content measured in the MGP wastes and the coherent sandy loam layer (Figure 26).

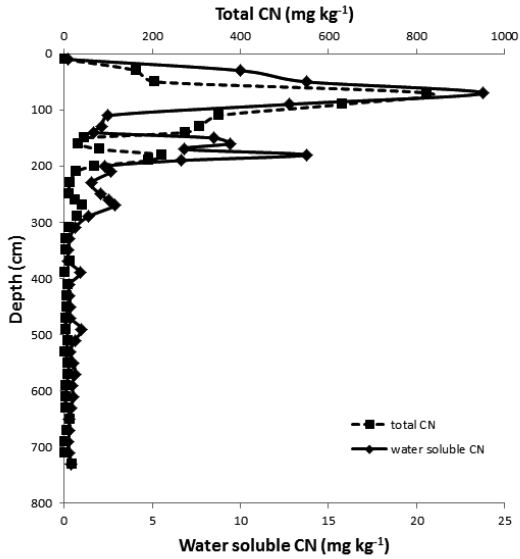

Figure 26: Total and water soluble cyanide concentration v/s depth in the soil borehole A-21.

XRF analysis (Table 30 in Appendix IV.1) revealed very high Fe concentrations along the borehole, whereas Ca, K and S concentrations were elevated up to 2.0 m depth. Soil samples collected at the depth of 0.4-0.5 m (representing the MGP waste layer) and at the depth of 1.5-1.6 m (representing the coherent sandy loam layer) were scanned with the FTIR spectrometer. The analysis revealed the infrared absorption bands at 2026 and 2087 cm^{-1}, in the waste material sample, indicating ferricyanide adsorbed on goethite and ferric ferrocyanide respectively (Rennert et al., 2007). The analysis of the coherent sandy loam material additionally indicated the presence of potassium manganese iron-cyanide ($K_2Mn[Fe(CN)_6]$) at the wavenumber 2067 cm^{-1} (Keizer et al., 1995; Rennert et al., 2007).

6.4.3 Borehole C-25

In order to confirm the analogous behavior of the cyanide in the soil at the MGP Cottbus, a second long borehole was investigated. The soil was collected up to 7.1 m (groundwater table) and every second 0.1 m of the material was subjected to further analysis. The properties of the soil are listed in Table 31 (Appendix IV.2). Visual observation of the collected material indicated dark, brown top soil up to 0.4 m depth mixed with the MGP wastes. Beneath a sandy layer occurred (up to 0.8 m), which was followed by the moist coherent material, analogues to the one found in the A-21 borehole and characterized by the blue color patches

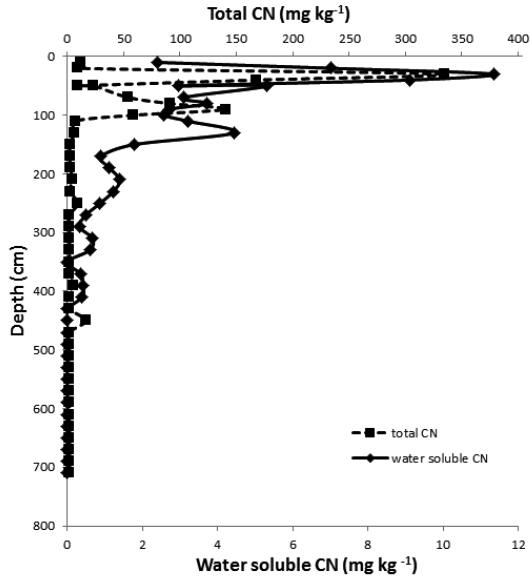

Figure 27: Total and water soluble cyanide concentration v/s depth in the soil borehole C-25.

(up to 1.3 m). Rest of the borehole was composed of sand. The soil pH varies between 5.3 and 7.9. Slightly elevated EC values at the depth of 1.1 to 1.3 m correlate with the increased sulfate and calcium concentrations (Table 32 in Appendix IV.2) and with the higher content of Fe, Mn, S, Ca and K obtained from the XRF analysis (Table 33 in Appendix IV.2).

Water soluble cyanide fraction reached up to 11.3 mg kg^{-1}, with the highest values measured in the MGP wastes close to the top soil (Figure 27). Total cyanide content deviated from 2.0 to 334.0 mg kg^{-1}, with the highest total cyanide content measured in the MGP wastes and coherent sandy loam (Figure 27). FTIR analysis was performed for the waste sample (0.3-0.4 cm deep) and for the sandy loam material (0.8-0.9 cm). The analysis revealed the infrared absorption bands at 2026 and 2087 cm^{-1}, in both samples, indicating ferricyanide adsorbed on goethite and ferric ferrocyanide respectively (Rennert et al., 2007).

6.4.4 Batch experiments

Laboratory analysis of the sample martial, originating from the two long boreholes (A-21 and C-25) collected at the MGP Cottbus, indicated the highest total and water soluble cyanide concentrations in the MGP wastes and the coherent sandy loam layer. Iron-cyanide complexes appeared to be transported/leached from the MGP wastes layer verti-

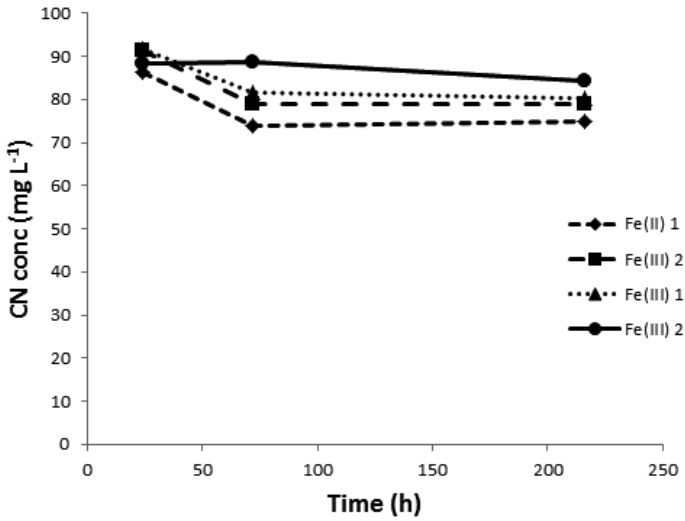

Figure 28: CN concentrations in the 100 mg L^{-1} (start concentration) solution v/s shaking time in the batch experiment.

cally through the profile, but seemed to be successfully held by the coherent sandy loam material.

Results obtained from the batch experiments indicated that the presence of sandy loam material leads to a decrease of the CN concentration in the solutions. In Figure 28 the CN concentration in the 100 mg L^{-1} (start concentration) solution v/s shaking time is shown. For the Fe (II) 1 & 2 solutions, the reduced CN amount was equal to 26 and 21 % respectively. Fe (III) solutions indicated slightly higher decrease, equal to 20 and 16 % (after 216 h). The pH of the solutions stays within the neutral range (6.9-7.1). In Figure 29 the CN concentration in the 1000 mg L^{-1} (start concentration) solution v/s shaking time is shown. During this experiment, disturbances with the measuring device (FIA) occurred, which can be observed in Figure 29 in the CN concentration measured at 120 and 192 h. As a consequence, the batch experiment was prolonged until 360 h of shaking. In Figure 29 it can be seen that the CN concentration decreases in both solutions (Fe (II) and (III)), which amounts to 27 % of CN amount reduced from the Fe (II) 1 solution and 17 % from the Fe (II) 2 solution, and 17 % and 19 % for the Fe (III) 1 & 2 solution respectively. The pH of the solutions is in the range of 6.7-7.2. Raw data of the both batch experiments is presented in the Appendix IV.3.

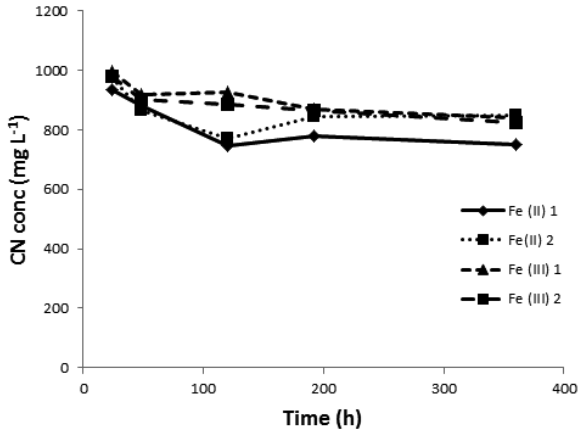

Figure 29: CN concentrations in the 1000 mg L^{-1} (start concentration) solution v/s shaking time in the batch experiment.

6.4.5 1st column experiment

The results of the batch experiments with the sandy loam material revealed a reduction of cyanide concentrations in the applied potassium hexacyanoferrat solutions. Generally, batch experiments promote destroying of soil aggregates and, as a consequence, can lead to artificial promotion of potential reactions, that in the reality would last longer or appear to limited extend. In order to more competently simulate cyanide behavior in soil profiles, a column experiment was conducted, imitating the boreholes A-21 and C-25, where the potassium hexacyanoferrat (III) solution, containing 1100 mg L^{-1} CN, was percolated through the sandy loam and quartz material (Picture 4a). In Figure 30, the measured CN concentration in the solution v/s percolation time is shown. In both columns, during the first two months of the experiment, a very minor loss of CN in the solution was measured. No blue patches or particles were noticed throughout the column material, indicating no reaction in form of ferric ferrocyanide precipitation (Picture 4a).

Subsequently a layer of FeS was implemented, which resulted in the presence of blue particles already within first 24 h of resumed percolation (Picture 4b). In the column filled only with the quartz material the blue-greenish color was visible throughout the whole profile as well as in the bottle containing the percolation solution (Picture 4b). The color of the solution changed from yellow to very dark blue-greenish pigment. In the column with the sandy loam layer, only the upper quartz layer was affected, the color of the quartz layer beneath, as well as the percolating solution, appeared intact (Picture 4b). The dark blue-greenish

solution was filtered twice with 0.45 and 0.2 µm syringe filters (Picture 5) revealing that the color is a result of very fine particles. The reaction of FeS and potassium hexacyanoferrat (III) can be explained in the following reactions:

$$FeS + 1\,{}^{1}/_{2}\,O_2 + H_2O \longleftrightarrow Fe^{2+} + SO_4^{2-} + 2H^+ \quad (6.2)$$

$$2K_3[Fe(CN)_6] + 3FeSO_4 \longleftrightarrow Fe_4[Fe(CN)_6]_3 + 3K_2SO_4 \quad (6.3)$$

The possible reaction of dissolved iron-cyanide complexes with FeS can be also noticed in Figure 30. In Figure 30 it can be seen that after implementing the FeS layer (after 63 days of percolation with potassium hexacyanoferrat solution) the measured CN concentration in both columns was reduced. In the quartz column, about 2 weeks of percolation with the additional FeS layer, CN concentration in the solution decreased by 18 %. In the column with the sandy loam layer, the amount of CN in the solution decreased by 41 %. In the column filled with quartz material the pH increased slightly from 5.9 to 6.5. In leachates obtained from the column filled with sandy loam material the pH value stayed relatively stable (6.2). Raw data of the 1st column experiment are presented in the Appendix IV.4.

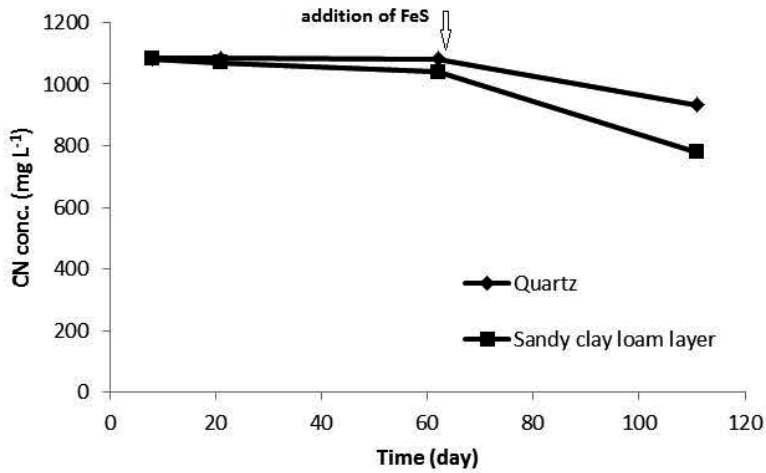

Figure 30: Measured CN concentration v/s percolation time in the 1st column experiment.

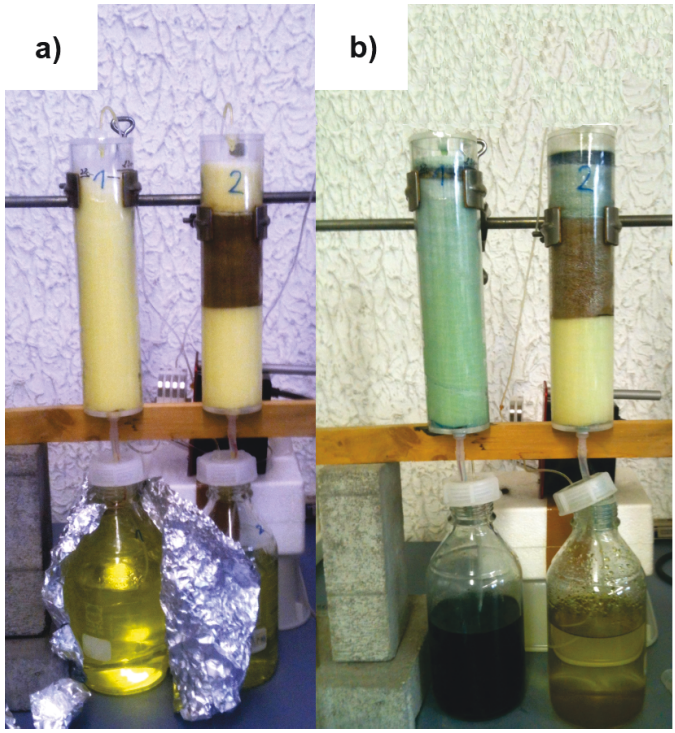

Picture 4: 1st column experiment after a) 1 month of percolation; b) adding FeS layer.

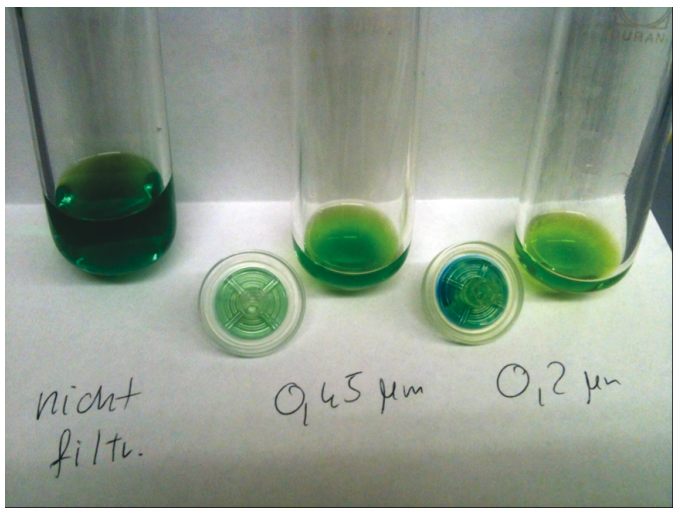

Picture 5: Filtration of the blue-greenish percolation solution from the column filled only with quartz.

6.4.6 2nd column experiment

1st column experiment resulted in no significant CN loss from the percolating solution, prior to the application of the iron sulfide layer, where the dissolved iron-cyanide complexes (in form of potassium hexacyanoferrat (III)) reacted with FeS producing blue-greenish precipitate. 2nd column experiment was performed to investigate the effect of the iron excess (FeS) and different quartz-sandy loam soil ratio on the potassium hexacyanoferrat (III) solution.

In Figure 31 the measured CN concentrations in the percolating solution v/s the infiltration time is shown. Analogous trend of the CN behavior can be noticed in all columns initiated by the strong decrease (first 5 days) and followed by the continuous reduction of the cyanide concentration on a low level (Figure 31). After 3 days of percolation the column with the inserted paper filter (column 4) became impermeable, the flow in the column was sustained, however under lower infiltration rate. Raw data of the 2nd column experiment are presented in Appendix IV.5. The pH of the percolating solutions increased from ≈ 6.4 (beginning of the experiment) to ≈ 7.2 (end of the experiment) (Appendix IV.5).

Visual observation of the bottles containing percolation solutions revealed strong green coloration, especially in column 1, 4 and 5 and slightly in column 2 (Picture 7), which during the experiment deposited in form of blue precipitate in the bottom of the bottles (Picture 6). The results of the cyanide balance calculations, obtained for the 2nd column experiment are presented in Table 44 in Appendix IV.5. Subtracting the mass of the precipitated cyanide

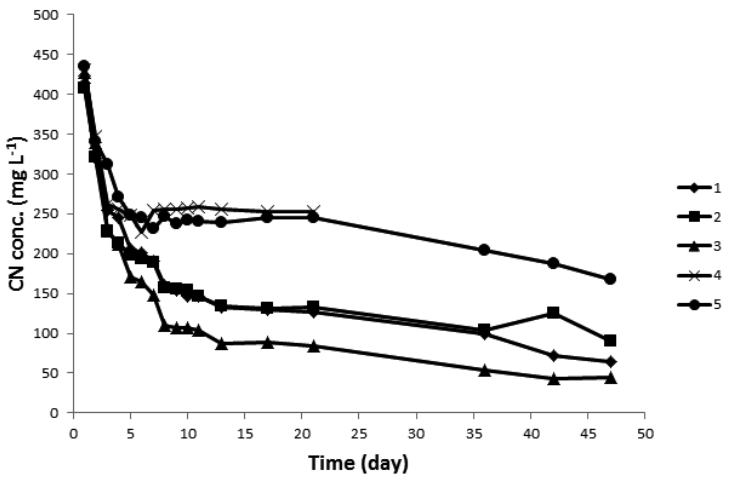

Figure 31: Measured CN concentration v/s percolation time in the 2nd column experiment.

Picture 6: Bottle with the percolation solution with the visible blue precipitate in the bottom.

and the mass of the cyanide present in the solution (in the end of experiment) from the starting CN mass revealed the highest decrease in the cyanide mass in column 3 and the lowest in column 5. A balance for column 4 was not obtained due to high loss of the solution during the experiment. According to Table 44 (Appendix IV.5), the lowest mass of the precipitated CN was weighted in column 3, whereas the highest was obtained in column 5.

Visual observation of column 5 revealed blue patches along the total length of the column and the change of the infiltrating solution to blue-greenish (Picture 7). In column 4, blue patches were visible only above the filter layer, however the color of the solution changed to blue-greenish (Picture 7 and 8). Visual observation of the column 1 revealed blue patches through the whole length of the column (Picture 9) and noticeable change in the color of percolating solution (Picture 7). In column 2, blue particles were also observed through the whole column, however the quartz layer beneath the sandy clay loam material was only slightly influenced (Picture 9). The color of the infiltration solution changed to very light green. In column 3, blue patches were observed within the sandy loam layer and above it (Picture 7), but the quartz material beneath was "clean" (Picture 9). The color of the infiltration solution didn't change (Picture 7).

After finalizing the experiment, the columns were carefully disassembled in order to make visual observation of the filling material (Picture 10). Picture 11 indicates analogous behavior (blue patches) of ferric ferrocyanide in the sandy loam layer, as well as in the quartz material to the one observed in the material collected from the boreholes at the MGP site in Cottbus. Results of the total and water soluble CN concentration in the different layers of column

3 are presented in Figure 32. The rest of the results are presented in the Appendix IV.5. Figure 32 indicates analogues spatial distribution of the cyanide concentration within the soil column to the ones observed in the boreholes A-21 and C-25 (Figures 24, 25 and 26), where the lower CN concentration is observed, in the sandy layer under the MGP wastes, prior to the increase within the coherent sandy loam material layer (column: 7-12 cm) and to the very low concentration in the sandy layer beneath.

Picture 7: The 2nd column experiment after 20 day of percolation.

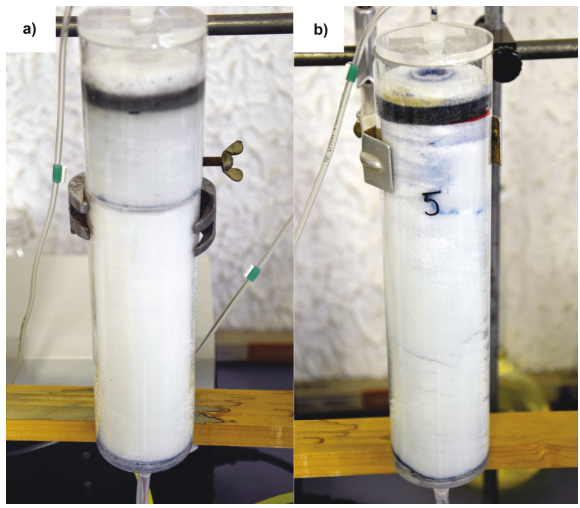

Picture 8: Columns filled with quartz material: a) with the paper filter, b) pure quartz.

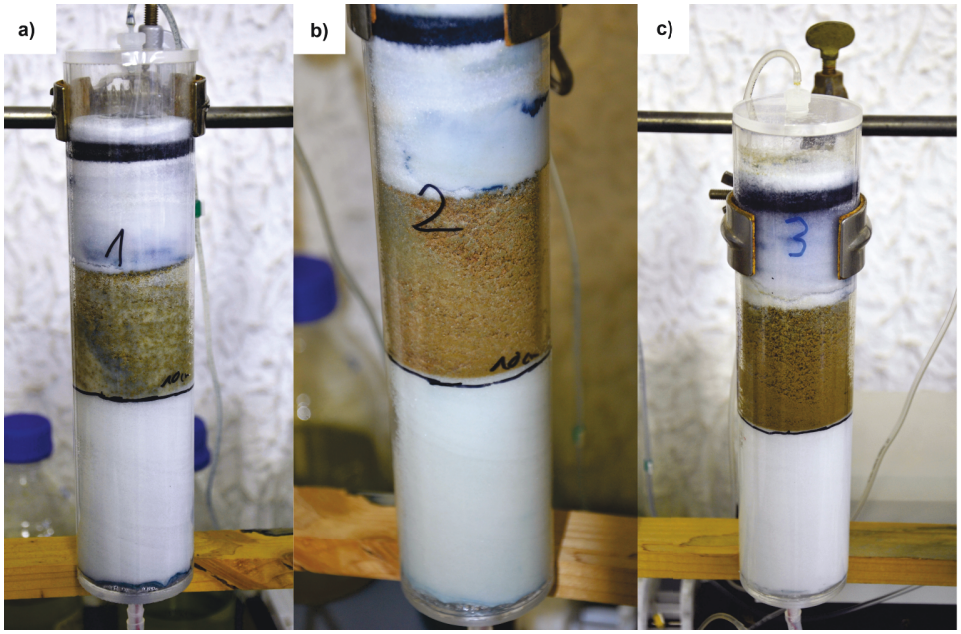

Picture 9: Columns filled with sandy loam layer and quartz material in ratio a) 1:3, b) 1:1 and c) 3:1.

Picture 10: Disassembling of the column experiment and investigating the material.

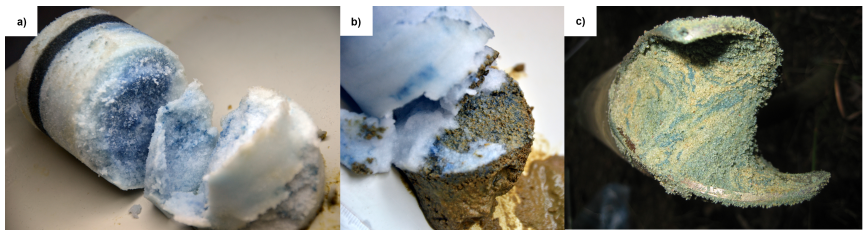

Picture 11: Blue patches occurring in the a) column quartz material, b) column sandy loam material and c) sample collected at the MGP Cottbus site.

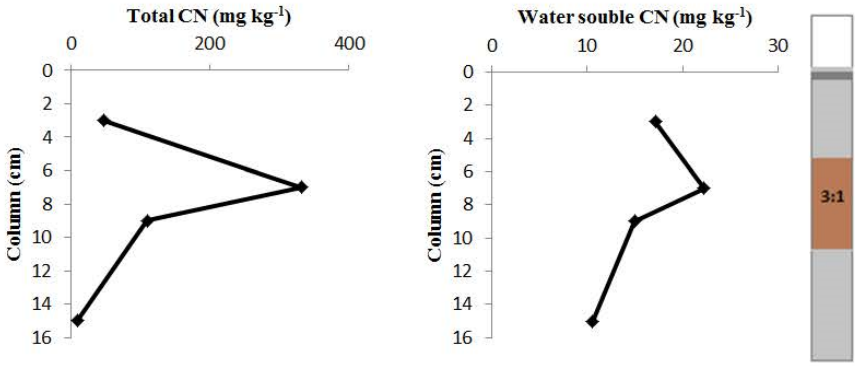

Figure 32: Vertical distribution of the total and water soluble cyanide concentration in the column 3.

Subsequently, the disassembled columns material was sampled and analyzed using the FTIR spectroscopy in order to characterize the iron-cyanide complexes. According to Rennert et al. (2007), the wavenumbers ranging from 2200 to 2000 cm^{-1} are relevant regarding the CN stretching vibrations. The FTIR spectra of the column no. 4 and 5 (quartz material) revealed the presence of ferric ferrocyanide (2092 and 2084 cm^{-1}), so called soluble Prussian Blue ($KFe(Fe(CN)_6$) with the absorption band at 2077 cm^{-1}. The presence of potassium ferrocyanide was revealed (2044 cm^{-1}), which is likely a product of a reduction of the potassium ferricyanide from the percolating solution.

The FTIR analysis of columns with the sandy loam soil revealed corresponding adsorption bands to the ones obtained for column 4 and 5. Additionally, a band that occurred at 2067 cm^{-1} was analogous to the spectral response in the borehole A-21 (100-110 cm sample), which according to Rennert et al. (2007) indicates the presence of the solid potassium manganese iron-cyanide ($K_2Mn[Fe(CN)_6]$).

6.5 Discussion

In this study batch and column experiments were conducted to investigate and simulate the retardation of the iron-cyanide complexes through the soil profiles. Own research (boreholes A-21 and C-25) conducted at the MGP Cottbus revealed the likely migration of the cyanide, from the MGP wastes layer through the sandy soil beneath it, towards the sandy loam layer, characterized by the high CN concentrations and agglomerations of blue patches. Very low CN concentrations were detected in the sandy layer below (Figure 26 and 27). The vertical distribution of the cyanide concentration in the boreholes A-21 and C-25 implies the retardation of the cyanide by the sandy loam material.

There are few studies dealing with the adsorption of iron-cyanide complexes on soil and minerals as a possible retention mechanism (Alesii and Fuller, 1976; Fuller, 1985; Meeussen et al., 1994; Kang et al., 2010) that commonly state that soils with acidic pH are the most effective in the retention of iron-cyanide complexes. Low soil pH enhances the adsorption of negatively charged Fe-CN complexes on iron or aluminum oxides and clay minerals, which are positively charged under acidic conditions. Additionally, under acidic pH, the dissolved iron-cyanide complexes may precipitate in the solid form ferric ferrocyanide, which additionally attenuate the movement of contaminants in the soil profile. According to Mansfeldt et al. (1998) and Rennert and Mansfeldt (2002), in acidic soils, the precipitated Prussian Blue can be subjected to colloidal vertical migration.

Batch experiments revealed a reduction of the CN concentration in the solutions, indicating slightly higher decrease for potassium ferrocyanide (≈ 22 %) than for potassium ferricyanide (≈ 18 %). According to Rennert (2002), ferrocyanide is possibly sorbed due to inner-sphere complexation on goethite, up to pH = 9. Theis et al. (1986) stated that ferricyanides form mainly outer-sphere complexes and that their formation is dependent on the electrostatic attraction that increases with decreasing pH value. Slightly higher reduction of the CN concentration in the potassium ferrocyanide solution can be attributed to the circum-neutral pH of both batch experiments that, according to the literature, decreases the electrostatic attraction, negatively influencing the outer-sphere complexation of ferricyanide.

Additionally, the decrease in CN concentrations in the batch solutions can be induced by the possible precipitation reaction in form of ferric ferrocyanide. Rennert (2002) proposed that part of the ferrocyanide, that is not absorbed on the goethite surface reacts with $Fe^{(3+)}$ ions in the solution and precipitate in form of Prussian Blue. Generally, the ferric ferrocyanide reaction has been considered to be dependent on the reduction of ferricyanide to ferrocyanide, and in the presence of the ferric ions, the consequent formation of Prussian Blue (Lillie and Donaldson, 1973). Both batch experiments were conducted under saturated

water conditions that decrease the reduction of ferricyanide to ferrocyanide and as a consequence, potential precipitation in the solid form.

On the basis of the batch experiments results it is difficult to define, which mechanisms (outer or inner-sphere sorption or precipitation reaction) influences the CN decrease in the solutions. Additional investigations of the sandy loam material from the MGP Cottbus, concerning the type of the clay mineral (Table 15), may help in closer interpretation of the sorption mechanisms.

Once the efficiency of the sandy loam material to reduce the CN concentration in the batch tests was demonstrated, a series of column experiments were performed to investigate this process. In the 1st column experiment, initially no change in the CN concentration was measured (Figure 30). 2 months of percolation with the potassium ferricyanide solution revealed only a very slight decrease: 2 % in the quartz and 6 % in the column with the sandy loam material. According to Theis and West (1986), ferricyanide complexes can sorb onto iron and aluminum oxides, especially at the lower (acidic) pH values. Ghosh et al. (1999c) stated that in the neutral pH range ferro and ferricyanide complexes do not absorb onto sand and gravel material. According to the results obtained in the 1st column test, the experimental conditions (slightly acidic pH and oxic environment: Table 38 in Appendix IV.4) were not favorable for the reduction of the cyanide concentration via sorption reactions.

As it was mentioned in the introduction, the purifier wastes contained large amounts of amorphous iron sulfide (Environmental Resources Limited, 1987), which could have an acidifying effect on soil due to the formation of sulfuric acid, causing protonation of the surfaces and supplying the iron excess, generated by the oxidation of iron sulfide, which could enhance the iron-cyanide complexes to precipitate in the solid form (ferric ferrocyanide). Subsequently, a layer of synthetic FeS mixed with quartz sand material was implemented on top of both columns, which resulted in a CN decrease in the solution amounting to 18 % in the quartz and 41 % in the sandy loam material (Figure 30). According to Ghosh et al. (1999a), Prussian Blue and Turnbull's Blue are two primer stable solids formed on addition of iron to solutions of cyanide or iron-cyanide complexes. Prussian Blue forms at lower pH and greater pE values, whereas Turnbull's Blue forms at a range of pH values, from low to high, but under anoxic conditions (Ghosh et al., 1999a).

Additionally, in the column containing exclusively quartz material, the percolating solution changed color from yellow to green (Picture 4). Ghosh et al (1999b) suggested that the decrease in the CN concentration in sand at pH below 7 is not a result of adsorption, but the precipitation due to the effectiveness of $Fe^{(2+)}$ and $Fe^{(3+)}$ dissolution. According to Ghosh et al., (1999c) cyanide in groundwater will be transported as a non-reactive species at sites with sand-gravel aquifer material. Filtering (< 2 µm) of the percolation solution obtained

from the quartz column indicated that the green coloration is a result of blue particles (Picture 5). The method used for the cyanide concentration measurement in column leachates (digestion with acid) does not digest the CN in the solid form (ferric ferrocyanide), which implies that the reduction of the CN concentration in the quartz column is attributed to the precipitation reaction, induced by introducing FeS, and the vertical transport of the colloids through the quartz material to the solution. According to Dzombak et al. (2006) many researchers highlight the potential importance of iron-cyanide solid colloidal transport in acidic soils, however this phenomenon has never been directly demonstrated. According to Mansfeldt et al. (1998) Prussian Blue is known to form colloids and its transport do not necessary require the dissolution and reprecipitation processes.

Visual observation of the column with sandy loam soil revealed no color change in the percolating solution (Picture 4a), which implies additional physical filtering properties of the coherent material. Vertical colloidal transport of the particles was most probably inhibited by the smaller pore spaces that physically induce the filtration effect and influence the water flux, which is not as steady as in the quartz matrix. Colloids are particles with effective diameters less than 10 μm (McCarthy and Zachara, 1989) so that transport is highly dependent on the colloid size and soil grain size distribution (Scott et al., 2002). Natural porous media exhibit a wide range in pore size due to variation in grain size, orientation and configuration and surface roughness (Scott et al., 2002). Another phenomenon affecting the colloid transport is straining, so the trapping of colloids particles in the down-gradient pores that are too small to allow physical particle passage (McDowell-Boyer et al., 1986), which can also be explained as a mechanical filtration. Generally, colloid straining is mainly controlled by the size of the colloid and the soil pore size distribution. However, many chemical factors, like pH, ionic strength, surface charge, chemical composition, influence the aggregating behavior of the colloids. Nevertheless, except of the apparent mechanical filtration properties of the sandy loam material, additional reduction of the CN concentration can be attributed to the possible chemical effects like sorption reactions or formation of new compounds.

Results obtained in the 2nd column experiment indicated cyanide reduction in the percolation solutions in all 5 columns (Figure 31). Despite of the analogous trend of the CN concentration decrease in Figure 31, it can be noticed that columns containing coherent sandy loam material more efficiently reduce the cyanide in the solution.

In column 4 and 5, visual observation of the quartz material and percolation solutions imply that CN reduction is a consequence of the precipitation reaction. This assumption is supported by the fact that paper filter, implemented in the column 4, was promptly impermeable due to accumulation of precipitated iron-cyanide complexes. The FTIR analysis of the quartz material from column 4 and 5 indicated the presence of ferric ferrocyanide and

soluble Prussian Blue, which is expected in the presence of additional K+ ions. Mansfeld et al. (1998) and Ghosh et al. (1999b) reported dark blue solids in the soil profiles from a MGP site and column experiment using a sand-gravel material, respectively. The agglomeration of the colloid iron-cyanide complexes (blue patches), observed in column 4 and 5 (Picture 8 and 11), can be a consequence of a time-dependent retention, which is reported to be a result of differences in the behavior of colloids on clean porous media and on media already containing colloids (Johnson and Elimelech, 1995). Therefore, colloids that are retained in the smaller pores decrease the effective pore size and may therefore increase subsequent particle retention in these pores (Scott et al. 2002). Visual observation of the 2nd column experiment indicated the capacity of the sandy loam material to physically filter the CN colloids from the percolating solution. This finding is supported by the cyanide balance presented in Table 44 in Appendix IV.5, where the mass of precipitated CN in the bottle is decreasing with increasing quartz-sandy loam soil ratio.

Noticeable difference in the reduction of cyanide concentration between columns containing a sandy loam layer and columns packed exclusively with quartz material indicate additional chemical effects of the coherent soil. The FTIR analysis of the disassembled column material, indicated the presence of the solid potassium manganese iron-cyanide ($K_2Mn[Fe(CN)_6]$) (Rennert et al., 2007). Keizer et al. (1995) suggested that for soils with higher pH (pH > 5) equilibrium exists with manganese iron cyanide ($Mn_2Fe(CN)_6$), which in the excess of K^+ ion can be found in the form of potassium manganese iron-cyanide. They suggested that the mobility of cyanide is highly influenced by the amount of available manganese and solubility of the manganese oxide present in soil. They stated that the iron cyanide solubility in non-acidic soils (pH > 5) is not a result of equilibrium with Prussian Blue, but rather with the solid compounds of manganese iron cyanide. Many authors have noted the strong adsorption capacity of the hydrous manganese oxides (Jenne et al., 1968) resulting in possible accumulation of large amounts of other ions from the soil solution (McKenzie, 1970). The XRF analysis of the uncontaminated sandy loam material from the MGP site revealed Mn concentration amounting to 180 mg kg^{-1}. Additional studies need to be conducted to investigate this process, including the speciation of the form in which the Mn present in the coherent soil. Nevertheless, as demonstrated in this study, reaction with the manganese oxides, resulting in forming the solid potassium manganese iron-cyanide, is partially inducing the reduction of the cyanide concentration in the percolating solution.

The RFA analysis of the uncontaminated sandy loam material, prior to column experiments, indicated high iron concentration (up to 13000 mg kg^{-1}), that correlate with the adsorption of ferricyanide on iron oxides as a potential retention mechanisms. The upper part of the sandy loam layer could possibly be affected by the oxidation of iron sulfides, which due to acidifying impact could cause protonation of the surfaces leading to potential sorption.

However, this is just a theory since the pH inside of the column was not determined.

Visual and chemical investigation of the disassembled column material (Picture 10 and 11) revealed analogous cyanide vertical distribution to the one observed in the boreholes A-21 and C-25. In columns 1-3, the highest total cyanide concentration was obtained within first 2 cm of the sandy loam layer, which decreased with increasing depth (Figure 32). Relatively low water soluble CN concentration (Figure 32) implied the presence of solid iron-cyanide complexes, which were proven to be in form of ferric ferrocyanide and potassium manganese iron-cyanide (FTIR analysis). Mansfeldt et al. (1998) investigated the soil profile from a former MGP site, where the layer of the glaciofluvial sand acted like a sink for the vertically transported iron-cyanide complexes that were mobilized from the MGP waste material, in form of ferric ferrocyanide colloids. Our findings are consistent with the study conducted by Mansfeldt et al. (1998), where the change in soil texture affects the pore size and the water flux which as a consequence filter the ferric ferrocyanide colloids. However, Mansfeldt et al. (1998) stated that this form of Prussian Blue transport is feasible in extremely acidic conditions. Our study indicated that with the excess of iron source and in circum-neutral pH conditions, colloid vertical movement of solid iron-cyanide complexes can be achieved.

6.6 Conclusions

Visual observation and the laboratory analysis of the soil material collected from two boreholes revealed potential vertical migration of the cyanide, from the MGP wastes towards the sandy loam layer, which appeared to act like a sink for iron-cyanide complexes. Acidic character of the MGP wastes, and the soil beneath it, collide with the high mobility of the cyanide. In this study, retention properties of the sandy loam soil and the potential vertical movement of the solid iron-cyanide complexes, co-existing with the dissolution, sorption and precipitation reactions were investigated.

Batch experiments revealed that in the circum-neutral pH conditions, the sandy loam material decreases the potassium ferro and ferricyanide concentration. However, in the 1st column experiment, no significant reduction in the cyanide concentration, both in the quartz and coherent soil, was obtained prior to implementing an additional iron source (FeS). The study revealed that the excess of the available iron, which induced the formation of the Prussian Blue colloids, was a very important factor in decreasing the cyanide concentration. Visual observation and chemical analysis of the quartz sand, sandy loam soil and percolation solutions implied that the CN concentration reduction was partially a result of precipitation reactions. Sandy loam soil appeared to retard the vertical migration of the iron-cyanide colloids due to mechanical filtering. In the quartz sand, precipitated ferric ferrocyanide was

vertically transported along the column as a non-reactive species, changing the color of the percolation solution.

Higher reduction of the cyanide concentration by the sandy loam material, indicate possible chemical effects of the coherent soil. Long-term acidification due to iron sulfide oxidation would enhance the extent of iron-cyanide complex sorption, because the surfaces of potential mineral sorbents become protonated and thus positively charged. Spectroscopic analysis of the MGP material suggested reaction with Mn oxides (formation of $K_2Mn[Fe(CN)_6]$) as a possible retention mechanism, despite the circum-neutral pH of the percolating solution. It is possible that the reduction of the cyanide concentration in the circum-neutral conditions is not only a result of equilibrium with Prussian Blue, but also with the solid compounds of manganese iron cyanide.

7 Supplementary discussion

In this Chapter the discussion concerning additional, unpublished measurements and experiment, obtained for the purposes of the studies presented in Chapters 3, 4 and 5, is shown.

7.1 Limitations of the FP NIR spectrometer

Diffuse reflectance occurs when light penetrates the surface of a sample material and it is partially reflected and transmitted, and the reflected radiation is passed back into the spectrometer. Spectral features of the soil material in the NIR region are based on molecular over tones and combination vibrations of C-H, O-H and N-H. NIR is comprised of combinations and overtones that is anharmonic oscillation, cause the bonds do not obey Hooke's law exactly. The anharmonicity of the covalent bonds allows the harmonic motion (overtones) to occur in the NIR region. Hydrogen, as a light atom, reveals the largest vibration and the greatest deviation from the harmonic behavior. The NIR region corresponds to bonds containing light atoms with single bonding, whereas the bands for bonds such as C=O, C≡N are much weaker or absent. Cyanide however, contains a carbon atom triple-bonded to a nitrogen atom that obtains lower anharmonic oscillations, which as a consequence produces weaker NIR response.

Depending on the soil constituents, the radiation will cause the individual molecular bonds to vibrate, either by bending or stretching, and they will absorb light, to various degrees, with a specific energy quantum corresponding to the difference between two energy levels, which is directly related to frequency and inversely related to wavelength (Stenberg et al., 2010). The result - absorption spectrum, can be further used for the analytical purposes. In the NIR region, the frequencies at which the light is absorbed occurs as a reduced signal of reflected radiation and are displayed in % reflectance (R), which can be transformed to apparent absorbance: A=log(1/R) (Stenberg et al., 2010).

The spectrometer (PHAZIR™) used for this study was an integrated handheld spectral analyzer that is designed to analyze diffuse reflection measurements from solids, powders or other reflective materials. According to the manufacturer (Polychromix), the FP NIRs are

currently used in a broad variety of applications from laboratories to industrial process controls, including material identification, quantitative analysis, purity analysis, quality control and material inspection. Screening the literature yielded some applications of the PHAZIR™ device in pharmacology and in the carpet industry, but for the soil science, as shown in Chapter 3, spectrometers in the laboratory set up and complex sample preparation methods were used. Personal communication established with the Senior Engineer from Polychromix revealed that preliminary studies of United States Geological Survey (USGS) data with the FP NIR were conducted, but particularly concerning minerals, due to the fact that the soil samples in the NIR region were inconclusive. The Polychromix employee recommenced using the mid IR range for the soil and cyanide analysis. This method was further applied as a reference for the NIR signal.

Spectral properties of bare soils are governed mainly by the soil constituents (e.g. soil organic matter, iron oxides, clay minerals and soil water) and soil roughness (e.g. particle size and aggregate size) (Atzberger, 2002), which affect the reflection of radiant energy from soils. According to Viscarra Rossel et al. (2006), both clay minerals and SOM are the fundamental constituents of the soil and have well-recognized absorption features in the NIR region, whereas other properties, including pH, extractable P, K, Fe, Ca, Na, Mg and CEC, are highly variable due to dependency on combinations of other soil properties (water, organics and minerals). Good examples are metals that do not absorb in the NIR region, but can be detected due to co-variation with spectrally active components like organic matter or clay minerals. Malley and William (1997) attributed most of the variance in the heavy metal concentration to organic matter content.

According to the literature and the information gathered from different specialist all over the world, FP NIR works more efficiently with simple matrixes. Particulate materials having low absorption, such as quartz, strongly scatter light in the forward direction with a maximum reflectance, which decreases the amount of the shadowed area (backscattering) (Atzberger, 2002). In the beginning of the project, the performance of the NIR spectrometer was evaluated by generating a simple model for the cyanide detection in a quartz matrix. Synthetic ferric ferrocyanide (used in Chapter 3) was mixed at the different ratios with the synthetic quartz. Scans of the samples were collected with the FP NIR, and preprocessed with the multivariate data analysis PHAZIR MG program, where the statistical methods like PLS, PCA were applied to the data set. The application for the device was generated and preinstalled. The performance of the spectrometer in predicting the CN concentration in the quartz matrix was more than satisfactory.

Unfortunately, soil matrix is much more complicated than quartz, including various particle size, different colors (which influence the absorbance), water signal, organic matter

coating or even signals of different elements or minerals that can inhibit the cyanide band. Moisture decreases the reflectance as the consequence the portion of energy is not reflected to space but is re-reflected between the surface of the particle and the surface of the water film covering the particle (Baumgardner et al., 1985). Water signal in the NIR region is between the 7143 and 6667 cm^{-1} so it does not interfere with the CN signal at 4215 cm^{-1}. However, multiple-reflection increases the absorption and decreases the reflection of the entire spectrum. It was quickly realized that the soil samples had to be dried prior to the spectra collection.

Variation in particle or aggregates size is another important issue in the NIR region. Generally, decrease in the particle size increases the reflectance and the contrasts of the absorption features (Atzberger, 2002). This becomes evident when considering that the surface of the particle becomes smoother with the decreasing size. When the light signal penetrates the coarse aggregates of irregular shape, it falls within the gaps and is absorbed there (Baumgardner et al., 1985). Sieving was the second necessary soil pretreatment prior to data collection with FP NIR.

Within the first few months of the study it was realized that using the device in-situ (without drying and sieving of the soil samples in the laboratory) would not progress the cyanide model development. Figure 33 shows the raw (not pre-processed), almost featureless, spectra of the few soil samples collected at the MGP Cottbus after drying in the laboratory. The particle size distribution of the sample affects the degree of scattering, as the coarser structure increases the scatter and the absorbance (baseline shifts). The spectra pre-processing (Figure 34) was very helpful in raising the important common features of the soil scans and enabled focusing on the part of the spectra that was essential for the cyanide signal. However, the soil samples, where CN concentration was lower than 1500 mg kg^{-1} showed no band at the 4215 cm^{-1}. This happened to be a big limitation for our project since almost 80 % of the samples used for calibration and available in this study had a cyanide concentration below 1000 mg kg^{-1}.

It is often suggested that smaller soil variation at the field scale would result in better calibration than a more general one (Stenberg et al., 2010). The soil used for this calibration was highly inhomogeneous and collected from different depths, which negatively influenced the calibration. Since the FP NIR performance for the samples with high CN concentrations (< 1750 mg kg^{-1}) was quite satisfactory, the next step would be to create a model for the samples were only CN concentrations higher than 1750 mg kg^{-1} occurred. The problem was to obtain the satisfactory amount of samples from the already planted MGP site in Cottbus. Generally, the higher the number of samples used for the calibration the better the models are. Unfortunately, the number of samples with such a high CN concentration was limited.

Additionally, random collection of the soil material, used for the FP NIR calibration, resulted in the samples containing high OM content (top soil), which has a strong influence on soil reflectance (OM content exceeding 2.0 %) (Atzberger, 2002). Malley and Williams (1997) reported that the predictive capability of the NIR region can be improved by separately calibrating for highly organic and highly inorganic samples. The influence of the OM content in the cyanide study was possibly reduced by the sample grinding, which decreased the particle coating effect.

Another sample pretreatment, possibly improving the feasibility of FP NIR to measure the CN concentration, is collecting the soil spectra at a stable temperature. According to De-Braekeleer et al. (1997), the variation in temperature results in an additional source of variation in the spectral response. Additionally sample sets can be divided according to the soil color (dark and light). Lighter samples have low absorption, whereas darker ones absorb light to the higher extent, which lowers the reflectance.

As pointed above, there are many potential ways to improve the feasibility of the FP NIR to measure the cyanide concentration in the soil, but every additional sample pretreatment step (drying, homogenizing, sieving, grinding, temperature measurement, division according to soil color and OM content, sample collection from the small field scale etc.) was bringing us back to the laboratory instead of making the measurements in-situ, which was the main aim of our study.

7.2 Additional measurements conducted for the purposes of the Prussian Blue stability study

The values of cyanide concentrations, measured with the FIA, for column and batch experiments are shown in the Tables 17, 18, 19 and 20 in the Appendix II.1. Chapter 4 mainly relates to the batch I experiment, since introducing all batch experiments (3) conducted during this study, would go beyond the scope of Chapter 4. Raw data of the batch 2 and 3 are shown in Table 19 and Table 20, respectively. Batch 3 was conducted only for 1 h, while batch 2 lasted for 382 h during which problems with the calibration of the measuring device (FIA) occurred, so it was decided not to include those results into the publication Sut et al. (2013). Soil used for the batch, as well as for the column experiment, was supplied by the German Railways (DB AG) in the big beakers (60 L), where each of the beaker was labeled with the letter related to the collection point (A, B, C and D). Soil in beakers was very inhomogeneous, so for each experiment a few kilos were taken from the big pull (beaker), homogenized and then used for the further analysis. The column experiment and the batch 3 experiment were conducted on the soil material collected from the beaker at the same time, which can explain a slightly better correlation in Figure 36 (R^2=0.9977).

Batch 1 (used for the study presented in Chapter 4) and batch 2 were conducted on the soil collected from the same beakers, but not at the same time as the material used for the column experiment, which, due to the high inhomogeneity of the material, explains slightly worse correlation obtained in the Figure 35 (R^2=0.9487) and in the Figure 17 (R^2=0.8468).

The correlations obtained for the column and the batch experiments were related to the cyanide concentrations in phase I. The phase I was based on the readily water soluble cyanide (Chapter 4) which were visually obtained from the graphs. Prior to data comparison, it was assumed that the cyanide concentrations used for the correlations should be based on the pore water volume. Our hypothesis assumed that all of the readily water soluble cyanide should be washed out of the columns within 2 pore volumes. Because this parameter was not determined prior to the experiment, it was attempted to obtain the reliable values using 3 different values: field capacity (Table 21), porosity (Table 22) and particle density determination via pycnometers (Table 23). Unfortunately, the values obtained for the pore water volume did not bring unambiguous results. The obtained pore water volumes differ according to the determination methods, so it was decided not to use this parameter in the correlation.

In order to primarily evaluate species distribution, focusing on cyanide and hexacynanoferrate speciation in the aqueous solutions of the soil column extracts, a chemical equilibrium program PHREEQC (Parkhurst and Appelo, 1999) was used. Prior to this study, speciation calculation was performed by Meeussen et al. (1992a; 1994), Ghosh et al. (1999c) and Weigand et al. (2001). The input file consisted of following extract characteristics: pH (measured for each soil column extract); redox potential (was assumed to be equal to an Eh of 500 mV, as the column experiment was performed under unsaturated condition); total amounts of the components involved (CN, Fe, Ca, K) (Table 4) and their equilibrium constants (Table 25); and the total amounts of selected constituents (Mg, Mn, SO_4^{2-}, NO_3^-, Cl) (Table 4).

The calculations were performed in order to evaluate and compare the cyanide species distribution for different columns extracts (A, B, C and D), at the beginning and the end of experiment, according to given components concentrations, pH and assumed redox potential. The Fe^{3+} activity was assumed to be controlled by equilibrium with soild $Fe(OH)_3$ and $Fe_3(OH)_8$ (reactions 1 and 2 in Table 25) and the $Fe(CN)_6^{-3}$ by the dissolution of ferric ferrocyanide (reaction 3 in Table 25).

Determination of the different cyanide species in the water (soil column extract) is extremely time consuming due to several different analyses that have to be performed on the single sample. Therefore experiments are frequently limited to 'total cyanide' and 'weak acid dissociable cyanide' analysis. Additionally, different methods (acid digestion, extrac-

tion with sodium hydroxide etc.) can change the chemistry of the water sample, which as a consequence alter the dissolved CN species.

In this study soil column leachate speciation was performed with a chemical equilibrium program PHREEQC. The distribution of cyanide species in the column extracts did not differ greatly, especially between starting and ending measurement. The exception is water from column D, where very low concentrations of cyanide were measured in the end of the experiment (Table 26). The speciation calculation revealed $Fe(CN)_6^{-3}$, $CaFe(CN)_6^{-}$, $CaFe(CN)_6^{-2}$ and HCN as predominant species for all soil column extracts (A, B, C, D). This result is most probably caused by basic pH (6.44-8.13) and assumed oxic conditions (Eh = 500 mV). In groundwater at MGP sites most abundant are the iron-cyanide complexes found in two oxidation states: $Fe(CN)_6^{-3}$ and $Fe(CN)_6^{-4}$ (Theis et al., 1994). Reducing conditions will reduce $Fe(CN)_6^{-3}$ to $Fe(CN)_6^{-4}$. Oxic conditions of our soil column extract explain the presence of $Fe(CN)_6^{-3}$ and production of labile complexes with Ca^{+2} ($CaFe(CN)_6^{-}$ and $CaFe(CN)_6^{-2}$) (Table 26). These findings are consistent with the study made by Meeussen et al. (1992a and 1994). Speciation modeling also revealed the presence of HCN in the soil column extracts. This is not consistent with the additional measurements performed with the FIA in order to determine the HCN concentration in the columns leachates. The analysis was performed directly on the water sample, without acid digestion, to exclude alternation of the sample chemistry. The obtained results indicated HCN concentration below limits of detection (< 0.02 mg L^{-1}).

According to Gosh et al. (1999; 2004) cyanide can occur in aqueous solutions in a free, uncomplexed form as hydrocyanic acid (HCN) and its dissociation product cyanide anion (CN-). As stated in the equilibrium calculations (Table 25) under oxic conditions iron-cyanide complexes should dissolve releasing free cyanide. This is not consistent with leaching experiments using spent bog iron ore performed by Theis et al. (1994), where no free cyanide was found in water. It is commonly known and accepted that the cyanide present in the groundwater and soil solution at the former MGP sites mainly occur in the form of iron-cyanide complexes. On the other hand equilibrium calculations performed by Meeussen et al. (1992a) indicated similar iron-cyanide complexes dissolution behavior demonstrating free cyanide as a predominant species. According to Rennert (2002) this result demonstrates that modelling the species distribution may not be performed under the assumption of a local equilibrium, because of the large differences between the modelled and the measured species distribution. The difference between the measured and calculated cyanide species in a water matrix can be additionally explained by very slow decomposition of these complexes in the dark. Water containing Fe-CN complexes when exposed to the light will release HCN, in the dark, this reaction (under this pH and pE conditions) might take 1000 of years (Meeussen et al., 1992a).

7.3 Long-term ''one-phase release'' of the iron-cyanide complexes from the acidic soil

The study of the long-term iron-cyanide complexes release from the MGP soils, presented in Chapter 5, assumes that the discharge is constrained by two phases: one available and one strongly fixed. Applying different isotherm and kinetic equations to the experimental results obtained from the column leaching experiment (Figure 19), without separating the data set into two phases, resulted in very low correlations. According to visual inspection of the release curves (Figure 19) and to the low correlations it was decided, in order to extract additional information concerning the CN release process, to divide the data set into two phases. This study is presented in Chapter 5. Applying the isotherm equations assumed that the CN release is separate in time, whereas using the kinetic equation considered that both phases occur simultaneously. The study revealed that the two phase approach does not exactly reflect the release of the iron-cyanide complexes from the soil C. Own preliminary studies had shown that the top soil C is acidic (pH = 5), has a very high total CN content and relatively low water soluble cyanide content (Table 3) when compared to the other soils used in this study. Furthermore, the CN release curve (Figure 19), obtained from the column leaching experiment, does not indicate a significant change in the release rate, rather pointing to the constant, but continuous process. Generally the release of iron-cyanide complexes is very pH dependent and is increasing with increasing pH, which was proven by the study conducted by Meeussen et al. (1990). They investigated leaching from soils contaminated with iron-cyanide minerals in a column experiment and a batch experiment under different pH conditions (pH 3 - 9). Low pH of the investigated soil C justify the low water soluble cyanide content and therefore interpret the presence of only one phase.

Another acidic soil used in the leaching column experiment, was soil B (pH = 5.7), however the slight increase of the pH, when compared to the soil C, resulted in the higher water soluble cyanide content (Table 3) and in the release of the iron-cyanide complexes constrained by two phases (Figure 19). This result proves how pH sensitive the stability of ferric ferrocyanide is. Another reason can be a low OM content of soil B. Soil C was collected as a top soil, whereas soil B was the sandy layer beneath the top soil A. According to Ghosh et al. (1999), both ferricyanide and ferrocyanide were not restrained by the sandy aquifer material and the lower release rate of the soil C can be additionally constrained by the possible sorption on the organic matter, which can take place through the hydrogen bonds under acidic conditions (Mansfeldt, 2003).

The isotherm and the kinetic equations used in the study presented in Chapter 5, where applied to model the release of iron-cyanide complexes from the soil C considering one phase release. The equations were applied to the entire data set, without dividing it into

phases. The parameters of the correlations are presented in Table 27. Modeling revealed the highest correlation coefficient when the Parabolic Diffusion equation was applied to the data set (R^2=0.98). The correlation obtained with the Freundlich and the First Order equation was also satisfactory (R^2=0.94). However the lowest standard error was obtained when Freundlich Equation was applied. The Elovich equation resulted in the lowest correlation (R^2=0.83) and the highest standard error (SE = 9.11). According to the visual representation of the applied equations (Figure 37), the best fit of the regression line was obtained when the Freundlich equation was applied to the data set.

The short study of the long-term iron-cyanide release form soil C revealed that the dissolution mechanism of the solid CN compounds is constrained by one phase. Due to the acidic nature of the soil, the readily dissolved CN amount is very low (Table 3), which only slightly changes (increases) the release rate within the first few days of leaching (Figure 19). Except for the Elovich, all the applied equations successfully described the data set. However, the best visual fit of the regression line (Figure 37) and the lowest SE was obtained by using the Freundlich equation, which was used by many scientists to describe the behavior of organic and inorganic compounds (Chien and Clayton, 1980; Aharoni et al., 1991). The Freundlich equation is often used for heterogeneous surfaces and describes desorption from solids to solutes in liquid and assumes that different sites with several adsorption energies are involved.

8 Synthesis

8.1 General conclusions

Both in public and private sector, there is a general awareness of the need for faster, better and cheaper methods for site characterization and remediation. The management of the former MGP sites can be very challenging due to the complex chemistry of the wastes. MGP sites can provide opportunities to try new methods for the contaminant detection, and to relate the obtained results to the existing knowledge based on other MGP sites. The main purpose of this research was to gain a deeper insight into detection and behavior of iron-cyanide complexes in the soil environment, in order to improve the efficiency of the phytoremediation projects, and to enable rapid and non-destructive measurement in the field. This chapter presents the major objectives of the research presented in this thesis and provides a brief conclusion concerning the obtained results.

The first aim of this research was to investigate the feasibility of FP NIR spectrometer to determine the CN concentrations in soil. The process of characterizing and remediating the MGP site involves first site screening, so determining the 'hot spots' of contaminants concentrations. Generally, diffuse reflectance spectroscopy provides an attractive alternative for the laboratory measurement, due to rapid, cost-effective and non-destructive in-situ analysis. However, as demonstrated in Chapter 3, the limits of detection for the determination of the cyanide concentrations are too high to replace the traditional laboratory methods. As described in Chapter 7.1, it was quickly realized that the limitations, resulting from the chemistry of the compound and the complexity of the soil matrix, would bring us back to the laboratory. The cyanide group consists of a carbon atom triple-bonded to a nitrogen atom that will produce less fundamental stretching and bending vibrational modes than for example the harmonics and overtones of X-H. In addition, the NIR spectra are also highly influenced by the physical structure of the material including different particle size, different colors (which influences the absorbance), water signal, organic matter coating or even the signal of different elements or minerals that can inhibit the cyanide band. Additionally, the study revealed that the feasibility of FP NIR to measure cyanides in the soil improves with advancing the sample preparation procedure.

The part, concerning advancing the knowledge of cyanide behavior in the soils of a for-

mer MGP sites, was initiated with the Prussian Blue stability study. Until recently, regulation and management of cyanide in water and soil have been focused on total (inorganic) cyanide content, which causes potential restraints in the remediation projects. Especially concerning implementation of phytoremediation strategies, the lack of a standard leaching procedure to determine the water soluble (plant available) cyanide fraction can be a key factor affecting the effectiveness of the project. Batch and column experiments, conducted for the purposes of this study, revealed continuous dissolution of the solid iron-cyanide complexes, for both alkaline and acidic soils, which question the solubility values reported in the literature and available procedures (suggested by Standard Methods) for defining water soluble cyanide fraction. The study revealed that dissolution of ferric ferrocyanide under circum-neutral pH, oxic conditions is a function of time and only the released amount is soil pH dependent, thus introducing one more fraction to specify cyanide release was recommended. In this research, an approach of long-term extraction or leaching of surface and near-surface cyanide contaminated soils with distilled water, as a reliable tool for assessing the potential environmental hazard, was suggested. It was proposed to specify 1 h of water extraction as a "readily soluble fraction", whereas the rest of the liberated cyanide can be determined as the "long-term water available fraction" that is difficult to be defined in time.

Another limitation, recognized while conducting the column leaching experiments, was the lack of rapid and noninvasive methods for determining different water soluble cyanide species. The chemical equilibrium modeling was performed to evaluate and compare the cyanide species distribution in the column leachates, in the beginning and the end of the experiment. The chemical equilibrium modeling revealed free cyanide and HCN as one of the main species, which does not correlate with the measured species distribution (FIA). According to the literature, the cyanides present in the groundwater and soil solutions at the former MGP sites mainly occur in form of iron-cyanide complexes. The evident difference between the modeled and measured cyanides implies that the chemical equilibrium modeling should not be performed considering local equilibrium conditions.

Furthermore, stability leaching experiment revealed that long-term release of iron-cyanide complexes from the MGP soils is governed by two phases: one readily dissolved and one strongly fixed. To design effective remediation strategies it is crucial to quantify and mathematically model the contaminant release rate, column studies can provide key information concerning the mechanism of the iron-cyanide complexes dissolution or desorption, where the release rate parameters can be estimated from the isotherms of the time dependent data using various mathematical models.

Applying the isotherm equations (Elovich, Freundlich and Parabolic Diffusion) to the col-

umn data assumed that both phases are separate in time. For phase I, obtained results imply that the transport process of the readily dissolved iron-cyanide complexes (hexacyanoferrats), taking place in the liquid phase, combined with the desorption of CN bound to heterogeneous surfaces that are in direct contact with aqueous phase (outer-sphere complexation) is the main release mechanism. Indefinite results for phase II, most probably indicate that the long-term iron cyanide release from the MGP soils is a complex phenomenon driven by various mechanisms involving desorption, diffusion and dissolution processes like the dissolution of precipitated ferric ferrocyanide or of inner-sphere complexed ferricyanides.

Applying a multiple first order equation to the experimental data, assumed simultaneous occurrence of both phases, which is considered to closer reflect the probable cyanide release mechanisms from the MGP soils. This non-equilibrium approach adequately described the CN release from soil A, B and D, except for the soil C, where the low pH justified the low water soluble cyanide content and therefore explained the presence of only one phase. Additional modeling, considering one phase release using different isotherm and kinetic equations, revealed that the soil C follows the mechanisms of desorption from solid heterogeneous surfaces to the liquid.

The iron-cyanide release rates revealed that the CN mobility is mainly influenced by the pH, by the initial CN concentration and by the possible sorption on soil organic matter. The cyanide release rates increased with increasing pH, decreased with low initial CN concentration and was retarded by an increase in OM content.

According to the literature, the mobility of iron-cyanide complexes in soil is mainly governed by dissolution and precipitation reactions. Very little is known about the potential vertical movement of the solid iron-cyanides via colloidal transport. The laboratory analysis of the two long soil boreholes, revealed the likely migration of cyanide from the MGP wastes layer through the sandy soil, towards the sandy loam material. The acidic character of the wastes and soil implied colloidal vertical transport of the ferric ferrocyanide as a potential process influencing the cyanide mobility. Characteristic blue patches (accumulation of precipitated Prussian Blue) and high CN concentrations detected in the sandy loam material pointed to the sink character of the coherent soil.

Lastly, the retardation of the iron-cyanide complexes by the sandy loam soil form the MGP Cottbus was studied in the column and batch experiments. The laboratory studies were successful in simulating the iron-cyanide complexes behavior in the contaminated soil of a former MGP site in Cottbus revealing the formation of ferric ferrocyanide, from reaction of potassium ferricyanide with iron sulfide, retardation of Prussian Blue colloids demonstrated by blue patches and by reduction of the CN concentration in the infiltrating solution. Sandy loam soil retarded vertical migration of iron-cyanide colloids due to mechanical filter-

ing. Spectroscopic analysis (FTIR) of the coherent soil suggested reaction with Mn oxides (formation of $K_2Mn[Fe(CN)_6]$) as a possible retention mechanism.

In the quartz sand, precipitated ferric ferrocyanide was vertically transported along the column as a non-reactive species, changing the color of the percolation solution to blue-green. A colloidal vertical transport of the Prussian Blue particles along the column profiles was demonstrated as a potential alternative process influencing cyanide mobility in the circum-neutral pH and under conditions of excess iron availability.

When evaluating the environmental fate of iron-cyanide complexes, dissolution of solid ferric ferrocyanide as well as colloidal transport should be taken into consideration. This research demonstrated the potential risk of soil and groundwater contamination due to high instability of solid iron-cyanide complexes in circum-neutral pH conditions. However, in acidic environment as well as in the excess of iron, mobility of Prussian Blue can be constrained by the vertical migration of colloids. This research demonstrated the lack of a standard leaching procedure to determine the water soluble cyanide fraction and the limitations of using the equilibrium modeling to determine dissolved cyanide species. Presently, many studies have been conducted to analyze the behavior and fate of cyanides in soil and groundwater. However, more investigations should be performed to reduce the inconsistency in the knowledge concerning the geochemistry of the iron-cyanide complexes.

8.2 Recommendations for further research

Although, as presented in this doctoral thesis, the behavior and fate of the cyanide in soil have been studied intensively, several questions and problems arose from this research that still remain to be solved. It is commonly known that phytoremediation is a promising technology for the remediation of the cyanide contamination, however it is limited by the lack of specific knowledge of the physicochemical mechanisms that influence the cyanides fate in the environment, biological mechanisms responsible for the transport and metabolism of cyanide species by plants, and cyanide uptake rates and factors that influence these rates.

In the field of in-situ cyanide determination, the approach presented in Chapter 3 is definitely a step in a right direction towards a simple, rapid and non-destructive method for the preliminary site screening concerning 'hot spots' of contamination. The future investigations should include larger amount of soil samples with CN concentration <1750 mg kg^{-1} to be used for calibration. Additionally, separately calibrating for highly organic and highly inorganic samples, grouping soil samples according to their color and collecting the scans at the same temperature can improve the predictive capabilities of the NIR region. Furthermore, one may also consider developing a small scale field portable lab, where the samples can be dried and ground in-situ prior to scanning with FP NIR.

Although a lot of work has been done and published concerning the behavior and dissolution of iron-cyanide complexes in soil, the study on the stability of these compounds (Chapter 4) revealed higher dissolution than reported in the literature. Probably of more importance is conducting the leaching and batch experiments using the contaminated soil instead of synthetic solutions. Future investigations should definitely include the effects in changes of pH and redox potential on the cyanide behavior simulating the environmental conditions. Additionally, more research has to be done to develop a standard method for determining the water soluble fraction of cyanides. Due to the fact that the stability study presented in Chapter 4 implied that at some conditions the water soluble fraction of cyanides could be as high as the total content, more investigations concerning the influence of the soil chemistry on the solubility of iron-cyanide should be performed.

Despite the fact that according to the previous research, the fundamental interaction of the dissolved iron-cyanide complexes with the soil solid phase is mainly influenced by the dissolution and precipitation of the solid ferric ferrocyanide, in the non-acidic soils the cyanide solubility might be governed by the equilibrium with another mineral like manganese iron cyanide. The precipitation of dissolved hexacyanoferrats in such form could also reduce the CN concentrations in the alkaline soils. Therefore further research concerning the presence of the different iron-cyanide phases and their dissolution behavior is recommended. In the ground water and in soil solutions of the former MGP sites, cyanide mainly exist as a dissolved iron-cyanide complexes, however the chemical equilibrium modeling revealed free cyanide as the predominant species. The evident difference between the modeled and measured cyanides implies that the chemical equilibrium modeling should not be performed without local equilibrium conditions.

Generally the mobility of the iron-cyanide complexes in the soils of a MGP sites is mainly governed by the dissolution and the precipitation of the ferric ferrocyanide. The high instability of Prussian Blue, demonstrated in this study, does not explain the limited transport indicated by still very high cyanide concentrations in the sandy loam layer after so many years from disposal (closure of the MGP in Cottbus was around the year 1960). The research presented in Chapter 6 suggested the vertical colloidal transport of the ferric ferrocyanide as a potential alternative movement. More insight into this process would be helpful in establishing physical barriers to "filter out" the particles and to generally improve the knowledge about the dissolution kinetics of solid iron-cyanide complexes. More research concerning the role of the pH and redox potential variation on the precipitation of Prussian Blue with the excess of iron is recommended to more precise study the release rates of mineral contaminants from waste material.

Appendix I: Additional data for the FP NIR calibration

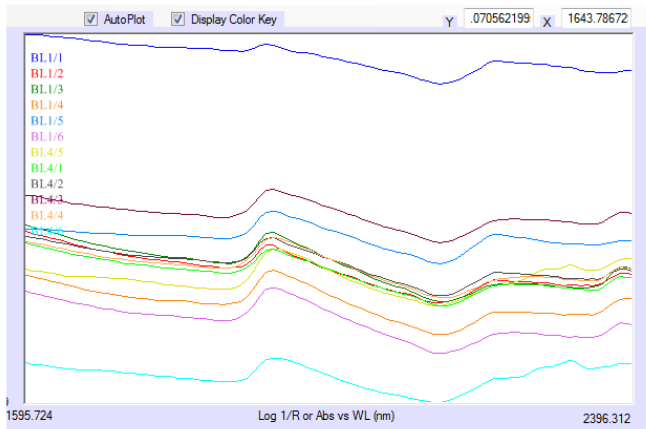

Figure 33: Example of the soil spectra (without preprocessing) collected with the FP NIR and visualized with the Phazir MG Polychromix Software.

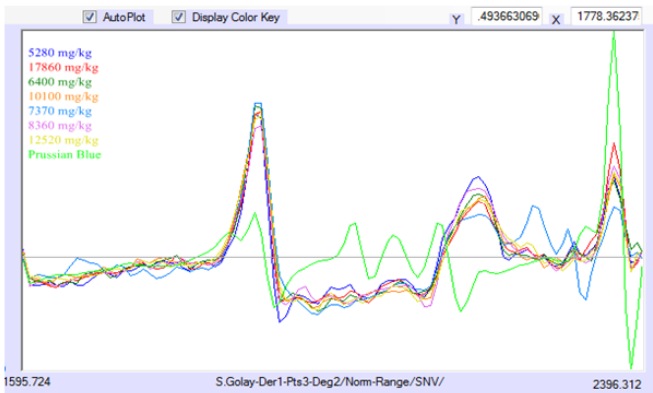

Figure 34: Example of the soil spectra, after preprocessing using SNV and S. Golay, collected with the FP NIR and visualized with the Phazir MG Polychromix Software.

Appendix II: Additional data concerning the stability of Prussian Blue

II.3 Raw data for the column and batch experiments

Table 17: Raw data of the column leaching experiment.

	Column							
Leachate collection	**A1**	**A2**	**B1**	**B2**	**C1**	**C2**	**D1**	**D2**
	Cyanide conc. (mg L^{-1})							
22.06.2013	2015	1865	720	620		175	25.6	29.6
23.06.2011	1523	1245	393	385	168	135	11.2	10.6
24.06.2011	1875	1320	320	348	128	120	8.8	8.2
28.06.2011	1058	1038	245	245	123	128	7.6	7.2
29.06.2011	868	1020	243	165	90	103	6.4	5.4
30.06.2011	840	798	108	145	88	115	4.6	13.0
01.07.2011	788	775	63		83	93	3.0	3.2
04.07.2011	743	850	50	97	88			1.9
06.07.2011	740	628	45	61	92	99	3.1	1.9
07.07.2011	403	470	38	48	94	95	2.9	2.1
08.07.2011	433	435	40	43	91	99	2.6	
12.07.2011	308	365	31	26	97	103	1.7	
13.07.2011	240	300	30	28	84	73		1.5
14.07.2011	250	323	23	32	81	68	1.9	1.8
15.07.2011	233	273	36	24	50	75	1.3	1.8
19.07.2011	117	154	22	17	36	66	1.1	2.0
20.07.2011	105	132	25	16	37	37	1.3	1.3
21.07.2011	173	185	25	16	39	36	0.9	
22.07.2011	158	145	38		30	39	0.9	1.3
26.07.2011	115	143	34	20	45	30	0.6	1.6
27.07.2011	143	145	36	19	49	44	0.8	1.7
28.07.2011	133	160	35	21	48	46		0.9
29.07.2011	105	130	34	21	46	48	0.7	2.1
02.08.2011	160	135	33	20	54	44	0.9	2.4
03.08.2011	135	135	42	25	52	33	0.9	3.0
04.08.2011	125	153	41	27	59	51	0.8	3.0
05.08.2011	113	125	19	23	49	62	0.7	3.0
08.08.2011	100	115	30	26	0	54	0.8	1.9
09.08.2011	85	108	36	19	33	43	0.9	1.8
10.08.2011	85	108	41	20	42	49	1.3	2.9
11.08.2011	93	110	41	20	42	52	0.7	2.2
12.08.2011	90	0	40	0	43	22		

Table 17 (continued)

Leachate collection	Column							
	A1	A2	B1	B2	C1	C2	D1	D2
	Cyanide conc. (mg L^{-1})							
16.08.2011	88	115	40	18	42	53	0.7	1.7
17.08.2011	88	83	41	22	45	49	0.6	1.5
18.08.2011	85	100	51	19	44	53	0.7	2.0
19.08.2011	88	98	43	22	37	51	0.8	2.0
26.08.2011	92	105	40	20	38	46	0.8	1.4
02.09.2011	70	87	42	18	37	45	0.7	1.2
09.09.2011	72	99	38	15	36	47	0.7	1.0
16.09.2011	60	76	34	5	30	42	0.6	0.7
23.09.2011	51	70	35	19	32	48	0.0	0.7
30.09.2011	56	69	29	36	29	41	0.6	0.6
07.10.2011	35	41	15	27	24	30	0.4	0.4
14.10.2011	28	36	13	22	22	28	0.5	0.5
21.10.2011	24	31	11	16	22	27	0.5	0.4
28.10.2011	24	35	11	18	0	27	0.5	0.7
04.11.2011	22	32	10	16		26	0.5	0.5
11.11.2011	20	26	9	8		31	0.4	0.4

Table 18: Raw data collected from the batch I experiment.

Sample	Time (h)										
	1	24	72	96	168	216	336	504	672	840	1344
	Cyanide conc. (mg kg^{-1})										
A1	140.0	178.2	176.5	205.4	262.2	242.5	344.1	398.4	458.6	470.7	576.7
A2	127.0	168.3	167.8	181.4	240.4	251.0	359.0	415.8	448.6	471.6	553.6
A3	138.0	172.3	172.7	195.8	250.8	260.4	378.5	455.4	542.4	539.1	657.7
B1	72.2	132.7	163.2	176.2	225.6	240.6	316.7	359.3	402.2	443.7	558.0
B2	67.2	88.1	106.9	127.7	157.7	159.8	245.5	289.3	310.8		418.3
B3	64.7	89.3	107.4	109.7	134.4	149.0	172.1	206.1	250.3	255.2	331.1
C1	30.0	51.1	58.2	64.6	94.1	100.8	166.2	206.1	275.3	312.3	396.9
C2	29.5	47.8	64.0	72.5	98.3	109.3	160.2	213.0	290.3	294.8	429.0
C3	28.6	46.5	65.2	74.4	96.9	114.4	173.2	238.7	315.3	330.8	472.6
D1	1.6	2.7	3.8	4.2	5.6	7.0	9.0	9.8	10.5	9.6	12.2
D2	1.7	2.7	3.6	3.8	4.0	5.3	6.9	8.1	9.8	9.4	10.9
D3	1.7	2.7	3.5	4.1	4.8	5.5	7.1	8.3	9.0	9.2	10.8

Table 19: Raw data collected from the batch II experiment.

Sample	Time (h) 1	24	48	72	144	216	310	382
	Cyanide conc. (mg kg^{-1})							
A1	71.0	97.0	120.5	121.3	142.1	192.9	404.2	424.1
A2	67.0	88.1	101.9	114.5	123.8	289.8	341.2	377.6
A3	77.0	119.8	140.1	158.1	187.2	212.8	516.1	513.4
B1	27.6	53.5	65.4	69.1	88.1	102.8	138.2	153.0
B2	26.5	52.5	65.2	71.3	85.9	101.2	171.1	181.4
B3	29.3	54.4	65.2	73.5	90.7	106.2	161.0	162.3
C1	10.7	28.9	41.8	55.6	61.6	68.2	106.0	131.6
C2	11.5	32.6	45.1	51.0	70.2	73.2	118.0	145.5
C3	10.2	28.2	41.1	45.3	56.7	58.9	108.3	126.9
D1	0.0	1.3	1.8	0.0	2.4	3.9	7.4	9.0
D2	0.0	1.1	1.6	1.8	2.4	4.0	7.8	7.7
D3	0.0	1.2	1.8	2.2	2.2	3.8	7.2	8.3

Table 20: Raw data collected from the batch III experiment.

Sample	Time (h) 1 Cyanide conc. (mg kg^{-1})
A1	152.4
A2	154.8
A3	136.3
B1	22.2
B2	28.9
B3	26.1
C1	21.4
C2	20.9
C3	21.2
D1	0.6
D2	0.7
D3	0.6

II.4 Correlation of column and batch experiment

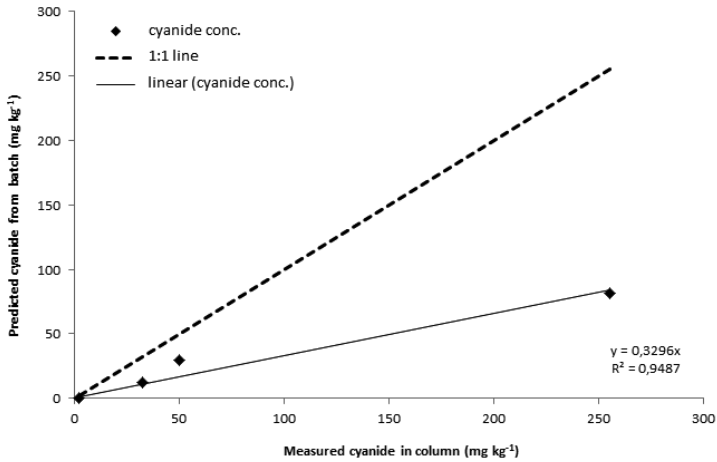

Figure 35: Columns v/s batch II cyanide concentration (phase I).

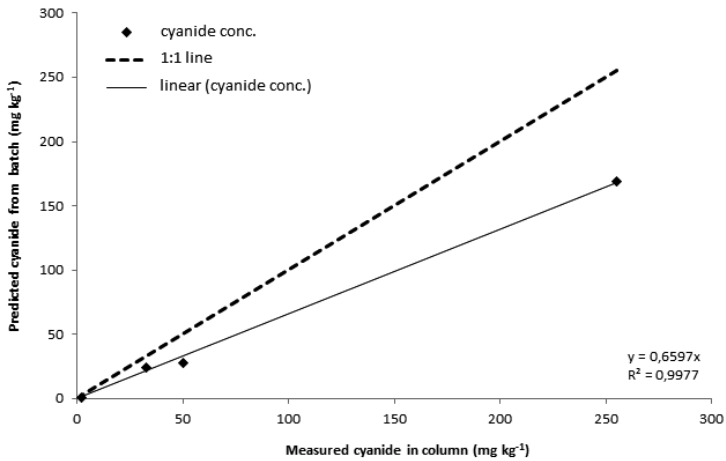

Figure 36: Columns v/s batch III cyanide concentration (phase I).

II.5 Pore volume determination for the column experiment

Table 21: Pore volume determination, for the column experiment, using field capacity value.

Soil column	mass wet	water content	mass water	mass dry	mass of the column	mass of column + soil	mass after 50 mL
	(g)	(%)	(g)	(g)	(g)	(g)	(g)
A1	693	12.6	87.4	605.6	230	927	697
A2	697	12.6	87.9	609.1	231	965	734
B1	734	6.4	47.3	686.7	229	987	758
B2	758	6.4	48.8	709.2	228	996	768
C1	768	12.9	98.7	669.3	232	1000	768
C2	768	12.9	98.7	669.3	228	904	676
D1	676	10.6	71.9	604.1	230	887	657
D2	657	10.6	69.9	587.1	230	887	657

Soil column	volume start	height end	volume end	filed capacity start	filed capacity end	pore volume start	pore volume end	2 pore volumes
	(cm^3)	(cm)	(cm^3)			(mL)	(mL)	(mL)
A1	431.8	19.80	388.58	0.21	0.24	91.4	91.4	183
A2	431.8	19.00	372.88	0.29	0.33	120.9	124.9	250
B1	431.8	19.00	372.88	0.17	0.19	71.3	71.3	143
B2	431.8	19.00	372.88	0.14	0.16	58.8	58.8	118
C1	431.8	22.00	431.75	0.23	0.23	98.7	98.7	197
C2	431.8							
D1	431.8	20.00	392.50	0.12	0.13	52.9	52.9	106
D2	431.8	19.20	376.80	0.16	0.19	69.9	69.9	140

Table 22: Pore volume determination, for the column experiment, using porosity values.

Soil column	mass wet	water content	mass of water	mass dry	volume start	height end	volume end
	(g)	(%)	(g)	(g)	(cm^3)	(cm)	(cm^3)
A1	693	12.61	87.38	605.62	431.75	19.8	388.58
A2	697	12.61	87.88	609.12	431.75	19.0	372.88
B1	734	6.44	47.29	686.71	431.75	19.0	372.88
B2	758	6.44	48.84	709.16	431.75	19.0	372.88
C1	768	12.86	98.74	669.26	431.75	22.0	431.75
C2	768	12.86	98.74	669.26	431.75		
D1	676	10.64	71.94	604.06	431.75	20.0	392.50
D2	657	10.64	69.92	587.08	431.75	19.2	376.80

Table 22 (continued)

Soil column	particle density (g cm^3)	φ start	φ end	pore volume start (mL)	pore volume end (mL)	total pore volume (mL)
A1	2.65	0.47	0.41	203.21	160.04	203.00
A2	2.65	0.47	0.38	201.89	143.02	209.30
B1	2.65	0.40	0.31	172.61	113.74	105.30
B2	2.65	0.38	0.28	164.14	105.27	104.82
C1	2.65	0.42	0.42	179.20	179.20	209.80
C2	2.65	0.42				207.80
D1	2.65	0.47	0.42	203.80	164.55	149.93
D2	2.65	0.49	0.41	210.21	155.26	149.91

Table 23: Particle density determination, for the column experiment, using pycnometers.

Pyknometer	Column	volume pyknom. (mL)	mass pyknom. (g)	mass pyknom.+ water (g)	mass pyknom.+ sample (g)	mass sample (g)	mass pyknom. (g)
1	A1	49.84	28.81	78.72	66.48	37.67	100.53
1	A2	49.84	28.81	78.72	57.82	29.02	95,.7
3	B1	49.82	28.14	78.04	72.88	44.74	104.38
1	B2	49.84	28.81	78.72	66.59	37.78	100.57
2	C1	49.88	28.09	78.04	64.64	36.55	99.19
3	D1	49.82	28.14	78.04	60.93	32.78	97.17
2	D2	49.88	28.09	78.04	66.12	38.04	99.75

Pyknometer	Column	mass sample + water (g)	mass water (g)	volume water (mL)	volume sample (cm^3)	particle density (g cm^{-3})
1	A1	71.72	34.05	34.14	15.70	2.40
1	A2	66.46	37.44	37.54	12.30	2.36
3	B1	76.24	31.50	31.58	18.24	2.45
1	B2	71.76	33.98	34.06	15.78	2.39
2	C1	71.10	34.55	34.64	15.25	2.40
3	D1	69.03	36.24	36.33	13.49	2.43
2	D2	71.67	33.63	33.71	16.17	2.35

Table 24: Pore volume determination, for the column experiments, using pyknometers

Soil column	mass wet (g)	water content (%)	mass of water (g)	mass dry (g)	volume start (cm^3)	height end (cm)
A1	693	12.61	87.38	605.62	431.75	19.8
A2	697	12.61	87.88	609.12	431.75	19
B1	734	6.44	47.29	686.71	431.75	19
B2	758	6.44	48.84	709.16	431.75	19
C1	768	12.86	98.74	669.26	431.75	22
C2	768	12.86	98.74	669.26	431.75	
D1	676	10.64	71.94	604.06	431.75	20
D2	657	10.64	69.92	587.08	431.75	19.2

Soil column	bulk density start ($g\ cm^{-3}$)	bulk density end ($g\ cm^{-3}$)	particle density ($g\ cm^{-3}$)	φ start	φ end	Pore volume start (mL)	Pore volume end (mL)
A1	1.40	1.56	2.40	0.42	0.35	179	136
A2	1.41	1.63	2.36	0.40	0.31	173	115
B1	1.59	1.84	2.45	0.35	0.25	152	93
B2	1.64	1.90	2.39	0.31	0.21	136	77
C1	1.55	1.55	2.40	0.35	0.35	153	153
C2							
D1	1.40	1.54	2.43	0.42	0.37	183	144
D2	1.36	1.56	2.35	0.42	0.34	182	127

II.6 Equilibrium modeling

Table 25: Equilibrium reactions and constants used in the cyanide speciation calculation (Meeussen et.al, 1994).

Reaction	Log $K°$	References
1. $Fe(OH)_{3(s)} + 3H^+ \longleftrightarrow Fe^{+3} + 3H_2O$	3.45	*(Lindsay, 1979)*
2. $Fe_3(OH)_{8(s)} + 8H^+ \longleftrightarrow 3Fe^{+3} + e^- + 8H_2O$	4.63	*(Lindsay, 1979)*
3. $Fe_4(Fe(CN)_6)_{3(s)} \longleftrightarrow 3Fe(CN)_6^{-3} + 4Fe^{+3} + 3e^-$	-84.5	(Meeussen et al., 1992b)
4. $6CN^- + Fe^{+3} \longleftrightarrow Fe(CN)_6^{-3}$	43.9	(Beck, 1987)
5. $6CN^- + Ca^{+2} + Fe^{+3} \longleftrightarrow CaFe(CN)_{6-}$	46.5	(Hanania, 1974)
7. $6CN^- + Fe^{+3} + K^+ \longleftrightarrow KFe(CN)_6^{-2}$	45.4	(Eaton, 1967)
8. $6CN^- + Fe^{+3} + e^- \longleftrightarrow Fe(CN)_6^{-4}$	49.9	(Beck, 1987)
9. $6CN^- + Fe^{+3} + H^+ + e^- \longleftrightarrow HFe(CN)_6^{-3}$	54.3	(Capone, 1986)
10. $6CN^- + Fe^{+3} + 2H^+ + e^- \longleftrightarrow H_2Fe(CN)_6^{-2}$	56.7	(Capone, 1986)
11. $6CN^- + Ca^{+2} + Fe^{+3} + e^- \longleftrightarrow CaFe(CN)_6^{-2}$	54.0	(Capone, 1986)
12. $6CN^- + 2Ca^{+2} + Fe^{+3} + e^- \longleftrightarrow Ca_2Fe(CN)_6$	55.3	(Capone, 1986)
13. $6CN^- + Ca^{+2} + Fe^{+3} + H^+ + e^- \longleftrightarrow CaHFe(CN)_{6-}$	57.0	(Capone, 1986)
14. $6CN^- + Fe^{+3} + K^+ + e^- \longleftrightarrow KFe(CN)_6^{-3}$	52.4	(Capone, 1986)
15. $6CN^- + Fe^{+3} + 2K^+ + e^- \longleftrightarrow K_2Fe(CN)_6^{-2}$	53.3	(Capone, 1986)
16. $6CN^- + Fe^{+3} + H^+ + K^+ + e^-\ KHFe(CN)_6^{-2}$	55.7	(Capone, 1986)
17. $HC + CN^-\ HCN_{(g)}$	9.2	(Capone, 1986)
18. $HCN_{(aq)} \longleftrightarrow HCN_{(g)}$	-2.8*	(Capone, 1986)

* Henry's constant given as $\log(mg\ CN(L\ air)^{-1}\ (mg\ CN(L\ water)^{-1})$

Table 26: The results of the modeling with the chemical equilibrium program PHREEQC for the columns A, B, C and D.

Column	start	end
A	$Fe(CN)_6^{-3}$	HCN
	$CaFe(CN)_6^-$	$Fe(CN)_6^{-3}$
	$CaFe(CN)_6^{-2}$	$CaFe(CN)_6^-$
	HCN	$CaFe(CN)_6^{-2}$
B	HCN	HCN
	$Fe(CN)_6^{-3}$	$Fe(CN)_6^{-3}$
	$CaFe(CN)_6^-$	$CaFe(CN)_6^-$
	CN^-	CN^-
C	HCN	HCN
	$Fe(CN)_6^{-3}$	$Fe(CN)_6^{-3}$
	$CaFe(CN)_6^-$	$CaFe(CN)_6^-$
	$CaFe(CN)_6^{-2}$	$CaFe(CN)_6^{-2}$
D	HCN	HCN
	CN^-	CN^-
	$Fe(CN)_6^{-3}$	
	$CaFe(CN)_6^-$	

Appendix III: Additional data concerning the modeling of the long-term iron-cyanide complexes release from the MGP soils

III.1 Long-term release of the iron-cyanide complexes from the acidic soil considering "one-phase" release

Table 27: Kinetic and isotherm equations parameters and correlation coefficient for the "one-phase" release of the acidic soil.

Soil C	**Elovich Equation**				
	α (mg CN kg^{-1} day^{-1})	a (mg CN kg^{-1})	R^2	SE	p
	0.04	25.69	0.83	9.11	< 0.01
	Freundlich Equation				
	$\nu \times 10^{-3}$	k (day^{-1})	R^2	SE	p
	782.5	2.99	0.94	2.94	< 0.01
	Parabolic Diffusion				
	K_d (mg CN kg^{-1} $day^{1/2}$)	a (mg CN kg^{-1})	R^2	SE	p
	12.22	21.69	0.98	4.93	< 0.01
	First Order Equation				
	k (day^{-1})	R^2	SE	p	
	0.018	0.94	4.94	< 0.01	

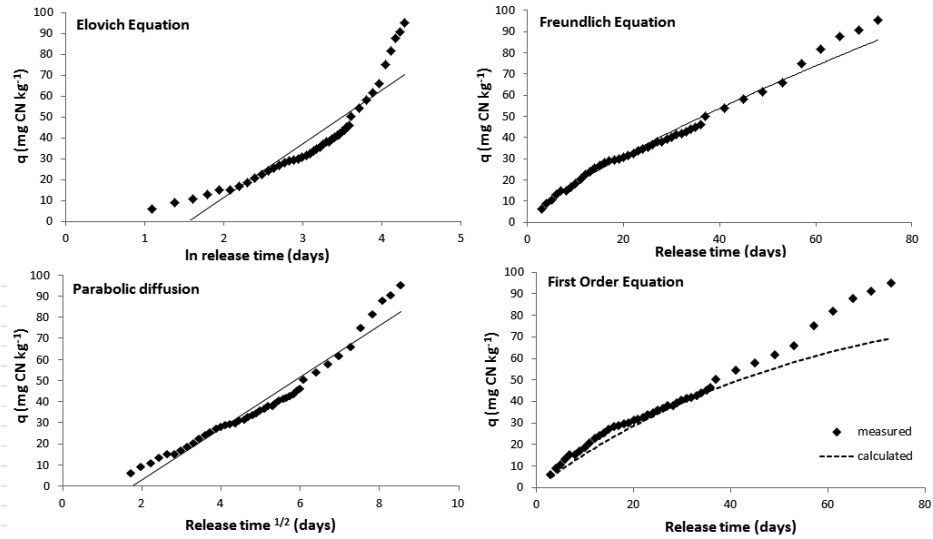

Figure 37: Kinetic and isotherm equation plots for the ''one-phase'' CN release from the acidic soil.

III.2 Correlation of the release rates, obtained after applying different isotherm and kinetic equations, with the soil pH, OM and total CN content

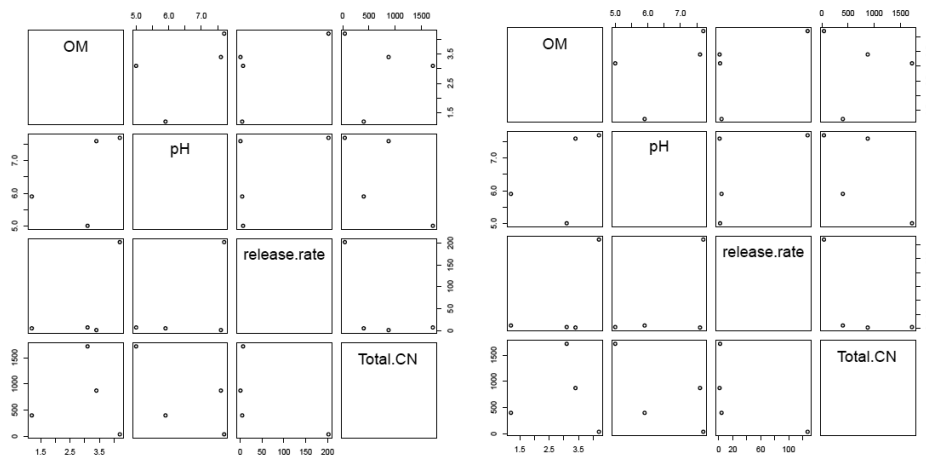

Figure 38: Correlation of the release rates, according to the Elovich Equation (α x 10^2) to the pH, OM and total cyanide content in a) phase I; and b) phase II.

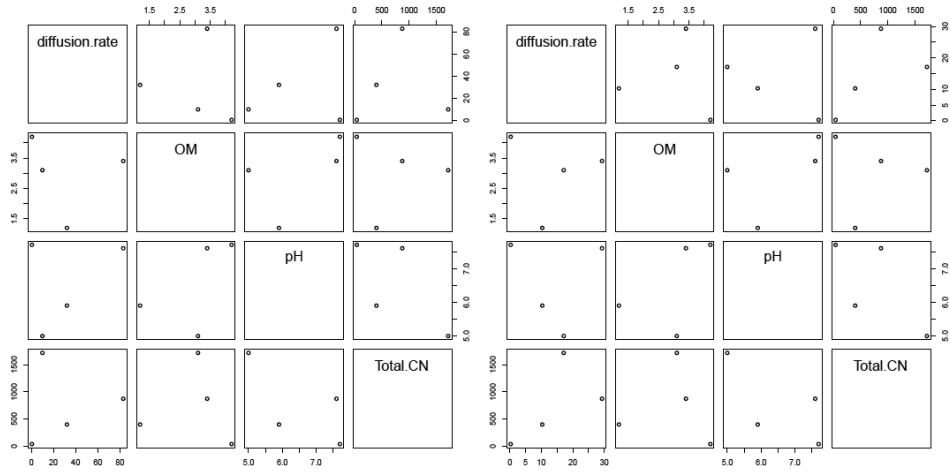

Figure 39: Correlation of the release rates, according to the Parabolic Diffusion Equation (K_d) to the pH, OM and total cyanide content in a) phase I; and b) phase II.

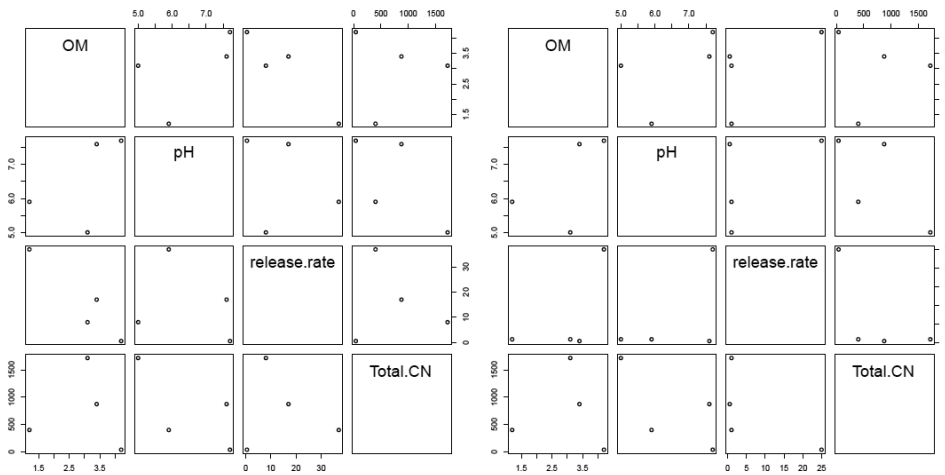

Figure 40: Correlation of the release rates, according to the First Order Equation (k_1 ; k_2 x 10^2) to the pH, OM and total cyanide content in a) phase I; and b) phase II.

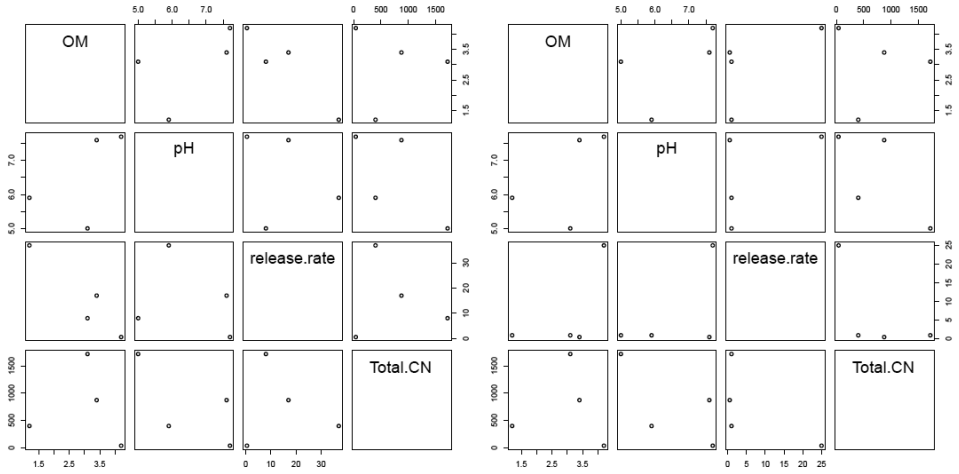

Figure 41: Correlation of the release rates, according to the Freundlich Equation (*k*) to the pH, OM and total cyanide content in a) phase I; and b) phase II.

Appendix IV: Additional data concerning the retardation of the iron-cyanide complexes in the MGP soils

IV.1 Borehole A-21

Table 28: Properties of the borehole A-21 soil samples, based on the fresh mass of the sample.

Depth (cm)	OM (%)	Water content (%)	pH	EC (µS cm^{-1})	Ecell (mV)	temp (°C)	Eref (mV)	Eh (mV)	Water soluble CN (mg kg^{-1})	Total CN (mg kg^{-1})
10	3.6	4.1	6.8	131.2	205.3	26.3	220	425.3	0.2	2.6
30	3.7	8.8	7.4	267.4	246.2	26.4	220	466.2	10.0	164.0
50	2.4	7.6	6.9	214.5	272.2	26.8	220	492.2	13.7	206.0
70	2.0	7.0	6.5	165.7	283.4	26.7	220	503.4	23.7	824.0
90	0.6	5.0	6.0	167.7	270.1	26.5	220	490.1	12.7	632.0
110	1.5	9.6	4.7	172.6	304.8	26.5	220	524.8	2.5	352.0
130	0.9	9.1	4.5	157.2	318.3	26.8	220	538.3	2.1	308.0
140	0.9	1.2	5.1	304.0	331.0	20.6	220	551.0	1.8	274.0
150	1.8	1.,0	6.5	1742.0	241.5	26.7	220	461.5	8.5	46.0
160	2.0	10.3	6.8	2701.0	291.0	20.6	220	511.0	9.4	31.2
170	1.4	12.1	6.9	1778.0	277.1	26.6	220	497.1	6.8	80.0
180	1.5	10.9	6.9	409.0	315.0	20.6	220	535.0	13.7	222.0
190	1.3	6.3	6.5	447.0	295.2	26.8	220	515.2	6.6	192.0
200	0.7	3.3	6.1	83.9	289.0	20.8	220	509.0	2.3	70.0
210	1.6	3.4	5.6	144.7	233.5	25.2	220	453.5	2.6	27.2
230	0.3	2.4	4.9	184.1	327.5	26.6	220	547.5	1.5	13.4
250	0.8	2.3	5.3	62.3	283.5	26.6	220	503.5	2.1	10.6
260	1.0	3.9	5.3	81.9	283.5	26.6	220	503.5	2.6	25.0
270	1.7	4.8	5.3	94.0	277.0	26.3	220	497.0	2.9	40.6
290	1.7	3.4	4.8	136.4	311.9	26.4	220	531.9	1.4	29.4
310	0.7	3.1	4.7	108.0	308.5	26.5	220	528.5	0.6	10.6
330	0.6	2.7	4.6	140.2	389.4	27.1	220	609.4	0.3	5.2
350	0.1	2.4	4.7	76.2	223.1	27.2	220	443.1	0.3	3.4
370	0.4	3.3	4.5	109.3	233.2	27.8	204	437.2	0.3	14.6
390	0.2	2.2	4.4	102.0	284.4	27.6	204	488.4	0.9	3.0
410	0.5	3.5	4.5	238.2	120.6	27.0	220	340.6	0.3	8.8
430	0.4	2.7	4.4	207.8	149.4	27.0	220	369.4	0.3	6.8
450	0.4	3.6	4.5	160.0	229.4	27.4	220	449.4	0.4	6.8
470	0.3	3.2	4.7	237.9	259.5	26.7	220	479.5	0.4	4.4
490	0.4	2.3	4.4	144.3	264.7	26.8	220	484.7	1.0	4.4
510	0.3	2.7	4.7	160.7	258.4	26.9	220	478.4	0.6	9.5

Table 28 (continued)

Depth (cm)	OM (%)	Water content (%)	pH	EC ($\mu S\ cm^{-1}$)	Ecell (mV)	temp (°C)	Eref (mV)	Eh (mV)	Water soluble CN ($mg\ kg^{-1}$)	Total CN ($mg\ kg^{-1}$)
530	0.5	1.3	5.2	85.6	220.9	26.8	220	440.9	0.4	3.0
550	0.0	2.8	5.9	121.4	243.5	26.9	220	463.5	0.5	9.4
570	0.1	2.2	6.2	91.5	226.9	26.6	220	446.9	0.6	9.4
590	0.0	2.2	6.8	87.2	215.7	26.6	220	435.7	0.4	5.0
610	0.1	2.0	6.9	113.7	150.8	28.1	204	354.8	0.5	4.8
630	0.1	1.3	5.1	115.4	177.9	27.3	220	397.9	0.4	3.7
650	0.1	1.9	5.8	43.8	165.8	27.5	220	385.8	0.3	13.5
670	0.4	2.2	5.5	52.2	185.0	27.4	220	405.0	0.3	6.3
690	0,3	2.1	5.9	38.7	129.6	27.2	220	349.6	0.3	2.8
710	0.1	6.1	6.54	42.1	140.4	27.2	220	360.4	0.3	2.3
730	0.2	14.2	6.7	57.7	146.6	27.1	220	366.6	0.4	17.1

Table 29: Ions concentrations for the borehole A-21 soil samples.

Depth (cm)	Chloride	Nitrate	Sulfate	Ca	Mg	Fe	Mn	Al	K
				($mg\ L^{-1}$)					
10	1.5	0.3	8.9	19.6	2.0	10.8	0.1	12.1	2.6
30	0.4	2.1	46.3	40.0	3.3	19.5	0.2	14.1	2.3
50	0.4	5.9	64.1	33.8	2.6	8.2	0.1	3.5	1.4
70	0.4	5.1	48.4	25.8	2.3	10.4	0.2	4.9	1.1
90	0.5	3.7	33.9	18.6	1.5	8.3	0.1	4.4	1.5
110	0.7	6.7	44.5	20.6	0.9	5.5	0.1	1.4	1.0
130	0.5	5.5	36.1	17.0	0.9	1.1	0.1	0.9	1.7
140	0.6	5.3	40.1						
150	0.6	4.7	596.0	436.4	4.2	1.1	0.3	0.0	0.4
160	0.5	8.2	15490						
170	0.7	4.0	705.9	489.4	4.0	0.6	0.2	0.0	0.8
180	0.5	7.4	177.0						
190	0.9	4.7	179.3	76.8	1.5 0.9	0.1	0.0	0.4	
200	0.2	2.2	26.2						
210	0.3	2.5	31.4	15.7	1.3	6.9	0.1	6.0	0.9
230	0.4	2.2	46.8	22.4	1.0	3.7	0.1	3.0	0.5
250	0.4	1.9	17.9	9.7	1.0	5.6	< NWG	5.7	1.0
260	0.2	2.8	24.9						
270	0.3	3.1	28.6	14.6	0.9	2.1	0.1	1.9	0.3
290	0.3	2.1	20.7	9.9	0.8	4.0	< NWG	2.7	0.4
310	0.3	1.3	17.2	8.0	0.7	5.2	< NWG	3.1	0.5
330	0.6	1.7	16.6	9.2	0.8	4.8	0.0	3.1	0.7
350	0.3	1.4	15.7	6.6	0.6	2.5	< NWG	1.8	0.4
370	0.3	1.6	20.4	8.4	0.7	1.1	0.0	0.8	0.5
390	0.2	1.3	26.9	11.3	0.5	0.2	0.1	0.2	0.3
410	0.3	2.0	63.6	25.6	1.1	0.0	0.1	0.0	0.3

Table 29 (continued)

Depth (cm)	Chloride	Nitrate	Sulfate	Ca	Mg	Fe	Mn	Al	K
				(mg L^{-1})					
430	0.2	1.6	43.8	18.1	1.0	0.0	0.1	0.0	0.2
450	0.3	2.5	57.6	22.0	1.4	0.0	0.1	0.0	0.3
470	0.2	1.7	74.9	29.1	1.4	0.0	0.1	0.0	0.4
490	0.4	1.7	38.6	14.3	1.0	0.0	0.1	0.0	0.2
510	0.6	2.0	35.2	13.8	1.0	0.2	0.2	0.0	0.2
530	0.5	3.1	19.3	8.1	0.9	1.8	< NWG	1.7	0.3
550	0.3	1.8	24.0	10.7	1.3	3.3	0.0	2.2	0.5
570	0.6	1.2	19.1	8.9	1.1	2.8	0.0	2.2	0.4
590	0.7	0.9	15.8	7.3	1.1	3.0	0.0	2.5	0.5
610	0.2	1.0	14.0	8.4	0.9	3.1	0.0	2.5	0.6
630	0.4	0.9	13.7	6.7	0.7	2.3	0.0	2.2	0.4
650	0.2	0.7	12.3	6.0	0.7	2.0	< NWG	1.8	0.4
670	0.4	1.0	16.3	7.1	0.8	2.5	0.1	2.4	0.4
690	0.2	0.9	10.9	4.5	0.8	3.3	0.0	3.2	0.6
710	0.3	1.4	11.2	5.8	0.8	2.6	< NWG	2.6	0.5
730	0.5	1.7	15.4	7.6	0.9	2.8	< NWG	2.4	0.4

Table 30: Concentrations of chosen elements in the borehole A-21 soil samples.

Depth (cm)	Fe	Mn	Ca	K	S
			(mg kg^{-1})		
10	7454	130	6656	11007	239
30	12946	242	12464	10630	506
50	9838	107	4458	10273	496
70	5376	122	2859	10113	144
90	3800	56	2256	10678	224
110	14678	121	3634	16314	< LOD
130	10354	104	3190	14568	< LOD
140	10562	95	3285	13142	177
150	9383	87	10143	15870	1567
160	7961	65	20536	12081	5951
170	8278	89	12096	14372	2287
180	8703	87	4257	12892	339
190	6976	81	2487	8074	316
200	2636	34	1235	5747	< LOD
210	3130	40	1480	7918	< LOD
230	1951	< LOD	1372	8027	< LOD
250	1328	< LOD	1208	7902	< LOD
260	1749	< LOD	1240	8168	< LOD
270	1514	30	1384	7290	< LOD
290	1021	< LOD	1015	7341	< LOD
310	1694	< LOD	1101	6745	< LOD

Table 30 (continued)

Depth (cm)	Fe	Mn	Ca (mg kg^{-1})	K	S
330	1408	< LOD	1120	7873	< LOD
350	2197	< LOD	1220	9927	< LOD
370	1983	< LOD	1267	12607	< LOD
390	1510	< LOD	1150	10596	< LOD
410	2202	34	1393	10002	< LOD
430	1941	< LOD	1316	12568	< LOD
450	2331	28	1564	13049	< LOD
470	2530	26	1375	9950	< LOD
490	3687	59	1512	7086	< LOD
510	3482	39	1640	8092	< LOD
530	1445	36	1380	11175	< LOD
550	1939	< LOD	1277	7304	148
570	1761	< LOD	1246	9380	< LOD
590	1067	< LOD	1350	6354	< LOD
610	1102	26	1326	7302	< LOD
630	908	< LOD	1186	7791	< LOD
650	769	< LOD	1062	7821	< LOD
670	975	< LOD	1165	9131	< LOD
690	846	< LOD	1177	7752	< LOD
710	1032	< LOD	1210	9316	< LOD
730	1246	< LOD	1435	9923	< LOD

IV.2 Borehole C-25

Table 31: Properties of the borehole C-25 soil samples, based on the fresh mass of the sample.

Depth (cm)	OM (%)	Water content (%)	pH	EC (µS cm^{-1})	Ecell (mV)	temp (°C)	Eref (mV)	Eh (mV)	Water soluble CN (mg kg^{-1})	Total CN (mg kg^{-1})
10	2.6	10.6	7.1	301.0	256.0	25.6	220.0	476.0	2.4	12.0
20	3.6	11.3	7.2	238.6	267.0	20.7			7.0	9.6
30	2.7	10.1	6.8	575.0	266.0	25.4	220.0	486.0	11.4	334.4
40	2.7	8.1	7.0	394.0	264.0	20.7			9.1	167.6
50	0.5	5.8	6.6	140.4	294.0	25.4	220.0	514.0	3.0	8.8
60	1.9	6.2	7.0	147.7	297.0	21.3			5.3	23.2
70	0.6	6.4	6.9	137.5	292.0	25.6	220.0	512.0	3.1	54.4
80	1.7	6.6	5.8	142.2	302.0	21.3			3.7	91.2
90	1.4	7.0	5.3	271.2	305.0	25.8	220.0	525.0	2.7	140.4
100	0.1	7.0	5.7	202.2	303.0	21.7			2.6	58.6
110	0.9	9.0	7.1	421.0	288.0	25.9	220.0	508.0	3.2	7.0
130	0.8	6.5	6.8	460.0	289.0	25.9	220.0	509.0	4.5	6.4
150	0.2	3.7	7.0	119.2	281.0	25.9	220.0	501.0	1.8	2.4
170	0.5	1.8	7.4	133.3	256.0	25.8	220.0	476.0	0.9	2.4
190	0.3	2.9	7.1	57.6	276.0	25.9	220.0	496.0	1.1	2.6
210	0.3	3.6	7.4	101.8	267.0	25.9	220.0	487.0	1.4	4.4
230	0.2	3.9	7.6	103.9	222.0	25.7	220.0	442.0	1.2	2.4
250	0.3	3.3	7.9	98.5	219.0	25.4	220.0	439.0	0.9	9.6
270	0.1	2.3	7.0	68.9	277.0	26.0	220.0	497.0	0.5	2.0
290	0.4	2.0	6.0	114.1	325.0	25.6	220.0	545.0	0.3	2.0
310	0.2	2.9	7.0	65.5	250.0	25.6	220.0	470.0	0.7	2.0
330	0.2	2.4	6.8	44.0	294.0	25.0	220.0	514.0	0.6	2.0

Table 31 (continued)

Depth (cm)	OM (%)	Water content (%)	pH	EC ($\mu S\ cm^{-1}$)	Ecell (mV)	temp (°C)	Eref (mV)	Eh (mV)	Water soluble CN ($mg\ kg^{-1}$)	Total CN ($mg\ kg^{-1}$)
350	0.5	2.8	6.9	43.0	293.0	25.1	220.0	513.0	0.0	2.0
370	0.3	2.1	7.0	71.5	277.0	25.0	220.0	497.0	0.4	2.0
390	0.3	4.0	6.7	70.1	268.0	22.8	220.0	488.0	0.4	5.4
410	0.4	3.8	7.0	57.3	292.0	24.7	220.0	512.0	0.4	2.0
430	0.5	4.8	7.2	60.9	284.0	23.7	220.0	504.0	0.0	2.0
450	0.1	3.7	7.0	35.3	292.0	24.0	220.0	512.0	0.0	16.2
470	0.3	1.4	7.1	60.4	268.0	24.4	220.0	488.0	0.0	2.0
490	0.3	1.5	6.9	71.2	290.0	24.0	220.0	510.0	0.0	2.0
510	0.4	2.1	6.3	88.2	302.0	23.6	220.0	522.0	0.0	2.0
530	0.1	2.9	6.3	23.3	301.0	24.0	220.0	521.0	0.0	2.0
550	0.2	3.4	6.7	48.4	300.0	24.0	220.0	520.0	0.0	2.0
570	0.4	4.6	7.0	58.2	284.0	23.9	220.0	504.0	0.0	2.0
590	0.1	3,1	6.9	37.7	274.0	24.0	220.0	494.0	0.0	2.0
610	0.1	1,9	6.8	29.0	304.0	24.0	220.0	524.0	0.0	2.0
630	0.2	2,0	6.7	20.3	319.0	23.9	220.0	539.0	0.0	2.0
650	0.2	2,5	6.6	19.7	313.0	24.0	220.0	533.0	0.0	2.0
670	0.1	2,0	6.6	18.3	310.0	23.9	220.0	530.0	0.0	2.0
690	0.1	7,4	6.9	49.3	292.0	23.9	220.0	512.0	0.0	2.0
710	0.1	16,6	7.0	81.1	296.0	23.9	220.0	516.0	0.0	2.0

Table 32: Ions concentrations for the borehole C-25 soil samples.

Depth (cm)	Chloride	Nitrate	Sulfate	Al	Ca	Fe	K	Mg	Mn
				($mg\ L^{-1}$)					
10	2.0	6.3	26.7	14.0	25.6	16.5	8.2	2.3	0.1
20	0.8	8.9	63.1						
30	1.0	0.2	191.0		91.4	1.9	6.5	5.1	0.0
40	1.0	7.0	118.0						
50	1.1	1.0	40.6	22.1	25.1	20.3	5.1	2.8	0.2
60	0.7	4.0	43.7						
70	0.7	0.3	48.7	23.8	24.5	24.8	5.8	2.9	0.2
80	1.0	3.6	50.9						
90	0.5	0.2	66.3	2.3	28.5	3.9	1.0	0.6	0.1
100	0.4	4.1	78.4						
110	0.6	1.6	168.0		76.7	0.6	0.6	0.8	<NWG
130	0.2	2.1	217.0		88.9	0.3	0.9	1.3	<NWG
150	0.3	1.4	34.6	12.7	20.8	16.2	3.2	2.0	0.1
170	0.2	0.3	25.6	7.9	18.3	11.1	2.0	1.2	0.1
190	0.5	0.6	15.3	5.0	8.7	6.1	1.2	0.8	0.0
210	0.5	0.6	28.5	8.9	18.0	10.9	2.2	1.5	0.1
230	0.4	0.9	24.8	3.7	15.9	4.8	1.0	0.7	0.0
250	0.2	0.2	15.2	5.4	11.1	5.3	1.5	0.9	0.0
270	0.3	0.2	11.6	9.4	7.6	9.5	2.2	1.3	0.1
290	0.3	0.2	8.5	7.7	6.3	9.3	2.1	1.2	0.0
310	0.2	0.3	13.3	5.1	10.4	4.9	1.4	0.9	0.1
330	0.6	0.4	11.6	5.3	6.5	5.8	1.6	1.1	0.1

Table 32 (continued)

Depth (cm)	Chloride	Nitrate	Sulfate	Al	Ca	Fe	K	Mg	Mn
				(mg L^{-1})					
350	0.2	1.3	11.7	2.0	6.1	2.1	1.1	0.7	0.0
370	0.2	0.2	11.1	18.2	7.7	18.7	4.3	2.6	0.1
390	0.5	0.3	11.3	14.8	8.1	18.5	3.6	2.0	0.1
410	0.6	0.2	14.2	10.0	8.6	11.3	2.6	1.6	0.1
430	0.7	0.3	15.0	6.6	8.4	6.1	2.5	1.2	0.1
450	0.4	0.1	7.4	9.8	5.4	11.1	2.2	1.3	0.1
470	0.2	0.2	7.5	3.7	5.5	4.5	1.3	0.9	0.1
490	0.3	0.3	7.8	3.6	5.4	3.9	1.2	0.8	0.1
510	0.4	1.1	8.3	3.4	5.4	3.5	1.2	0.8	0.1
530	0.5	0.9	5.0	4.3	3.2	4.5	1.2	0.6	0.1
550	1.1	0.8	10.5	5.8	7.1	6.4	1.8	1.2	0.1
570	0.8	0.6	12.9	8.7	8.9	8.7	3.1	1.5	0.2
590	0.7	0.1	7.7	4.0	5.0	4.0	1.8	0.8	0.1
610	0.8	0.2	5.6	3.0	4.0	3.3	1.4	0.7	0.1
630	0.4	0.3	3.6	4.3	2.9	4.2	1.3	0.6	0.1
650	0.3	0.4	2.8	3.6	3.2	3.9	1.4	0.6	0.0
670	0.5	0.4	3.1	3.5	3.0	3.4	1.1	0.5	0.0
690	2.7	1.9	7.4	2.0	6.3	2.3	0.9	0.7	0.0
710	3.9	3.8	12.8	1.8	10.5	5.8	1.2	1.2	0.0

Table 33: Concentrations of chosen elements in the soil samples of borehole C-25.

Depth	Fe	Mn	Ca	K	S
(cm)			(mg kg^{-1})		
10	8121	139	6414	10687	275
20	7081	129	6874	9525	295
30	20265	228	14107	11034	722
40	14384	199	7324	9250	366
50	6124	138	3736	12930	< LOD
60	6172	142	3236	10667	< LOD
70	5870	136	3281	12623	216
80	6216	133	2950	11283	< LOD
90	5122	158	2857	11640	< LOD
100	5375	189	2750	10822	148
110	7404	335	4743	12150	308
130	6176	192	4345	13236	305
150	3803	65	1867	9795	< LOD
170	5991	49	1589	8872	< LOD
190	1857	< LOD	1324	9986	< LOD
210	2683	25	1345	9221	< LOD
230	3649	55	1534	8245	< LOD
250	1427	< LOD	1156	6709	< LOD
270	1247	< LOD	1211	7978	< LOD
290	1804	33	1303	11178	< LOD
310	1555	33	1361	9988	< LOD
330	3007	46	1395	10536	< LOD

Table 33 (continued)

Depth	Fe	Mn	Ca	K	S
(cm)			(mg kg^{-1})		
350	2749	49	1322	8865	< LOD
370	2455	47	1355	8563	< LOD
390	3999	104	1578	8682	< LOD
410	2533	43	1342	8521	< LOD
430	2128	24	1322	10462	< LOD
450	2097	23	1310	9387	< LOD
470	1637	44	1326	7109	< LOD
490	1644	33	1255	7127	< LOD
510	1601	38	1386	7647	< LOD
530	1424	34	1184	8371	< LOD
550	1447	< LOD	1221	7128	< LOD
570	2071	33	1472	9048	< LOD
590	1170	< LOD	1184	9898	< LOD
610	1144	< LOD	1131	10057	< LOD
630	1140	25	1132	9188	< LOD
650	1498	30	1154	7251	< LOD
670	1404	< LOD	1154	7190	< LOD
690	1589	< LOD	1204	9392	< LOD
710	3851	36	1348	6864	< LOD

IV.3 Batch Experiment

Table 34: Raw data of the cyanide concentration measured in the batch experiment (start CN conc. 100 mg L^{-1}).

Solution	Time (h)		
	24	72	216
	CN conc. (mg L^{-1})		
Fe (II) 1	86.2	73.8	75.0
Fe (II) 2	91.4	78.8	79.0
Fe (III) 1	91.6	81.6	80.4
Fe (III) 2	88.2	88.6	84.4

Table 35: Results of the pH measurement for the batch experiment (start CN conc. 100 mg L^{-1}).

Solution	Time (h)		
	24	72	216
	pH		
Fe (II) 1	6.92	7.09	7.14
Fe (II) 2	7.09	7.13	7.11
Fe (III) 1	7.01	7.05	7.11
Fe (III) 2	6.98	7.03	7.09

Table 36: Raw data of the cyanide concentration measured in the batch experiment (start CN conc. 1000 mg L^{-1}).

Solution	Time (h) 24	48	120	192	360
			CN conc. (mg L^{-1})		
Fe (II) 1	937	880	745	780	750
Fe (II) 2	976	865	770	845	850
Fe (III) 1	995	917	925	870	840
Fe (III) 2	980	902	885	865	822

Table 37: Results of the pH measurement for the batch experiment (start CN conc. 1000 mg L^{-1}).

Solution	Time (h) 24	48	120	192	360
			pH		
Fe (II) 1	6.67	6.94	6.95	7.08	7.12
Fe (II) 2	7.37	6.92	7.02	7.14	7.24
Fe (III) 1	6.85	6.69	6.85	6.81	6.92
Fe (III) 2	6.92	6.71	6.77	6.86	6.81

IV.4 1st column experiment

Table 38: Results of the pH measurement for the 1st column experiment.

Column	pH 8 (day)	21 (day)	62 (day)	111 (day)
Quartz	5.97	5.71	5.98	6.51
Sandy loam	6.26	6.18	5.84	6.26

Table 39: Results of the EC measurement for the 1st column experiment.

Column	EC (mS cm^{-1}) 8 (day)	21 (day)	62 (day)	111 (day)
Quartz	3.4	3.5	3.5	2.8
Sandy loam	2.4	2.4	2.4	2.4

Table 40: Raw data of the cyanide concentration in the 1st column experiment.

Column	Time (day)			
	8 (day)	21 (day)	62 (day)	111 (day)
	CN conc. (mg L^{-1})			
Quartz	1084	1084	1081	932
Sandy loam	1082	1070	1039	778

IV.5 2nd column experiment

Table 41: Raw cyanide data of the 2nd column experiment.

Column	Time (day)									
	1	2	3	4	5	6	7	8	9	10
	Cyanide (mg L^{-1})									
1	414.44	320.00	254.44	245.56	205.56	201.78	190.67	160.44	154.22	147.11
2	407.78	321.11	228.89	213.33	197.78	193.56	188.89	156.44	155.56	153.78
3	427.78	338.89	227.78	211.11	171.11	165.33	148.44	109.33	106.22	107.11
4	431.11	346.67	262.22	255.56	248.89	226.67	253.78	255.56	256.44	257.33
5	434.44	341.11	312.22	271.11	248.89	245.56	231.56	246.67	236.89	242.22

Column	Time (day)						
	11	13	17	21	36	42	47
	Cyanide (mg L^{-1})						
1	145.78	132.44	130.40	126.40	100.00	72.40	64.00
2	146.22	134.22	131.60	132.00	104.40	124.40	90.00
3	103.56	87.11	88.00	84.00	53.20	43.60	44.40
4	259.11	256.44	253.20	252.40			
5	240.44	238.67	244.40	245.20	204.80	187.40	168.20

Table 42: Results of the pH measurement for the 2nd column experiment.

Column	Time (day)									
	1	2	3	4	5	6	7	8	9	10
	pH									
1	6.31	6.8	6.77	6.94	7.21	7.14	7.09	7.12	6.92	6.64
2	6.41	6.74	7.01	7.23	7.28	7.23	7.33	7.33	7.26	7.16
3	6.58		6.98	7.27	7.19	7.34	7.32	7.42	7.41	7.51
4	6.36	7.01	7.02	7.05	7.46	7.57	7.51	7.72	7.35	7.59
5	6.52	7.11	7.08	7.16	7.26	7.53	7.47	7.32	7.33	7.21

Table 42 (continued)

Column	Time (day)						
	11	13	17	21	36	42	47
	pH						
1	7.2	7.42	7.31	7.32	6.91		7.11
2	7.46	7.43	7.51	7.43	6.98		7.04
3	7.61	7.65	7.65	7.64	7.4		7.24
4	7.37	7.52	7.53	7.71			
5	7.16	7.22	7.28	7.38	7.03		7.02

Table 43: Results of the EC measurement for the 2nd column experiment.

Column	Time (day)									
	1	2	3	4	5	6	7	8	9	10
	EC (mS cm^{-1})									
1	1281	1148	976	1321	1086	1080	1097	1096	1377	1014
2	1035	931	755	819	722	826	794	699	706	802
3	964	792	624	633	589	585	682	576	576	644
4	1280	1114	1027	1012	1026	1025	1022	1041	1041	1044
5	1269	1102	1046	1018	990	980	979	975	972	979

Column	Time (day)						
	11	13	17	21	36	42	47
	EC (mS cm^{-1})						
1	1308	1304	1501	1450	1206		1934
2	804	959	760	824	834		1064
3	720	744	625	824	681		747
4	1037	1038	978	934			
5	978	978	986	980	950		949

Table 44: Cyanide balance in the 2nd column experiment.

Column	Mass of CN in the percolation solution (mg)		Mass of the CN precipitated in the bottle (mg)	Mass of the CN reduced the column material (mg)	Reduced CN mass by the column material (%)
	start	end	end	calculated	calculated
1	250	32.0	30.5	187.5	75.0
2	250	45.0	10.5	194.5	77.8
3	250	22.2	7.8	220.0	88.0
4	250	-	-	-	-
5	250	84.1	41.1	124.8	49.9

Table 45: Determination of the vertical distribution of total cyanide concentration within the columns (2nd column experiment).

Column/Sample	Total CN		
	FIA	Factor	CN conc. (mg kg^{-1})
1: 3-5cm	0.235	200	47.0
1: 9-11cm	0.417	200	83.4
1: 15-17cm	0.076	200	15.2
2: 3-5cm	0.265	200	53.0
2: 7-9cm	0.104	2000	208.0
2: 9-11 cm	0.087	2000	174.0
2: 15-17cm	0.113	200	22.6
3: 3-5cm	0.239	200	47.8
3: 7-9cm	0.166	2000	332.0
3: 9-11cm	0.055	2000	110.0
3: 15-17cm	0.046	200	9.2
4: filter up	0.174	200	34.8
4: filter down	0.23	200	46.0
5: quartz up	0.362	200	72.4
5: quartz down	0.47	200	94.0

Table 46: Determination of the vertical distribution of water soluble cyanide concentration within the columns (2nd column experiment).

Sample	Water soluble CN		
	FIA	Factor	CN conc. (mg kg^{-1})
1: 3-5cm	0.465	25	11.6
1: 9-11cm	0.042	250	10.5
1: 15-17cm	0.459	25	11.5
2: 3-5cm	0.078	250	19.5
2: 7-9cm	0.111	250	27.7
2: 9-11 cm	0.089	250	22.2
2: 15-17cm	0.951	25	23.8
3: 3-5cm	0.687	25	17.2
3: 7-9cm	0.089	250	22.2
3: 9-11cm	0.06	250	15.0
3: 15-17cm	0.424	25	10.6
4: filter up	0.763	25	19.1
4: filter down	0.149	250	37.2
5: quartz up	0.121	250	30.2
5: quartz down	0.093	250	23.2

References

Aharoni, C., Sparks, D. L., Levinson, S. and Ravina, I. (1991). Kinetics of Soil Chemical Reactions: Relationships between Empirical Equations and Diffusion Models. *Soils Science Society of American Journal*, 55, 1307-1312.

Allen, J. F. and Bonnette, A. K. Jr. (1974). Thermal decomposition of Prussian Blue: Isotopic labeling with Mössbauer-inactive Fe-56. *Journal of Inorganic and Nuclear Chemistry*, 36(5), 1011-1016.

Alesii, B. A. and Fuller, W. H. (1976). The mobility of three cyanide forms in soils. *Proceedings Residual Management by Land Disposal, Hazardous Waste Research Symposium*, EPA-600/9-76-015, U.S. Environmental Protection Agency, Cincinnati, OH.

APHA/AWWA/WEF, Method 4500-CN (1998). Cyanide. In L. S. Clesceri, A. E. Greenberg, A.D. Eaton (Eds.), *Standard Methods for the Examination of Water and Wastewater*. 20th American Public Health Assoc., American Water Works Assoc., and Water Environment Federation, Washington, DC.

Atkinson, R. J., Hingston, F. J., Posner, A. M. and Quirk, J. P. (1970). Elovich Equation for the Kinetics of Isotope Exchange Reaction at Solid-Liquid Interfaces. *Nature*, 226, 148-149.

Atzberger, C. (2002). Soil optical properties - A review. University of Trier, Remote sensing Department, Trier, Germany.

Baumgardner M. F. (1985). Reflectance properties of soils. *Advances in Agronomy*, 38, 1-44.

BBodSchG (1998). Gesetz zum Schutz des Bodens vom 17. März 1998, Bundesgesetzblatt Jahrgang 1998.- Teil I, Nr.16, S. 505-510.

BBodSchV (1999). Bundes-Bodenschutz- und Altlastenverordnung vom 12. Juli 1999 (BGBl. I S. 1554).

Beck, M. T. (1987). *Pure Applied Chemistry*, 59, 1703-1720.

Blanco, M., Coello, J., Iturriaga, H., Maspoch, S. and Pagès, J. (1999). Calibration in non - linear near infrared reflectance spectroscopy: a comparison of several methods. *Analitica Chimica Acta*, 384(2), 207-214.

Blanco, M. and Villarroya, I. (2002). NIR spectroscopy: a rapid-response analytical tool. *Trends in analitical chemistry*, 21(4), 240-250.

Bodenkundliche Kartieranleitung (2005). AG Boden, Bodenkundliche Kartieranleitung, 5. Aufl., 438 S., 41 Abb., 103 Tab., 31 Listen, Hannover.

Bokobza, L. (2002). Origin of near-infrared absorption bands. In H. W. Siesler, Y. Ozaki, S. Kawata, H. M. Heise (Eds.), *Near-infrared spectroscopy. Principles, instruments, applications* (pp. 11-41). Weinheim: Wiley-VCH.

Capone, S., De Robertis, A., Sammartano, S. and Rigano, C. (1986). *Thermochimica Acta*, 102, 1-14.

Chang, C. W., Laird, D. A., Mausbach, M. J. and Hurburgh, C. R. Jr. (2001). Near-infrared reflectance spectroscopy-principal components regression analysis of soil properties. *Soil Science Society of America Journal*, 65, 480-490.

Chapman, S. J., Campbell, C. D., Fraser, A. R. and Puri, G. (2001). FTIR spectroscopy of peat in bordering Scots pine woodland: relationship with chemical and biological properties. *Soil Biology and Biochemistry*, 33(9), 1193-1200.

Cheng, W. P. and Huang, C. (1996). Adsorption Characteristics of Iron - Cyanide Complex on $\gamma - Al_2O_3$. *Journal of Colloid Interface Science*, 181(2), 627-637.

Chien, S. H. and Clayton, W. R. (1980). Application of Elovich Equation to the Kinetics of Phosphate Release and Sorption in Soils. *Soils Science Society of American Journal*, 44(2), 265-268.

Chien, S. H., Clayton, W. R. and McClellan, G. H. (1980). Kinetics of Dissolution of Phosphate Rocks in Soil. *Soils Science Society of American Journal*, 44(2), 260-264.

Confalonieri, M., Fornasier, F., Ursino, A., Boccardi, F., Pintus, B. and Odoardi, B. (2001). The potential of near infrared reflectance spectroscopy as a tool for the chemical characterization of agricultural soils. *Journal of Near Infrared Spectroscopy*, 9, 123-131.

Cozzolino, D. and Moro'n, A. (2006). Potential of near-infrared reflectance spectroscopy and chemometrics to predict soil organic carbon fractions. *Soil & Tillage Research*, 85, 78-85.

DIN EN ISO 14 403 (2002). Bestimmung von gesamt Cyanid und freiem Cyanid mit der kontinuerlichen Fließanalytik-Teil D.

DeBraekeleer, K., Sanchez, F. C., Hailey, P. A., Sharp, D. C. A., Pettman, A. J. and Massart, D. L. (1998). Influence and correction of temperature perturbation on NIR spectra during the monitoring of a polymorph conversion process prior to self-modeling mixture analysis. *Journal of Pharmaceutical and Biomedical Analysis*, 17, 141-152.

DEIP (1995). Gas works, coke works and other coal carbonization plants, Industry Profile sponsored by Contaminated Land and Liabilities Division.

Dimitrova, T. (2010). Determination of Cyanides in Contaminated Soils Using Micro Distillation - and Spectrophotometric Flow Injection System. *Master Thesis*, Faculty of Environmental Sciences and process Engineering, Brandenburg University of Technology, 37-43.

Durig, J. R. (2002). Utility of Isotopic Data. In J. M. Chalmers, P. R. Griffiths (Eds.), Handbook of vibrational spectroscopy: *Sample characterization and spectral data processing; Volumne 3*, (pp.1935-1947). Chichester: John Wiley & Sons, LTP.

Dzombak, D. A., Ghosh, R. S. and Young, T. C. (2006). Physical - chemical properties and reactivity of cyanide in water and soil. In D. A. Dzombak, R. S. Ghosh, G. M. Wong-Chong (Eds.), *Cyanide in Water and Soil: Chemistry, Risk and Management*, (pp. 57-88). Boca Raton, FL: Taylor and Francis/CRC Press.

Eaton, W. A. (1967). *Journal of Physical Chemistry*, 71, 2016-2021.

Ebbs, S., Bushey, J., Poston, S., Kosma, D., Samiotakis, M. and Dzombak, D. (2003). Transport and metabolism of free cyanide and iron cyanide complexes by willow. *Plant Cell Environment*, 26,1467-1478.

EC (2006). Directive 2006/118/EC of the European Parliament and of the Council of 12 December 2006 on the protection of groundwater against pollution and deterioration, Commission of the European Communities, Brussels, Belgium.

Ebel, M. (2007). Cyanid - Phytoremediation mit *Eichhornia crassipes* - Eine alternative Methode zur Aufbereitung cyanid- und kupferhaltiger Abwässer aus dem Goldbergbau. *Doctor Thesis*, Fakultät für Mathematik, Informatik und Naturwissenschaften der Rheinisch-Westfälischen Technischen Hochschule Aachen.

EEA environmental statement (2007). Copenhagen EPA 542-R-99-005, 1999, A Resource for MGP Site Characterization and Remediation, Office of Solid Waste and Emergency Response (5102G), Washington, DC 20460.

Efron, B. and Tibshirani, R. J. (1993). *An introduction to the bootstrap* (Vol. 57 of monographs on statistics and applied probability). Boca Raton, FL: Chapman and Hall CRC.

Egekeze, J. O. and Oehme, F. W. (1980). Cyanides and their Toxicity: A literature review. *The Veterinary Quarterly*, 2, 104-114.

Elkhatib, E. A., ElShebiny, G. M. and Balba, A. M. (1992). Comparison of Four Equations to Describe the Kinetics of Lead Desorption from Soils. *Zeitschrift für Pflanzenernährung und Bodenkunde*, 155, 285-291.

Elkhatib, E. A., Mahdy, A. M., Saleh, M. E. and Barakat, N. H. (2007). Kinetics of Copper Desorption from Soils as Affected by Different Organic Ligands. *International Journal of Envirnomental Science Technology*, 4(3), 331-338.

Ellerbrock R. H., Gerke H. H., Bachmann J. and Goebel M. O. (2005). Composition of organic matter fractions for explaining wettability of three forest soils. *Soil Science Society of America Journal*, 69, 57-66.

Environmental Resources Limited (1987). Problems Arising from the Redevelopment of Gas Works and Similar Sites. 2nd edition. Department of the Environment, London.

EPA (1999). A Resource for MGP Site Characterization and Remediation Expedited Site Characterization and Source Remediation at Former Manufactured Gas Plant Sites. U.S. Environmental Protection Agency Office of Solid Waste and Emergency Response Technology Innovation Office Washington, DC.

Evans, R. L. and Jurinak, J. J. (1976). Kinetics of Phosphate Release from a Desert Soil. *Soil Science*, 121(4), 1205-1208.

Farmer, V. C. (1974). The layer silicates. In V. C. Farmer (Ed.), *Infrared Spectra of Minerals* (pp. 331-363). London: The Mineralogical Society Monograph 4.

Fidencio, P. H., Poppi, R. J. and de Andrade, J. C. (2002). Determination of organic matter in soils using radial basis function networks and near infrared spectroscopy. *Analytica Chimica Acta*, 453, 125-134.

Fischer, T., Veste, M., Schaaf, W., Dümig, A., Kögel-Knabner, I., Wiehe, W., Bens, O. and Hüttl, R. F. (2010). Initial pedogenesis in a topsoil crust 3 years after construction of an artificial catchment in Brandenburg, NE Germany. *Biogeochemistry*, 101(1-3), 165-176.

Freese, D. (1994). Criteria and Methods for the Assessment of Long-Term Phosphate Sorption and Desorption in Soils. *Habilitationsschrift, Landwirtschaftlich - Gärtnerischen Fakultät*, Humboldt-Universität zu Berlin.

Fuller, W.H. (1985). Cyanides in the environment with particular attention to the soil. In D. van Zyl (Ed.), *Cyanide in the Environment* (pp. 19-44). Colorado State University, Fort Collins.

Geladi, P. and Kowalski, B. R. (1986). Partial least-squares regression: A Tutorial. *Analytica Chimica Acta*, 185, 1-17.

Ghosh, R.S., Dzombak, D.A., Luthy, R.G. and Nakles, D. V. (1999a). Subsurface fate and transport of cyanide species at a manufactured gas plant site. *Water Environment Research* 71, 1205.

Ghosh, R.S., Dzombak, D.A., Luthy, R.G. and Smith, J. R. (1999b). In Situ Treatment of Cyanide - Contaminated Groundwater by Iron Cyanide Precipitation. *Water Environment Research*, 71(6), 1217-1228.

Ghosh, R.S., Dzombak, D.A. and Luthy, R.G. (1999c). Equilibrium precipitation and dissolution of iron cyanide solids in water. *Environmental Engineering Science*, 16(6), 501-501.

Ghosh, R.S., Nakles, D.V., Murarka, I. and Neuhauser, E.F. (2004). Cyanide speciation in soil and groundwater at manufactured gas plant (MGP) sites. *Environmental Engineering Science*, 21, 752-767.

Gorge, W. O. and Lewis, Rh. (2002). Hydrogen Bonding. In J. M. Chalmers, P. R. Griffiths (Eds.), Handbook of vibrational spectroscopy: *Sample characterization and spectral data processing; Volumne* 3, (pp. 1919-1934). Chichester, John Wiley & Sons, LTP.

Haaland, D. M. and Thomas, E. V. (1988). Partial least-squares methods for spectral analyses: 1. Relation to other quantitative calibration methods and the extraction of qualitative information. *Analytical Chemistry*, 60, 1193-1202.

Haberhauer, G., Rafferty, B., Strebl, F. and Gerzabek, M. H. (1998). Comparison of the composition of forest soil litter derived from three different sites at various decompositional stages using FTIR spectroscopy. *Geoderma*, 83(3-4), 331-342.

Hanania, G. I. H. and Israelian, S. A. (1974). Journal of Solution Chemistry, 3, 57-71.

He, Y., Song, H., Pereira, A. G. and Gomez, A. H. (2005). A new approach to predict N, P, K and OM content in a loamy mixed soil by using near infrared reflectance spectroscopy. *Lecture Notes in Computer Science*, 3644, 859-867.

Hester, R. E. and Harrison R. M (1997). *Contaminated land and reclamation*. Cambridge, UK: The Royal Society Of Chemistry.

Hingston, F. J., Posner, A. M. and Quirk, J. P. (1974). Anion Adsorption by Goethite and Gibbsite. II. Desorption of Anions from Hydrous Oxide Surfaces. *Journal of Soil Sciences*, 25(1), 16-26.

Hollemann, A. and Wiberg, N. (2001). *Inorganic Chemistry*. Berlin: Walter de Gruyter GMBH & CO. KG.

Hürkamp, K., Raab, T. and Völkel, J. (2009). Two and three-dimensional quantification of lead contamination in alluvial soils of a historic mining area using field portable X-ray fluorescence (FP XRF) analysis. *Geomorphology*, 110, 28-36.

Janik, L. J., Merry, R. H. and Skjemstad, J. O. (1998). Can mid infra-red diffuse reflectance analysis replace soil extractions? *Australian Journal of Experimental Agriculture*, 38, 681-696.

Jannusch, B., Mansfeldt, T. and Specovius, J. (2002). Characterization of cyanides in soils and industrial wastes by Fourier transform infrared spectroscopy. *Zeitschrift für Umweltchemie und Ökotoxikologie*, 14, 90-95.

Jardine, P. M. and Sparks, D. L. (1984). Potassium - Calcium Exchange in Multireactive Soil System. I. Kinetics. *Soils Science Society of American Journal*, 48(1), 39-45.

Jenne, E. A. (1968). Controls on Mn, Fe, Co, Ni, Cu and Zn concentrations in soils and water: the dominant role of hydrous manganese and iron oxides. *Advances in Chemistry* Series, 73, 337-387.

Johnson, P. R., and Elimelech, M. (1995). Dynamics of colloid deposition in porous media: Blocking based on random sequential adsorption. *Langmuir*, 11, 801-812.

Kamra, S.K., Lennartzb, B., VanGenuchtenc, M. Th. and Widmoser, P. (2001). Evaluating non - equilibrium solute transport in small soil columns. *The Journal of Contaminant Hydrology*, 48, 189-212.

Kang, D. H., Schwab, A. P., Johnston, C. T. and Banks, M. K. (2010). Adsorption of iron cyanide complexes onto clay minerals, manganese oxide, and soil. *Journal of Environmental Science and Health*, Part A, 45, 1391-1396.

Keizer, M. G., van Riemsdijk, W. H. and Meeussen, J. C. L. (1995). Manganese iron cyanide as a possible mineral form in contaminated nonacidic soil. *Land Contamination and Reclamation*, 3, 7-9.

Kjeldsen, P. (1998). Behavior of cyanides in soil and groundwater: A review. *Water, air and soil pollution*, 115, 279-307.

Knowles, C. J. (1976). Microorganisms and cyanide. *Bacteriological Reviews*, 40, 652-680.

Kurzbericht DB-AG (2011). GW-Monitoring Leuchtgasanstalt Cottbus, p.7.

Laidler, K. J. (1965). *Chemical Kinetics*. New York: McGraw-Hill.

Larsen, M., Trapp, S. and Pirandello, A. (2004). Removal of cyanide by woody plants. *Chemosphere*, 54, 325-333.

Larsen, M. and Trapp, S. (2006). Uptake of iron cyanide complexes into willow trees. *Environmental Science and Technology*, 40, 1956-1961.

Larsen, M., Ucisik, A. S. and Trapp, S. (2005). Uptake, metabolism, accumulation and toxicity of cyanide in willow trees. *Environmental Science and Technology*, 39, 2135-2142.

Lewis, J. and Sjöstrom, J. (2010). Optimizing the experimental design of columns in saturated and unsaturated transport experiments. *The Journal of Contaminant Hydrology*, 115, 1-13.

Linder, M., Bugmann, H., Lasch, P., Fleschig, M. and Cramer, W. (1997). Regional impacts of climatic change on forests in the state of Brandenburg, Germany. *Agricultural and Forest Meteorology*, 84, 123-135.

Loch, J. P. G., Lagas, P. and Haring, B. J. A. (1981). Behaviour of heavy metals in soil beneath a landfill; results of model experiments. *Science of the Total Environment*, 21, 203-213.

Low, M. J. D. (1960). Kinetics of Chemisorption of Gases on Solids. *Chemical Reviews*, 60(3), 267-312.

Madari, B. E., Reeves, J. B., Machado, P. L. O. A., Guimaraes, C. M., Torres, E. and McCarty, G. W. (2006). Mid- and near-infrared spectroscopic assessment of soil compositional parameters and structural indices in two Ferralsols. *Geoderma*, 136(1-2), 245-259.

Malley, D. F. and Williams, P. C. (1997). Use of near-infrared reflectance spectroscopy in prediction of heavy metals in freshwater sediment by their association with organic matter. *Environental Science and Technology*, 31, 3461-3467.

Mansfeldt, T. (2003). Mobilität und Mobilisierbarkeit von eisenkomplexierten Cyaniden. Materialien zur Altlastensanierung und zum Bodenschutz (MALBO). *Landesumweltamt Nordrhein - Westfalen* (LUA NRW), 16, 17-44.

Mansfeldt, T. and Biernath, H. (2001). Method comparison for the determination of total cyanide in deposited blast furnace sludge. *Analitica Chimica Acta*, 435, 377-384.

Mansfeldt, T. and Dohrmann, R. (2001). Identification of a Crystalline Cyanide-Containing Compound in Blast Furnace Sludge Deposits. *Journal of Environmental Quality*, 30(6), 1927-1932.

Mansfeldt, T., Gehrt, S.B. and Friedl, J. (1998). Cyanides in a soil of a former coking plant site. *Zeitschrift für Pflanzenernährung und Bodenkunde*, 161, 229.

Mansfeldt, T., Leyer, H., Barmettler, K. and Kretzschmar, R. (2004). Cyanide Leaching from Soil Developed from Coking Plant Purifier Waste as Influenced by Citrate. *Vadose Zone Journal*, 3, 471-479.

Martens, H. and Næs, T. (1989). *Multivariate Calibration*. New York: Wiley.

Maruyama, A., Saito, K. and Ishizawam, K. (2001). b-cyanoalanine synthase and cysteine synthase from potato: molecular cloning, biochemical characterization, and spatial and hormonal regulation. *Plant Molecular Biology*, 46, 749-760.

MacCarthy, J. F., and Zachara, J. M. (1989). Subsurface transport of contaminants. *Environmental Science and Technology*, 23, 496-502.

McCarty, G. and Reeves, J. (2001). Development of rapid instrumental methods for measuring soil organic carbon. In R. Lal (Ed.), *Assessment methods for soil carbon* (pp. 371-380). Boca Raton, FL: Lewis Publ.

McDowell-Boyer, L. M., Hunt, J. R. and Sitar, N. (1986). Particle transport through porous media. *Water Resources Research*, 22, 1901-1921.

McKenzie, R. M. (1970.) The reaction of cobalt with manganese dioxide minerals. *Australian Journal of Soil Research*. 8, 97-106.

Meeussen, J. C. L. (1992). Chemical Speciation and Behavior of Cyanide in Contaminated Soils. Doctoral thesis, Wageningen Agricultural University, Wageningen, The Netherlands.

Meeussen, J. C. L., Keizer, M.G. and F.A.M. de Haan (1992a). Chemical stability and decomposition rate of iron cyanide complexes in soil solutions. *Environmental Science and Technology*, 26, 511-516.

Meeussen, J. C. L., Keizer, M.G. and Van Riemsdijk, W.H. (1990). The Solubility of Iron - Cyanide in Soils. In F. A. M Hinsenveld, Van den Brink W. J (Eds.), *Contaminated Soil* '90 (pp. 367). Dordrecht: Kluwer Acadmic Publishers.

Meeussen, J. C. L., Keizer, M. G., Van Reimsdijk, W. H. and De Haan, V. (1992c). *Environmental Science and Technology*, 26, 1832.

Meeussen, J. L., Keizer, M.G., van Riemsdijk, W.H. and de Haan, F.A.M. (1992). Dissolution behavior of iron cyanide (Prussian Blue) in contaminated soils. *Environmental Science and Technology*, 26(9), 1832-1838.

Meeussen, J. C. L., Keizer, M. G., van Riemsdijk, W. H., and de Haan, F. A. M. (1994). Solubility of cyanide in contaminated soils. *Journal of Environmental Quality*, 23, 785-792.

Meeussen, J.C.L., Van Riemsdijk, W.H. and Van der Zee, S.E.A.T.M. (1995). Transport of complexed cyanide in soil. *Geoderma* 67(1), 73-85.

Micro dist Rapid Distillation Unit, http://ats-scientific.com/products/micro-dist, 15.10.2013

Morillo, E., Undabeytia, T., Maqueda, C. and Ramos, A. (2000). Glyphosate adsorption on soils of different characteristics. Influence of copper addition. *Chemosphere* 40, 103-107.

Müller, H. W., Dohrmann, R., Klosa, D., Rehder, S. and Eckelmann W. (2009). Comparison of two procedures for particle-size analysis: Köhn pipette and X-ray granulometry. *Journal of Plant Nutrition and Soil Science*, 172 (2), 172-179.

Nakamoto, K. (2002). Infrared and Raman Spectra of Inorganic and Coordination Compounds. In J. M. Chalmers, P. R. Griffiths (Eds.), Handbook of vibrational spectroscopy: *Sample characterization and spectral data processing*; Volumne 3, (pp.1872-1892). Chichester: John Wiley & Sons, LTP.

National Environment Protection Council (NEPC) (1999). National Environment Protection (Assessment of Site Contamination) Measure: Schedule B(1) Guideline on the Investigation Levels for Soil and Groundwater.

Nederlof, M. M., Van Riemsdijk, W. H. and Koopal, L. K. (1994). Analysis of the Rate of Dissociation of Ligand Complexes. *Environmental Science and Technology*, 28, 1048-1053.

Nielsen, P., Dresow, B., Fischer, R. and Heinrich, H. C. (1990). *Archives of Toxicology*, 64, 420.

Lillie, D. R and Donaldson, P. T (1973). The mechanism of the ferric ferricyanide reduction reaction. *Histochemical Journal*, 6, 679-684.

Ohno, T. (1990). Levels of Total Cyanide and NaCl in SurfaceWaters Adjacent to Road Salt Storage Facilities. *Environmental Pollution*, 67(2), 123-132.

Parkhurst, D. L., Appelo, C. A. J. (1999). User's guide to PHREEQC (Version 2): a computer program for speciation, batch-reaction, one-dimensional transport, and inverse geochemical calculations. USGS Water-Resources Investigations Report, 99-4259.

Peel, M. C., Finlayson, B. L. and McMahon, T. A. (2007). Updated world map of the Köppen Geiger climate classification. *Hydrology and Earth System Sciences*, 11, 1633-1644.

Pierzynski, G. M, Vance, G. F. and Sims, J. T. (2005). *Soils and environmental quality*. Boca Raton, FL: Taylor and Francis.

Pfaff-Schley, H. (1996). *Bodenschutz und Umgang mit kontaminierten Böden: Bodenschutzgesetze, Prüfwerte, Verfahrensempfehlungen*. Berlin: Springer.

Proffit, D., Marion, P. and Rouillier, M. C. (2001). Cyanide polluted solids - A combined leachate and solid characterization. In C. A. Young, L. G. Twidwell and C. G. Anderson (Eds.), *Cyanide: Social, Industrial, and Economic Aspects* (pp. 133-140). Warrendale: TMS.

Rhind, S. M. (2009). Anthropogenic pollutants: a threat to ecosystem sustainability? *The Philosophical Transactions of the Royal Society B*, 364, 3391-3401.

Rennert, T. (2002). Sorption of Iron-Cyanide Complexes on Iron Oxides and in Soils, Doctoral Thesis, Fakultät für Geowissenschaften der Ruhr-Universität Bochum.

Rennert, T. and Mansfeldt, T. (2002). Sorption of Iron-Cyanide Complexes on Goethite. *European Journal of Soil Science*, 52(1), 121-128.

Rennert, T. and Mansfeldt, T. (2002). Sorption of Iron-Cyanide Complexes in Soil. *Soils Science Society of American Journal*, 66(2), 437-444.

Rennert, T., Ufhold, S. and Mansfeldt, T. (2007). Identification of Iron - Cyanide Complexes in Contaminated Soils and Wastes by Fourier Transform Infrared Spectroscopy. *Environmental Science and Technology*, 41, 5266-5270.

Repmann, F., Freese, D., Dimitrova, T. and Sut, M. (2012). Erkundung und Monitoring der LGA Fläche Feld, Labor und Gewächshausuntersuchungen, Im Rahmen des Projekts Stabilisierung des DB AG Standortes "ehem. Leuchtgasanstalt Cottbus" durch Verfahren der Bioremediation (Phytoremediation), not published, released on 07.12.2012

Saffron, C. M., Park, J. H., Dale, B. E. and Voice, T. C. (2006). Kinetics of Contaminant Desorption Form Soil: Comparison of Model Formulations Using the Akaika Information Criterion. *Environmental Science Technology*, 40, 7662-7667.

Savitzky, A. and Golay, M. J. E. (1964). Smoothing and differentiation of data by simplified least squares procedures. *Analitical Chemistry*, 36(8), 1627-1639.

Schenk, B. and Wilke, B. M. (1984). Cyanidadsorption an Sesquioxiden, Tonmineralen und Huminstoffen. *Zeitschrift für Pflanzenernährung und Bodenkunde*, 147(6), 669-679.

Scott, A. B., Scott, R. Y., Bettahar, M. and Simunek J. (2002). Physical factors affecting the transport of colloids in saturated porous media. *Water Resources Research*, 38(12), 1327.

Shenk, J. S., Workman, J. J. Jr. and Westerhaus, M. O. (1992). Application of NIR spectroscopy to agricultural products. In D. A. Burns and E. W. Ciurczak, (Eds.), *Handbook of near-infrared analysis* (pp. 383-431). New York: Marcel Dekker.

Shefsky, S. (1997). Comparing Field-Portable X-Ray Fluorescence (XRF) to Laboratory Analysis of Heavy Metals in Soil. *International Symposium of Field Screening Methods for Hazardous Wastes and Toxic Chemicals*, Las Vegas, NV.

Shifrin, N. S., Beck, B. D., Gauthier, T. D., Chapnick, S. D. and Goodman, G. (1996). *Regulatory Toxicology and Pharmacology*, 23, 106.

Siebielec, G., McCarty, G. W., Stuczynski, T. I. and Reeves, J. B. III (2004). Near- and Mid-Infrared Diffuse Reflectance Spectroscopy for Measuring Soil Metal Content. *Journal of Environmental Quality*, 33, 2056-2069.

Slaughter. D. C., Pelletier, M. G. and Upadhyaya, S. K. (2001). Sensing soil moisture using NIR spectroscopy. *Applied Engineering in Agriculture*, 17, 241-247.

Smith, A. and Mudder, T. (1991). *The Chemistry and Treatment of Cyanidation Wastes*. Londin: Mining Journal Books.

Stenberg, B., Viscarra Rossel, R. A., Mouazen, A. M. and Wetterlind, J. (2010). Visible and Near Infrared Spectroscopy in Soil Science. In D. L. Sparks (Ed.), *Advances in Agronomy*, Vol. 107, Burlington: Academic Press.

Stevenson, F. J. (1994). *Humus Chemistry. 2nd edition*. New York: John Wiley & Sons.

Sut, M., Fischer, T., Repmann, F., Raab, T. and Dimitrova, T. (2012). Feasibility of Field Portable Near Infrared (NIR) Spectroscopy to Determine Cyanide Concentrations in Soil. *Water Air and Soil Pollution*, 223(8), 5495-5504.

Sut, M., Repmann, F. and Raab, T. (2013). Stability of Prussian Blue in Soils of a Former Manufactured Gas Plant Site. *Soil and Sediments Contamination an International Journal*, 23, 504-522.

Sut, M., Fischer, T., Repmann, F. and Raab, T. (2013). Long-term release of iron-cyanide complexes from the soils of a former Manufactured Gas Plant site. *Journal of Environmental Protection*, 4 (11B), 8-19.

Theis, T.L. and West, M.L. (1986). Effects of cyanide complexation on the adsorption of trace metals at the surface of goethite. *Environmental Technology Letters*, 7, 309-318.

Theis, T.L., Young, T.C., Huang, M. and Knutsen, K.C. (1994). Leachate characteristics and

composition of cyanide-bearing wastes from manufactured gas plants. *Environmental Science and Technology*, 28(1), 99-106.

Torrent, J. (1987). Rapid and Slow Phosphate Sorption by Mediterranean Soils. Effect of Iron Oxides. *Soils Science Society of American Journal*, 51, 78-82.

Trapp S., Larsen M. and Christiansen H. (2001). Experimente zum Verbleib von Cyanid nach Aufnahme in Pflanzen. *Umweltwissenschaften- und-Schadstoff-Forschung*, 13, 29-37.

Umpleby II, R. J., Baxter, S. C., Bode, M., Berch Jr., J. K., Shah R. N. and Shimizu, K. D. (2001). Application of the Freundlich Adsorption Isotherm in the Characterization of Molecularly Imprinted Polymers. *Analitica Chimica Acta*, 435(1), 35-42.

USEPA, Method 10-204-00-1-X (2008). Lachat USEPA Approved and Equivalent Method, Revision 3, 22.01.

USEPA, Method 9010B (1998). Total and amenable cyanide: Distillation. In SW-846: *Test Methods for Evaluating Solid Waste: Physical/Chemical Methods*, Rev 5, U.S. Environmental Protection Agency, Office of Solid Waste, Washington, DC.

USEPA, Method 1311 (1998). Toxicity characteristic leaching procedure. In SW-846: *Test Methods for Evaluating Solid Waste: Physical/Chemical Methods*, Rev 5, U.S. Environmental Protection Agency, Office of Solid Waste, Washington, DC.

USEPA, Method 1312 (1998). Synthetic precipitation leaching procedure. In SW-846: *Test Methods for Evaluating Solid Waste: Physical/Chemical Methods*, Rev 5, U.S. Environmental Protection Agency, Office of Solid Waste, Washington, DC.

Wang, T.H., Lib, M.H. and Teng, S.P. (2009). Bridging the gap between batch and column experiments: A case study of Cs adsorption on granite. *Journal of Hazardous Materials*, 161, 409-415.

Wehrer, M., T. Rennert, T. Mansfeldt and Totsche, K. U. (2011). Contaminants at former manufactured gas plants: Sources, properties, and processes. *Critical Reviews in Environmental Science and Technology*, 41, 1883-1969.

Weigand, H., Totsche, K.U., Mansfeldt, T. and Kögel-Knabner, I. (2001). Release and mobility of polycyclic aromatic hydrocarbons and iron cyanide complexes in contaminated soil. *Journal of Plant Nutrition and Soil Science*, 164, 643-649.

Wilson, D. J. and Clarke, A. N. (1994). *Hazardous Waste Site Soil Remediation: Theory and Application of Innovative Technologies*. New York, NY: M. Dekker.

Wu, F. C., Tseng, R. L. and Juang, R. S. (2009). Characteristics of Elovich Equation Used for the Analysis of Adsorption Kinetics in Dye-Chitosan Systems. *Chemical Engineering Journal*, 150, 366-373.

Vaidyanathan, R. and Tien, C. (1991). Hydrosol deposition in granular media under unfavorable surface conditions, *Chemical Engineering Science*, 46, 967-983.

Vandegrift, G. F., Reed, D. T. and Tasker, I. R. (1992). *Environmental Remediation: Removing Organic and Metal Ion Pollutants*. Washington, DC: American Chemical Soc.

Van der Zee, S. E. A. T. M. and Van Riemsdijk, W. H. (1998). Model for Long-Term Phosphate Reaction Kinetics in Soil. *Journal of Environmental Quality*, 17(1), 35-41.

Viscarra Rossel, R. A., Walvoort, D. J. J., McBratney, A. B., Janik, L. J. and Skjemstad, J. O. (2006). Visible, near infrared, mid infrared or combined diffuse reflectance spectroscopy for simultaneous assessment of various soil properties. *Geoderma*, 131, 59-75.

Zornoza, R., Guerrero, C., Mataix-Solera, J., Scow, K. M., Arcenegui, V. and Mataix-Beneyto, J. (2008). Near infrared spectroscopy for determination of various physical, chemical and biochemical properties in Mediterranean soils. *Soil Biology & Biochemistry*. 40(7), 1923-1930.

Young, T. C. and Theis, T. L. (1991). Determination of cyanide in manufactured gas plant purifier wastes. *Environmental Technology*, 12, 1063-1069.

Acknowledgments

My greatest appreciation and gratitude goes to my supervisor Prof. Raab for providing me the opportunity to take part in the IGS program and achieve the doctor title. I would like to thank him for his trust and support, for advising me during all phases of my doctoral thesis, but also for giving me the freedom to find my own way.

I would like to thank Dr. Fischer and Dr. Repmann for a great support and long hours of discussions. They were both very helpful in providing advices, designing the experiments and most important in preparing the publications. I am very grateful for their time and patience, it would not be possible for me to complete my degree without their help.

I would like to thank my friend Katharine Bendele for checking my English. She read and corrected all my papers and the thesis, and she still picks up the phone when I call! Thank you Kate!

I thank Tsvetelina Dimitrova for being always there for me when "FIA" broke. I am also very grateful for your previous work that helped me with progressing on my project.

I would like thank to Florian Jenn for his patience and time (many evenings) in explaining me the secrets of “R project”. I am very grateful to Prof. Freese for advices on my work and publications. Additionally I would like to thank Michael Kanzler for the support in collecting field samples.

I thank Florian Hirsch for many helpful advices and beneficial discussions. I would like to thank Alexander Nicolay for helping me with the soil analysis. I am very grateful to Annika Badorreck for her advices on modeling with Hydrus. I thank Steffi Schillem for always helping me with the organizational issues. Also I thank Anna Schneider for advises concerning the formatting and finalizing of my thesis.

It would not have been possible to finalize this thesis without the huge support and help from the labor staff. I would like to express my great gratitude to Gabriele Franke, Anita Maletzki , Regina Müller and Philipp Lange.

I am especially grateful to my IGS colleges: Penka Tsonkova, Tanya Medinski, Ina Pohle, Xiaoying Gu and Dario Mantovani. It was a blast sharing those last 3 years with you guys! Having you around made it so much easier. Thank you!

For financial support, I thank the Brandenburg Ministry of Science, Research and Culture (MWFK) as part of the International Graduate School at Brandenburg University of Technology (BTU) and Deutsche Bahn AG.

My Mom and Dad, for their unconditional love and care, and for not hanging up the phone when I was complaining over and over again about a miserable life of a doctoral student. I owe them much more then I would ever be able to express, they helped me to become a strong and confident person that I am today.

Finally, I would like to thank Jonas Lohmann for being the more loving, supportive, encouraging, and patient than I could ever imagine. You are my best friend and you have given me so many happy and beautiful memories throughout this journey. I would not be able to be the person that I am today without having you by my side. There are no words that can express my gratitude and appreciation for all you've done and been for me. Thank you.

In dieser Reihe bereits erschienen

- Raab, T., Raab, A., Gerwin, W., Schopper, F. (Hrsg., 2013): Landschaftswandel - *Landscape Change*. - GeoRS Vol. 01.
- Raab, T., Hirsch, F., Raab, A., Schopper, F., Freytag, K. (Hrsg., 2013): Arbeitskreis Geoarchäologie - Jahrestagung 2013, 2. - 4.5.2013, BTU Cottbus. Tagungsband und Exkurionsführer. - GeoRS Vol. 02.
- Schneider, A. (2014): Spatial and temporal development of sediment mass balances during the initial phase of landform evolution in a small catchment. - GeoRS Vol. 03